

PROPERTIES OF THE NON-CATALYTIC NUCLEOTIDE SITE OF THE  
 $\text{Ca}^{2+}$ -ATPase OF SARCOPLASMIC RETICULUM

Thesis presented for the degree of  
Doctor of Philosophy of the  
University of Cape Town

by

George A. Davidson M.B.,Ch.B. (UCT)

August 1986

The University of Cape Town has been given  
the right to reproduce this thesis in whole  
or in part. Copyright is held by the author.

The copyright of this thesis vests in the author. No quotation from it or information derived from it is to be published without full acknowledgement of the source. The thesis is to be used for private study or non-commercial research purposes only.

Published by the University of Cape Town (UCT) in terms of the non-exclusive license granted to UCT by the author.

To Gaia

## ACKNOWLEDGEMENTS

I wish to thank Professor Mervyn C. Berman for his guidance and supervision, and for creating the opportunity for me to perform this study.

I wish to express my sincerest thanks to Drs David B. McIntosh, James E. Bishop and Florent Guillain for valuable discussion and constructive criticism: to Mr David Woolley and Dr Melanie Ziman for technical assistance: to Messrs R.D. Alexander and M. Smith for help in the routine preparation of sarcoplasmic reticulum vesicles: to Mr David Greengrass for electronic and computing assistance: to Messrs Christopher Seebregts for assistance in the synthesis of [ $^{14}\text{C}$ ]TNP-ATP and David Ross for Gel electrophoresis studies. I thank Mrs Ripley Bommen for support and encouragement.

The South African Medical Research Council provided financial support during the period of graduate studies.

## ABSTRACT

Properties of the regulatory nucleotide binding site of the  $\text{Ca}^{2+}$ -ATPase of skeletal muscle sarcoplasmic reticulum have been investigated. Previously, several lines of evidence have indicated the existence of both catalytic and regulatory nucleotide binding sites on the same polypeptide species. The present study concentrates on the interaction of the ATP analogue, 2'-3'-O-(2,4,6-trinitro-cyclohexadienylidene) adenosine 5'-triphosphate, (TNP-ATP), with sites on the non-phosphorylated and phosphorylated enzyme. In particular those conformational transitions linking TNP-ATP fluorescence to the phosphoenzyme subspecies have been sought.

Previous studies have demonstrated a close relationship between TNP-ATP fluorescence and phosphoenzyme formed from ATP plus  $\text{Ca}^{2+}$ , or from inorganic phosphate (Pi) in the absence of  $\text{Ca}^{2+}$ , in the reverse direction of the cycle. However, the precise relationship of TNP-ATP fluorescence to the energy transducing conformations of the ATPase is controversial.

TNP-ATP binding was investigated by spectrophotometric methods and by the synthesis of [ $^{14}\text{C}$ ]TNP-ATP. [ $^{14}\text{C}$ ]TNP-ATP bound to the ATPase site with high affinity ( $[\text{TNP-ATP}]_{0.5} = 0.12 \mu\text{M}$ ), and a stoichiometry of 5.4 nmol/mg. [ $^{14}\text{C}$ ]ATP binding stoichiometry was 6.1 nmol/mg, demonstrating that TNP-ATP binds to a single family of sites.

The nature of the phosphoenzyme intermediate species that results in enhanced TNP-ATP fluorescence was investigated. NEM derivitization,  $\text{Sr}^{2+}$ -transport and  $\text{Ca}^{2+}$ -oxalate uptake have previously been found to alter the distribution or relative levels of phosphoenzyme intermediates. Modification of thiol groups responsible for phosphoenzyme decomposition (SHd), using N-ethylmaleimide (NEM) (0.4 mM) with 50  $\mu\text{M}$   $\text{Ca}^{2+}$ ,

1 mM AMP-PNP at pH 7.0, resulted in a 50% decrease in  $\text{Ca}^{2+}$ -uptake,  $\text{Ca}^{2+}$ -ATPase activity and ADP-insensitive E-P ( $\text{E}_2\text{-P}$ ), while total EP ( $\text{E}_1\text{-P} + \text{E}_2\text{-P} = 3.2 \text{ nmol/mg}$ ), remained unaltered.

ATP-dependent TNP-ATP enhanced fluorescence decreased by 50% under these conditions.  $\text{Ca}^{2+}$ -oxalate induced turnover has previously been shown to decrease steady-state  $\text{E}_2\text{-P}$  levels by prevention of  $\text{Ca}^{2+}$  gradient formation. Oxalate (5 mM) caused a 40% decrease in ATP-induced TNP-ATP fluorescence levels while total EP levels remained relatively unaltered.

Previous studies have shown that  $\text{Sr}^{2+}$ -induced turnover favours higher levels of  $\text{E}_2\text{-P}$  by inhibiting the reverse reaction from  $\text{E}_2\text{-P}$  to  $\text{E}_1\text{-P}$ . Strontium-induced turnover increased TNP-ATP fluorescence by 10% as compared to that of  $\text{Ca}^{2+}$ , without affecting steady-state E-P levels, consistent with an  $\text{E}_2\text{-P}$  conformation relationship to enhanced TNP-ATP fluorescence.

The binding site for TNP-ATP on the enzyme was investigated by chase studies using millimolar concentrations of nucleotides. ATP and ADP diminished TNP-ATP fluorescence competitively, with apparent  $K_m$  values of 1.25 and 0.54 mM respectively, consistent with their affinities of binding to the regulatory site. The rates of decrease of fluorescence (25 and 34  $\text{sec}^{-1}$  at 5°C, respectively), were of the same order of magnitude as the derived "off" rate of TNP-ATP from the site of enhanced fluorescence (33  $\text{sec}^{-1}$ ), consistent with TNP-ATP being bound to the regulatory site of the enzyme.

Enhanced TNP-ATP fluorescence has previously been related to decreased water activity of the probe site. Alteration of water activity by structure-forming (Deuterium oxide) and structure-breaking solutes (KSCN) in relation to fluorescence were explored. Replacement of  $\text{H}_2\text{O}$  by  $\text{D}_2\text{O}$  altered the fluorescence of unbound TNP-ATP. The

apparent for TNP-ATP binding to the E<sub>2</sub>-P conformation of the regulatory site. The regulatory site appears to be a modified form of the phosphorylated catalytic site. It is proposed that TNP-ATP fluorescence monitors an enzyme conformation related to Ca<sup>2+</sup> binding to an inward oriented site of low affinity. The mechanism of K<sup>+</sup> fluorescence quenching appears to be via an acceleration of dephosphorylation, as opposed to a change in affinity of the enzyme for TNP-ATP, as previously suggested. The K<sup>+</sup> sensitivity of TNP-ATP fluorescence has proved useful in demonstrating a direct interaction of valinomycin with the enzyme through the monovalent cation binding site. Valinomycin appears to bind directly to the enzyme and to selectively accelerate the "off" rate of K<sup>+</sup> from this site.

fluorescence quantum yield was increased by 30% and "blue-shifted" the emission peak from 560 to 545 nm, but there was no change in fluorescence characteristics of TNP-ATP bound to the enzyme. KSCN decreased TNP-ATP fluorescence levels ( $[KSCN]_{0.5} = 10 \text{ mM}$ ) at a rate ( $52 \text{ sec}^{-1}$ ) equivalent to the "off" rate constant of TNP-ATP from the binding site, consistent with previous studies that suggested displacement of ATP from the hydrophobic clefts that constitute binding sites on the polypeptide.

Monovalent cations decreased steady-state TNP-ATP enhanced fluorescence in the series  $K^+ > Rb^+ > Cs^+ > Na^+ \gg Li^+$  ( $K_{0.5} = 49, 73, 75, 94, \text{ and } 246 \text{ mM}$ , respectively), consistent with the known specificities and affinities of the monovalent cation site, that stimulates turnover and accelerates phosphoenzyme hydrolysis. The apparent affinity of the phosphoenzyme for TNP-ATP was decreased with  $K_d$  values of 0.76 and 3.1  $\mu\text{M}$  in the absence and presence of  $K^+$  respectively.  $K^+$  decreased fluorescence monoexponentially at a rate ( $0.027 \text{ sec}^{-1}$ ), 1000-fold slower than the "off" rate of TNP-ATP at  $5^\circ\text{C}$ . It is concluded that the fluorescence was decreased by a  $K^+$ -induced decrease in  $E_2\text{-P}$  levels alone, and not due to decreased TNP-ATP binding.

$K^+$  sensitivity provides a useful tool for analysis of monovalent cation interaction. Valinomycin (0.2 nmol/mg), in the absence of monovalent cations, decreased ATPase activity by 30%, and abolished the stimulatory effects of 150 mM  $K^+$  or  $Na^+$  on turnover. The ionophore alone enhanced TNP-ATP fluorescence by 20 %, but also altered the specificity and affinity of the site that inhibited TNP-ATP fluorescence, to  $Cs^+ > Rb^+ > K^+ > Na^+ \gg Li^+$ , ( $K_{0.5} = 79, 111, 134, 136 \text{ and } 270 \text{ mM}$ , respectively), which follows the Hofmeister series for the effectiveness of monovalent lyotropic cations.

In conclusion, the findings of this study indicate that TNP-ATP binds with high affinity to a single family of nucleotide binding sites. Enhanced TNP-ATP fluorescence is

## ABBREVIATIONS

AcP	Acetylphosphate
AMP-CPP	Adenosine 5'-( $\alpha$ , $\beta$ , methylene) triphosphate
AMP-PCP	Adenosine 5'-( $\beta$ , $\gamma$ , methylene) triphosphate
AMP-PNP	Adenosine 5'-( $\beta$ , $\gamma$ , imino) triphosphate
Me <sub>2</sub> SO	Dimethylsulfoxide
EGTA	Ethyleneglycol-bis-( $\beta$ -amino-ethyl ether) N,N,N',N'- tetraacetic acid
E	The Ca <sup>2+</sup> -ATPase
E <sub>1</sub> , E <sub>2</sub>	Conformational forms of the enzyme, E
EP	Phosphoenzyme
E <sub>1</sub> -P	High energy phosphoenzyme with high affinity outwardly oriented Ca <sup>2+</sup> binding sites
E <sub>2</sub> -P	Low energy phosphoenzyme with low affinity inwardly oriented Ca <sup>2+</sup> binding sites
FITC	Fluorescein isothiocyanate
Mops	3-(N-morpholino) propanesulfonic acid
NEM	N-ethyl maleimide
[ <sup>3</sup> H]NEM	N-[ethyl-2- <sup>3</sup> H]-ethylmaleimide
NTP	Nucleotide triphosphate
PCA	Perchloracetic acid
Pi	Inorganic phosphate
SR(V)	Sarcoplasmic Reticulum (vesicles)
TNP-ATP	2',3',-O-(2,4,6-trinitrocyclohexyldienylidene)-adenosine 5'-triphosphate: TNP-ADP, TNP-AMP; di- and monophosphates, respectively
Tris	Tris (hydroxymethyl)aminomethane

## CONTENTS

	Page
Acknowledgements	i
Abstract	ii
Abbreviations	vi
Contents	vii
1.0 <u>INTRODUCTION</u>	1
1.1    The Calcium pump of sarcoplasmic reticulum as a prototype for energy transduction in biological membranes	1
1.2    The sarcoplasmic reticulum of skeletal muscle	2
1.2.1    Structure and composition of sarcoplasmic reticulum vesicles	3
1.2.2    The catalytic cycle of the Ca <sup>2+</sup> -ATPase	5
1.2.3    Influence of ligands on the catalytic cycle	13
1.2.4    Catalytic requirements for energy coupling	18
1.2.5    Characteristics and role of regulatory nucleotide binding sites	23
1.3.    Aspects of water structure relevant to protein function	25
1.4.    TNP-ATP as a probe of nucleotide binding sites of ATPases	33
1.5    Interaction of ionophores with energy transducing membranes	40
1.5.1    Anomolous effects of the ionophore valinomycin	44

2.0	<u>EXPERIMENTAL PROCEDURES</u>	48
2.1	Materials	48
2.2	Preparative methods	48
2.2.1.	Isolation and purification of sarcoplasmic reticulum vesicles	48
2.2.2	Determination of protein concentrations	49
2.2.3	TNP-ATP synthesis	51
2.2.4	[ <sup>14</sup> C]TNP-ATP synthesis	51
2.3	Analytical methods	55
2.3.1	Radioactive ligand binding	55
2.3.2	Fluorescence measurements	58
2.3.3	Kinetic fluorescence measurements	61
2.3.4	Absorbance measurements	61
2.3.5	ATPase assays	61
2.3.6	<sup>45</sup> Ca <sup>2+</sup> uptake	62
2.3.7	[ <sup>32</sup> P]EP levels	63
2.3.8	Covalent modification with NEM	65
2.3.9	Binding parameters	65
3.0	<u>RESULTS</u>	66
3.1	Interaction of TNP-ATP with the Ca <sup>2+</sup> -ATPase	66
3.2	TNP-ATP binding affinity and stoichiometry	69
3.3	The effect of millimolar ATP and ADP concentrations on phosphoenzyme-dependent TNP-ATP fluorescence	78
3.4	Effects of alterations of distribution of the E-P intermediates on ATP-induced TNP-ATP fluorescence	83
3.4.1	Effects of NEM on partial reactions of the catalytic cycle	83
3.4.2	Effects of Oxalate	92
3.4.3	Effects of Strontium	97

3.5	Effects of modification of water activity on TNP-ATP fluorescence	103
3.6	Effects of monovalent cations on TNP-ATP fluorescence	109
3.7	Interaction of valinomycin with monovalent cation binding sites on the $\text{Ca}^{2+}$ -ATPase	114
4.0	<u>DISCUSSION</u>	123
4.1	TNP-ATP binding stoichiometry	123
4.2	TNP-ATP binding to the phosphorylated enzyme	125
4.3	Competition of ADP and ATP with TNP-ATP	126
4.4	TNP-ATP fluorescence and enzyme conformational change	127
4.5	The role of water during $\text{Ca}^{2+}$ pump activity	133
4.6	Interaction of $\text{K}^{+}$ and Valinomycin with the $\text{Ca}^{2+}$ -ATPase	137
4.7	Effects of valinomycin on monovalent cation binding	138
5.0	<u>CONCLUSION</u>	142
6.0	<u>BIBLIOGRAPHY</u>	

## 1.0 INTRODUCTION

### 1.1 THE $\text{Ca}^{2+}$ PUMP OF SARCOPLASMIC RETICULUM AS A PROTOTYPE FORENERGY TRANSDUCTION IN BIOLOGICAL MEMBRANES

Energy transduction is discussed in this section as an introduction to the role of associated ligand interactions with membrane-linked enzyme systems. Common to all membranous cation-pump types is either the redirection of chemical potential energy toward useful work as osmotic potential developed or the reverse of this process. Well characterized pumps fall into four groups (Tanford, 1983) :-

- a) ATP-driven pumps with phosphoryl enzyme intermediates, such as the  $\text{Ca}^{2+}$  pump of the sarcoplasmic reticulum, the  $\text{Na}^+/\text{K}^+$  pump of plasma membranes and the  $\text{H}^+$  pump of Ascomyces;
- b) Multisubunit ATP-linked proton transport systems without detectable phosphoryl enzyme intermediates such as the mitochondrial, bacterial and chloroplast  $\text{F}_0/\text{F}_1$  ATPases;
- c) Light-driven proton pumps, such as bacteriorhodopsin; and
- d) Obligatory exchange transport systems (antiports). Although these pumps vary considerably in molecular composition, stoichiometry, electrical and osmotic work, 10 to 14 kcal/mol energy is expended to solve identical functional problems (Tanford, 1983). Several authors have attempted a unified approach to various pump types on the basis that evolution conserves appropriate mechanisms for energy coupling (Hastings-Wilson and Maloney 1976).

The  $\text{Ca}^{2+}$ -ATPase of skeletal muscle sarcoplasmic reticulum, involved with the signaling ion  $\text{Ca}^{2+}$ , is a relatively well characterized and probably the most experimentally accessible coupled vectorial systems available (deMeis and Vianna, 1979). Efficiency of the pump is high, with tight coupling between scalar and vectorial events. Coupling has been described according to a set of rules that define pump operation in terms of switch mechanisms operated

by ligand binding (Jencks, 1980). Ligand binding energy also effects the rates of catalysis and dissipates energy over the whole catalytic cycle resulting in equivalent levels of most partial reaction intermediates. Tanford (1980) favours an alternate model in which the energy of hydrolysis of ATP is expended in a single step,  $E-P:2Ca^{2+}_{out}$  to  $E-P:2Ca^{2+}_{in}$ . Whereas these formulations are based on pump mechanisms that possess an integral stoichiometry, variable stoichiometry in the  $Ca^{2+}$ -ATPase has been recently described (For review, see Berman, 1982).

## 1.2 THE SARCOPLASMIC RETICULUM OF SKELETAL MUSCLE

The Sarcoplasmic reticulum membranes are the main constituents of muscle intracellular membranes, and consist of a transverse tubular network linked to the longitudinally oriented sarcoplasmic reticulum proper (Peachey, 1965). The transverse tubules are narrow invaginations of the plasma membrane that allow inward propagation of electrical excitation signals. The architecture of the system is closed to free communication of vesicular and intracellular fluids (Huxley, 1964; Somlyo *et al.*, 1977), but form an extended network of tubules that encompass the muscle fibrils.  $Ca^{2+}$  ions are maintained at various concentrations, being high in the extracellular, low in the intracellular, and high in the intravesicular domains (Porter, 1961).

The SR therefore acts as an amplifier of efferent electrical signals of neurosystem origin, resulting in the release of  $Ca^{2+}$  from the vesicular compartment to the myoplasm that activates the contractile proteins. The  $Ca^{2+}$ -ATPase plays a key role in the  $Ca^{2+}$  transport mechanism. Following their release,  $Ca^{2+}$  ions are rapidly removed from the myoplasm, (to levels  $< 0.1\mu M$ ), and restored to the SR lumen by the membrane bound  $Ca^{2+}$ -ATPase, for deactivation of the contractile proteins, and preparatory to

execution of the following cycle. Various reaction intermediates for the mechanism of energy transduction of the ATPase isolated from this system have been resolved (see section 1.2.4).

### 1.2.1 STRUCTURE AND COMPOSITION OF SARCOPLASMIC RETICULUM VESICLES

Homogenization of skeletal muscle cells fragments the SR membranes, which reseal to form vesicles with the external surface corresponding to the cytoplasmic surface of vesicles in vivo.  $\text{Ca}^{2+}$  ions are pumped across the membrane into the vesicle lumen (Ebashi and Lipmann, 1962).

The major proteins of SR are the  $\text{Ca}^{2+}$ -ATPase (Mr 105 000), two intrinsic glycoproteins (Mr 53 000 and 160 000), and Calsequestrin (Mr 63 000), constituting 80%, upto 20% and less than 5%, respectively (MacLennan, 1970; Michalak et al., 1980). Calsequestrin is involved in  $\text{Ca}^{2+}$  storage within the vesicle lumen (MacLennan and Wong, 1971). The 160 and 53 KDa glycoproteins have similar properties, both being transmembrane proteins largely exposed on the cytoplasmic surface of the SR (Campbell and MacLennan, 1981). Although they have been shown to bind the photo-affinity probe, 8-Azido-ATP, their function is largely unknown. Their origin is probably from lighter membranes such as the transverse tubular or sarcolemmal membranes (Campbell and MacLennan, 1983).

The SR membrane surrounding the ATPase is composed of a lipid bilayer, comprising 80% phospholipid and 20% neutral lipids (Tada et al., 1978). The phospholipid component consists mainly of phosphatidylcholine (ca. 70%), with phosphatidylethanolamine (15%) phosphatidylinositol (9%). The remainder includes phosphatidylserine, sphingomyelin and cardiolipin. Neutral lipids comprise largely of cholesterol (for review, see Bennet et al., 1980).

There is still uncertainty whether the  $\text{Ca}^{2+}$ -ATPase exists as a monomer or dimer within the SR membrane (For comprehensive reviews, see Ikemoto, 1982, and Moller et al., 1982). Protein-protein interactions have been widely studied and although there is evidence that the  $\text{Ca}^{2+}$ -ATPase can function as a monomer, there is an equal body of evidence indicating function of aggregated states (Napolitano et al., 1983).

The primary sequence and various functionally important amino acids have been recently elucidated by the laboratories of MacLennan and Green. More than half the protein is exposed to the outside of the SR membrane and there appears to be little protein mass on the interior surface (Dupont 1973, Fleisher et al., 1979; Herbette et al., 1977). Predictions from the primary structure, and also from N-ethylmaleimide (NEM) labelling, suggest that the protein consists of an intramembranous region, and three globular domains with a stalk section (Klip et al., 1980; MacLennan et al., 1985). The molecular weight calculated from complementary DNA clones, is 109763 Da (MacLennan et al., 1985).

Limited digestion with trypsin cleaves the protein into fragments A ( $M_r = 55\ 000$ ) and B ( $M_r = 54\ 000$ ). Further cleavage of the A subfragment yields A1 ( $M_r = 33\ 000$ ) and A2 ( $M_r = 22\ 000$ ). SDS gel electrophoresis shows that covalent  $^{32}\text{P}_i$  migrates with the A1 subfragment indicating that the phosphorylation site is on this component (Thorley-Lawson and Green 1973, 1977). FITC labelling shows that B contains the ATP binding site (Pick, 1981; Mitchinson et al., 1982). It has been suggested that A2 constitutes an energy transduction domain (MacLennan et al., 1985), since, according to dicyclohexylcarbodiimide (DCCD) studies, it binds  $\text{Ca}^{2+}$  (Pick and Racker, 1979), and confers  $\text{Ca}^{2+}$  conductivity on black lipid layers (Shamoo et al., 1976).

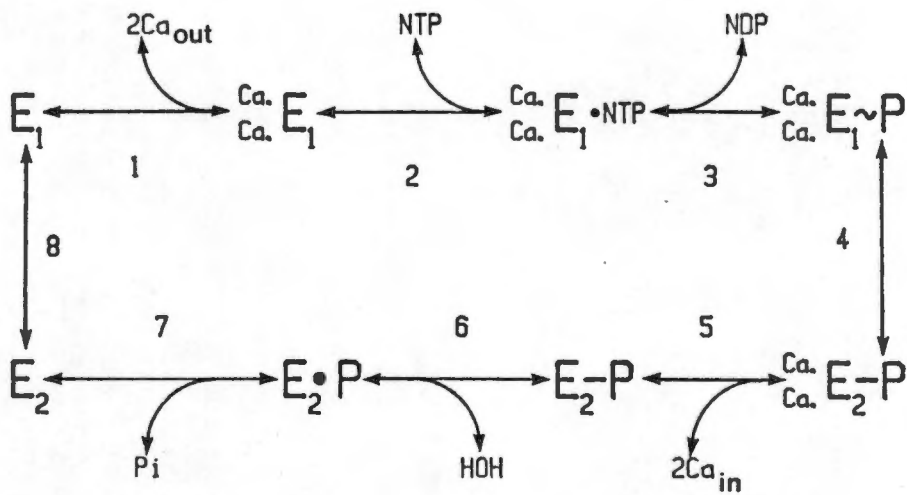
Of the 25 Cysteiny1 residues, 4-SH groups are reactive

to NEM, two being essential for  $\text{Ca}^{2+}$  transport. Two classes of functionally relevant -SH groups have been identified. SHd labelling inhibits phosphoenzyme decomposition, while SHf labelling inhibits phosphoenzyme formation (Kawakita et al., 1980). SHd labelling is dependent on the conformation induced by  $\text{Ca}^{2+}$  binding and has been located on the A1 subfragment (Saito et al., 1984).

### 1.2.2 THE CATALYTIC CYCLE OF THE $\text{Ca}^{2+}$ -ATPase

Isolated Sarcoplasmic reticulum vesicles of rabbit skeletal muscle sequester  $\text{Ca}^{2+}$  with high affinity (Ebashi, 1960; Ebashi and Lipman, 1962) at the expense of ATP hydrolysis (Hasselbach and Makinose, 1961; Makinose and Hasselbach, 1963). It was initially questioned whether  $\text{Ca}^{2+}$  uptake involved active transport or whether  $\text{Ca}^{2+}$  bound to sites on surfaces were sequestered during phosphorylation. The addition of anions, such as oxalate or phosphate, which can diffuse through the membrane and form  $\text{Ca}^{2+}$  precipitates of low solubility, increased the maximum uptake of  $\text{Ca}^{2+}$  (Hasselbach and Makinose, 1963; Martonosi and Feretos, 1964; Weber et al., 1966). Precipitation of  $\text{Ca}^{2+}$  was visible as electron opaque deposits in electron micrographs (Deamer and Baskin, 1969). In addition, the  $\text{Ca}^{2+}$  ionophores, X537A and A23187, promoted  $\text{Ca}^{2+}$  release from  $\text{Ca}^{2+}$  loaded vesicles confirming the hypothesis that  $\text{Ca}^{2+}$  ions were actively transported across the membrane (Scarpa et al., 1972).

Two  $\text{Ca}^{2+}$  ions are transported per ATP hydrolysed under optimal conditions. The process is reversable, and accumulated  $\text{Ca}^{2+}$  can generate ATP from ADP and Pi (for review see Inesi, 1985). However, under certain conditions the pump may be irreversibly uncoupled (For review, see Berman, 1982) and also exhibits variable stoichiometry with change in temperature, pH, and external  $[\text{Ca}^{2+}]$  (Meltzer and Berman, 1984).

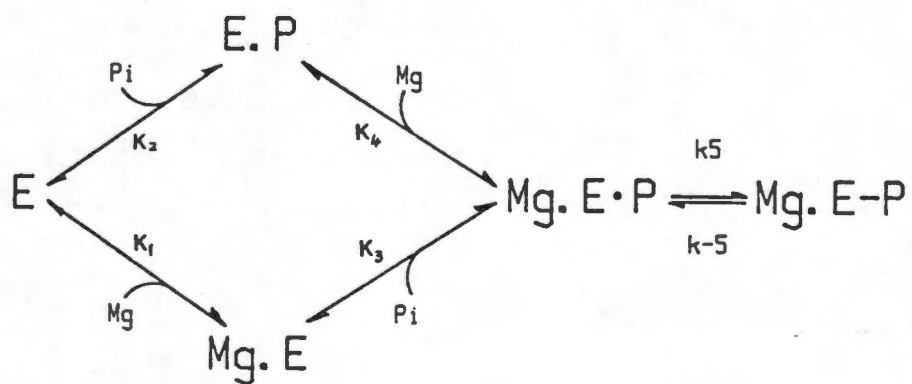


**Scheme I** The catalytic cycle of the Ca<sup>2+</sup>-ATPase, as proposed by deMeis and Vianna (1979)

a) The forward reaction

Steady state and rapid kinetic studies have established the following reaction sequence (see Scheme I), (deMeis and Vianna, 1979). Two  $\text{Ca}^{2+}$  ions interact cooperatively ( $nH = 1.8$ ), (Inesi, 1980) and with high affinity ( $K_m = 0.1$  to  $0.3 \mu\text{M}$ ), (step 1), with the enzyme (Yamamoto et al., 1979). Nucleotide triphosphate (step 2) binds and the  $\gamma$ -phosphate is transferred and covalently bound to an aspartyl residue that has the characteristics of an acyl phosphate (Degani and Boyer, 1973). The high energy phosphoenzyme intermediate formed,  $E_1\text{-P}$ , is associated with externally oriented, high affinity  $\text{Ca}^{2+}$  binding sites. There is a marked decrease in affinity ( $0.6 - 1 \text{ mM}$  at  $\text{pH } 7.0$ ) of the  $\text{Ca}^{2+}$  binding sites for  $\text{Ca}^{2+}$  and an associated change in site orientation, with the formation of the low energy phosphoenzyme,  $E_2\text{-P}$  (step 4), (Ikemoto 1975; Carvalho et al., 1976). Dephosphorylation (step 6 and 7) of the enzyme occurs only after  $\text{Ca}^{2+}$  is released to the inside of the vesicle (step 5), (Makinose, 1973; Ikemoto, 1975, 1976; Kurzmack et al., 1977; Sumida et al., 1974). The nucleotide diphosphate (step 3) and  $\text{P}_i$  (step 7) are released to the cytoplasmic side of the membrane (Knowles and Racker, 1975). The cycle is completed by a relatively slow isomerization of  $E_2$  to  $E_1$  (step 8), (Masuda and deMeis, 1973; Kanazawa and Boyer, 1973; Guillain et al., 1980).

The  $\text{Ca}^{2+}$  transport ATPase hydrolyses a wide range of phosphate compounds coupled to  $\text{Ca}^{2+}$  transport in addition to ATP. These include ITP, GTP, CTP (Makinose and The, 1965; deMeis and deMello, 1973), p-nitrophenyl phosphate (Inesi, 1971), and acetyl phosphate (Pucell and Martonosi, 1971). Even the the ATP analogue adenylyl-5'-imido diphosphate (AMP-PNP) is cleaved at a slow rate (Taylor, 1981).



**Scheme II** Proposed reaction pathways for phosphorylation of the  $\text{Ca}^{2+}$ -ATPase by  $\text{P}_i$  (Punzengruber et al., 1978)

b) Reversibility of the  $\text{Ca}^{2+}$  pump.

The osmotic potential energy of  $\text{Ca}^{2+}$  accumulation, against a concentration gradient, can be transduced into chemical energy by direct reversal of the pump. Barlogie et al., (1971), first showed that passive  $\text{Ca}^{2+}$  release from  $\text{Ca}^{2+}$ -filled vesicles is accelerated 10 to 50 -fold by the addition of ADP and Pi. Simultaneously, ATP is generated by  $\text{Ca}^{2+}$  efflux with a stoichiometry of  $\text{Ca}^{2+} : \text{ATP}$  of 2:1, similar to that of the forward reaction (Makinose and Hasselbach, 1965). Both  $\text{Ca}^{2+}$  release and phosphorylation from Pi are half maximally inhibited by medium  $[\text{Ca}^{2+}] = 1 \mu\text{M}$ , indicating that at this concentration range  $\text{Ca}^{2+}$  bind to sites on the enzyme and do not modify the  $\text{Ca}^{2+}$  gradient (Masuda and deMeis 1973; deMeis and Masuda, 1974). During  $\text{Ca}^{2+}$  release the enzyme is phosphorylated by Pi from the outside medium only, and the reaction is inhibited by ATP, suggesting involvement of the same catalytic site (Makinose 1971; Yamada et al., 1972). There is an absolute requirement for magnesium in the phosphorylation of the enzyme from Pi. No phosphoenzyme is formed in the absence of  $\text{Mg}^{2+}$ , regardless of the size of the transmembrane gradient (Makinose, 1973; Yamada et al., 1972).

The free energy values, calculated for the  $\text{Ca}^{2+}$  gradient are compatible with those for synthesis of ATP in its hydrated form (Makinose 1973; Makinose and Hasselbach, 1971). The conditions for (ADP plus Pi)-induced  $\text{Ca}^{2+}$  release however, are unlikely to occur in vivo, because inorganic phosphate levels in the resting muscle are below 10  $\mu\text{M}$ , which is insufficient to activate  $\text{Ca}^{2+}$  release.

The phenomenon of pump reversibility has provided much information about the mechanism of energy transduction, especially after the discovery that osmotic energy is not required for phosphorylation of the enzyme by Pi (Kanazawa and Boyer 1973). The phosphoenzyme formed in the absence of

a  $\text{Ca}^{2+}$  gradient cannot transfer its phosphate to ADP. The addition of  $\text{Ca}^{2+}$  to leaky vesicles, phosphorylated from Pi, will synthesize ATP in a single cycle only (Knowles and Racker 1975). There have been numerous studies on enzyme phosphorylation from Pi at equilibrium. The reaction is inhibited by decreased temperature (Masuda and Demeis 1977, Martin and Tanford 1981), alkaline pH, (optimal pH = 6.0), (Masuda and deMeis, 1976; deMeis et al., 1980; Beil et al., 1977), millimolar [KCl] (Punzengruber et al., 1978; Chaloub and deMeis 1980) and by millimolar [ATP] (McIntosh and Boyer 1983).

Punzengruber et al.(1978) formulated a probable mechanism, derived from the stoichiometry of the phosphoryl enzyme, as a function of free phosphate and  $\text{Mg}^{2+}$  (Scheme II). The rates of binding of Pi ( $K_2, K_3$ ) and  $\text{Mg}^{2+}$  ( $K_1, K_4$ ) are fast compared to the rate of formation of phosphoenzyme,  $k_5$  (Chaloub and deMeis, 1980). On this basis, it would appear that the most straightforward method of determining the phosphorylation stoichiometry was to derive  $k_5$  and  $k_{-5}$  from measurement of the "on" and "off" rate constants of the phosphorylation and dephosphorylation reaction (Inesi, 1982). However, determination of the time dependence of  $\text{Mg}^{2+}$ .E-P species formation by simulation, using a wide range of rate constants, indicate that this method is not sufficient to obtain a kinetic model leading to the stoichiometry of the Pi phosphorylation by SR vesicles (Guillain et al., 1984).

Medium Pi- $^{18}\text{O}$  Oxygen exchange is a potentially powerful tool for determining rate constants for the E.Pi to E-P equilibrium (Guillain et al., 1984; McIntosh and Boyer, 1983). Phosphorylation of the enzyme by  $\text{P}^{18}\text{O}_4$  in a medium containing  $\text{H}_2^{16}\text{O}$ , allows direct observation of oxygen exchange between water and oxygens bound to Pi. The "on" rate of substrate binding is found to be slow compared to its "off" rate, whereas the establishment of the covalent bond from the bound substrate, is a favourable process ( $k_5 > k_{-5}$ ),

showing that the enzyme is almost entirely phosphorylable (Guillain et al., 1984). The stoichiometry in this study was similar to that of ATP binding (5.5 and 6.0 nmol/mg, respectively).

KCl accelerates the hydrolysis of E-P ( $k_{-5}$ , Scheme II), (Chaloub and deMeis 1980; Guillain et al., 1984). Alkaline pH also decreases the stoichiometry of E for Pi. Initially it was proposed that this effect came about from changes in substrate and enzyme ionization (Inesi et al., 1980). Dissociation of  $H^+$  from carboxyl groups at the binding site at low pH favours  $H^+$  removal from  $H_2O$ . Nucleophilic attack by  $HO^-$  on phosphorus promotes cleavage of Pi from its bound carboxyl (Inesi et al., 1984). However, recent studies have shown that an alteration in  $Mg^{2+}$  sensitivity at alkaline pH favours the formation of an E. $Mg^{2+}$  dead-end complex (Loomis et al., 1982) that drives the enzyme away from a form that can react with Pi (Martin and Tanford, 1981; Loomis et al., 1982; Guillain et al., 1984). A similar effect of  $Mg^{2+}$  on the prevention of  $Ca^{2+}$  binding to the  $E_2$  form has been demonstrated (Guillain et al., 1982; Champeil et al., 1983).

Water structure plays an important role in phosphoenzyme hydrolysis. Although water is required in the hydrolysis of the acyl-phosphate covalent bond to non-covalently bound phosphate (deMeis et al., 1980; deMeis and Vianna, 1979), catalytic site water is unaltered by organic cosolvents. Energy of hydrolysis of phosphate compounds depends on the different solvation energies of reactants and products (deMeis et al., 1985). Alteration of the hydrophobicity of the bulk medium favours partitioning of Pi from solution to the catalytic site, and promotes acyl-phosphate formation in the reverse cycle (deMeis et al., 1980). Water structure within the binding domain therefore appears to be unaltered by the effects of structure altering factors in the bulk medium.

c) Occluded  $\text{Ca}^{2+}$  and ADP sensitivity.

Transient occlusion of divalent cations by the  $\text{Ca}^{2+}$ -ATPase, occurring during transport, may provide further understanding of energy transduction mechanisms. The initial rapid phase of  $\text{Ca}^{2+}$  disappearance upon phosphorylation is followed by a slower steady-state phase where further  $\text{Ca}^{2+}$  uptake occurs with Pi production. It had initially been suggested that  $\text{Ca}^{2+}$  ions, bound to an external site, were transported simultaneously with phosphoenzyme formation (Yamada and Tonomura, 1972; Tada et al., 1978). However, a phosphoenzyme species with high affinity  $\text{Ca}^{2+}$  sites exposed to the external medium has recently been demonstrated (Takakuwa and Kanazawa, 1981). The sites have comparable affinity to the  $\text{Ca}^{2+}$  sites in the nonphosphorylated enzyme. Several authors have shown that two  $\text{Ca}^{2+}$  ions are occluded immediately upon phosphorylation (Chiesi and Inesi, 1979; Sumida et al., 1978; Dupont 1980; Fassold et al., 1981), and that most of the occluded  $\text{Ca}^{2+}$  that remains after EGTA treatment is rapidly released to the medium on the addition of ADP (Takisawa and Makinose, 1983). Occluded  $\text{Ca}^{2+}$  has been shown to have decreased contact with solvent  $\text{H}_2\text{O}$ , consistent with its dehydration for high affinity binding (Klemens et al., 1986).

Various methods have been used to resolve the kinetics of the initial events associated with  $\text{Ca}^{2+}$  translocation. Phosphoenzyme intermediates have been differentiated into two types on the basis of their ADP sensitivity. These studies are performed by the addition of EGTA (Sumida and Tonomura, 1974), and ADP (Kurzmack 1977; Ikemoto, 1981) to the phosphoenzyme, followed by rapid filtration (Dupont 1980) or by optical monitoring with a  $\text{Ca}^{2+}$ -sensitive dye (Takisawa and Makinose, 1981; Pierce 1983). Further  $\text{Ca}^{2+}$ -dependent phosphorylation is prevented by EGTA while ADP binds to 'ADP-sensitive EP' and forms ATP. The phosphoenzyme that does not

bind ADP productively continues in the forward cycle, releasing  $\text{Ca}^{2+}$  to the lumen of the vesicle and liberating Pi. Phosphoenzyme decay is therefore biphasic, and the process of ATP generation is rapid, while that of Pi release is slow (Shigekawa and Dougherty, 1978; Shigekawa and Akowitz, 1979).

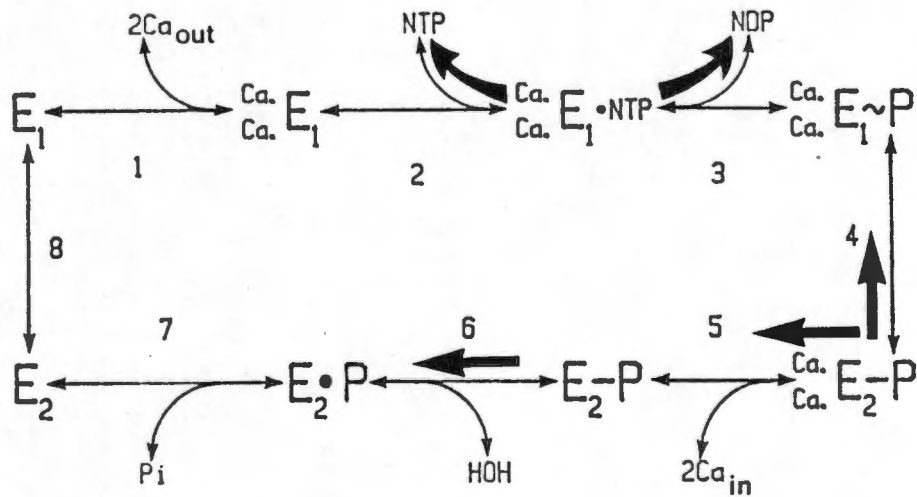
The relationship between the ADP-insensitive phosphoenzyme or  $\text{E}_2\text{-P}$  of Scheme I and occluded  $\text{Ca}^{2+}$ , is not well defined. Froehlich and Heller (1985) have shown that  $\text{E}_2\text{-P}$  formation from ATP is rapid ( $k_{\text{obs}} = 500 \text{ sec}^{-1}$ ), whereas  $\text{Ca}^{2+}$  release to the lumen of vesicle is delayed with respect to  $\text{E}_2\text{-P}$  formation. They suggest that  $\text{Ca}^{2+}$  is still occluded after phosphoenzyme isomerization, and that the energy transducing step associated with the phosphoenzyme may run to completion before the two  $\text{Ca}^{2+}$  ions become accessible to the vesicle lumen.

Whereas initial findings suggested that formation of the ADP-sensitive E-P intermediate is not usually associated with Pi release (Glynn and Karlsh, 1975 ;Tada et al.,1978), a subsequent study by Hobbs et al.(1985) has shown that ADP accelerates phosphoenzyme decomposition, and that a rapid release of Pi occurs simultaneously to the rapid phase of decrease in EP levels. These authors concluded that the measurement of 'ADP-sensitive EP' may over-estimate  $\text{E}_1\text{-P}$  at  $25^\circ$ .

### 1.2.3 THE INFLUENCE OF LIGANDS ON THE CATALYTIC CYCLE

#### a) The effect of monovalent cations

Early studies on the effects of  $\text{K}^+$  and monovalent cations on the catalytic cycle of the  $\text{Ca}^{2+}$ -ATPase were contradictory. Potassium ions were shown to stimulate, inhibit or have no effect (for review see Duggan, 1977). Varying amounts of mitochondrial fragment contamination, which showed decreased activity in the presence of  $\text{K}^+$ , and



**Scheme III** Effects of KCl on the catalytic cycle of Ca<sup>2+</sup>-ATPase. Thick arrows indicate the partial reactions accelerated by K<sup>+</sup>.

also the use of salt containing nucleotides and salt requiring co-enzyme systems appeared to be the main reasons for these conflicting reports. Monovalent cations stimulate ATPase activity in the series  $K^+ > Na^+ = Rb^+ > Cs^+ > Li^+$ , under conditions of equal ionic strength (Duggan, 1976).  $K^+$  and  $Na^+$  do not act synergistically. Unlike the  $(Na^+, K^+)ATPase$ , the  $Ca^{2+}$  uptake and ATPase activity are insensitive to Oaobain.

The mechanism of action of monovalent cations, accelerating uptake and concomitant ATPase, operates through a 3- to 4- fold increase in the rate limiting step of the cycle (see Scheme III) that accelerates phosphoenzyme decomposition (step 6 & 7, Scheme III) under conditions of low [ATP], (Shigekawa and Pearl, 1976). Phosphoenzyme levels from Pi are decreased in the presence of  $K^+$  (Chaloub and deMeis, 1980).  $K^+$  accelerates the rate constant for phosphoenzyme hydrolysis 6-fold at pH 6.5 (step 6, Scheme III) (Guillain et al., 1984) but has no effect on the steady state levels of E-P from ATP (Shigekawa and Akowitz, 1979).

The relative levels of phosphoenzyme intermediates are altered by  $K^+$ . Low  $Mg^{2+}$  and high  $Ca^{2+}$  concentrations favour accumulation of the ADP-sensitive intermediate in the presence of  $K^+$  (Shigekawa et al., 1978). Although the rate of conversion of  $E_1-P$  to  $E_2-P$  is inhibited by  $K^+$ , the acceleration of phosphoenzyme decomposition has the net effect of accelerating turnover 1.8 to 2-fold, (Shigekawa and Pearl, 1976).

It has recently been reported that  $K^+$  effects an earlier step in the reaction cycle.  $K^+$  decreases the forward reaction for the formation of E.ATP precursor complex (step 2, Scheme III), but also increases E.ATP to  $E_1-P$  conversion as well as accelerating the "off" rate of ADP 11-fold (step 3, Scheme III), with  $[K^+]_{0.5} = 52$  mM, (Shigekawa et al., 1982). Since the initial reaction of E.ATP formation is very much slower than the latter two reactions, the net effect is

to decrease the lifetime of the E.ATP precursor complex. Acceleration of the ADP "off" rate is more responsive to the anions of  $K^+$  salts and it is therefore presumed to be a chaotropic anion effect (Shigekawa et al., 1982). The affinity of the enzyme for TNB-ATP, an ATP analogue, is decreased 5fold by  $K^+$  with  $([K^+]_{0.5} = 50 \text{ mM})$  (see introductory section 1.4).

A parallel pathway for E-P decomposition has been proposed for the  $Na^+/K^+$  ATPase (Fukushima and Tonomura, 1975) and for the  $Ca^{2+}$  ATPase (Nakamura and Tonomura, 1978).  $P_i$  can be liberated directly from both the ADP-sensitive and insensitive phosphoenzymes during p-nitrophenylphosphate hydrolysis. However, these results could not be reproduced under ATP-dependent turnover (Shigekawa and Akowitz, 1979).

#### b) The role of $Mg^{2+}$

$Mg^{2+}$  appears to play complex roles in the function of the  $Ca^{2+}$ ATPase. The  $Mg$ ATP complex has been considered to be the physiological substrate for the  $Ca^{2+}$ -ATPase (Weber et al., 1966; Yamamoto et al., 1979; deMeis and Vianna, 1979; Makinose and Boll, 1979), whereas Yamada and Ikemoto (1980) have demonstrated that the complex of  $Ca^{2+}$  with ATP serves as a substrate for enzyme phosphorylation. The  $Mg^{2+}$  ion from the  $Mg$ ATP complex is occluded during phosphorylation and released from the cycle after phosphoenzyme decomposition (Garrahan et al., 1976).

$Mg^{2+}$  has been implicated in acceleration of the hydrolysis of the E-P intermediate (step 6, Scheme III) (Martinosi, 1969; Inesi et al., 1970; Panet et al., 1971; Kanazawa et al., 1971; Garrahan et al., 1976).  $Mg^{2+}$  was also shown to accelerate the conversion of ADP-sensitive to insensitive phosphoenzymes (Shigekawa and Dougherty, 1978; Shigekawa et al., 1984). Phosphorylation of the ATPase by  $P_i$  was also shown to be  $Mg^{2+}$ -dependent (Kanazawa and Boyer,

1973; Masuda and deMeis, 1973). These actions of  $Mg^{2+}$  can be antagonized by  $Ca^{2+}$ . High  $Ca^{2+}$  concentrations ( $>250 \mu M$ ) inhibit phosphoenzyme hydrolysis (Martonosi, 1969; Inesi et al., 1970; Panet et al., 1971). Low pH favours the formation of an  $E_2-Mg^{2+}$  complex that inhibits  $Ca^{2+}$  binding (Loomis et al., 1982; Guillain et al., 1984) and also inhibits phosphorylation from Pi (Guillain et al., 1982).

The apparently different functions of  $Mg^{2+}$  described above may arise from  $Mg^{2+}$  binding to more than one  $Mg^{2+}$  binding site. Makinose and Boll (1979) and Takakuwa and Kanasawa (1982) have shown that the ATPase has a  $Mg^{2+}$  site involved in direct activation of the enzyme, but is distinct from the substrate site for MgATP.  $Mg^{2+}$  is required to bind on the outer surface of the  $Ca^{2+}$ -ATPase, prior to  $Ca^{2+}$  release from the low affinity inward-oriented sites. There is no direct evidence implicating  $Mg^{2+}$  as a counter-ion in  $Ca^{2+}$  transport (Nagasaki and Kasai, 1980; Chiesi and Inesi, 1980).

### c) The interaction of Strontium

Strontium can substitute for  $Ca^{2+}$  as the ion engaged in vectorial transfer by the  $Ca^{2+}$ ATPase (Mermier and Hasselbach, 1976). Accumulation of  $Sr^{2+}$ , in the absence of precipitating anions, such as Pi or oxalate, is greater and faster than that of  $Ca^{2+}$ . The hydrolysis of ATP is higher during  $Sr^{2+}$  uptake, with a stoichiometry of ATP :  $Sr^{2+}$  of 1:1 (Mermier and Hasselbach, 1976). The high  $Sr^{2+}$  gradient formed at the expense of ATP hydrolysis is attributed to the inability of the enzyme to generate ATP from  $Sr^{2+}$  release, since  $Ca^{2+}$  efflux is inhibited in vesicles loaded with both  $Sr^{2+}$  and  $Ca^{2+}$  (Guimartes-Motta et al., 1984).

Strontium competes with  $Ca^{2+}$  for the low affinity  $Ca^{2+}$  binding sites oriented toward the lumen of the vesicle, and also competes for  $Mg^{2+}$  binding sites (Guimares-motta et

al.,1984). However,  $\text{Sr}^{2+}$  is not a functional substitute for  $\text{Mg}^{2+}$  (MacLennan, 1970). Strontium competes for the high affinity  $\text{Mg}^{2+}$  site for E-P formation from ATP and accelerates phosphoenzyme hydrolysis at high concentrations at a rate similar to that produced by the removal of  $\text{Mg}^{2+}$  by EDTA. The net effect of  $\text{Sr}^{2+}$  substitution in these three modes of action is the accumulation of  $\text{E}_2\text{-P}$  under steady-state turnover conditions (Guimares-motta et al., 1984). The use of  $\text{Sr}^{2+}$  in the present study is to observe its effects on phosphoenzyme redistribution to the  $\text{E}_2\text{-P}$  conformation, in the absence of  $\text{Sr}^{2+}$  competition for  $\text{Mg}^{2+}$ .

#### 1.2.4 CATALYTIC REQUIREMENTS FOR ENERGY COUPLING

Several authors have reported conformational changes in the  $\text{Ca}^{2+}$  ATPase during various parts of the cycle. Binding of NTP, or  $\text{Ca}^{2+}$ , modifies the electron spin resonance spectrum of vesicles labelled with iodoacetamide spin label (Coan and Inesi, 1977; Coan et al., 1979; Champeil et al., 1978; Laggner et al., 1981). Fluorescence from intrinsic tryptophans in the  $\text{Ca}^{2+}$ -ATPase changes upon binding of  $\text{Ca}^{2+}$  (Dupont, 1976, 1978; Dupont and Liegh, 1978; Dupont and leMaire, 1980), and upon phosphorylation, and is kinetically related to rates of phosphorylation (Guillain et al., 1980). In addition, the reactivity of sulphhydryls is sensitive to the conformational state of the enzyme (for review, see Ikemoto, 1982). The rate of labelling is accelerated by the presence of  $\text{Ca}^{2+}$  at concentrations stoichiometric to the  $\text{Ca}^{2+}$  site (Murphy, 1976). Similarly, nucleotide binding decelerates sulphhydryl reactivity (Thorley-Lawson and Green, 1977; Andersen and Moller, 1977). The reactivity of the  $\text{Ca}^{2+}$  ATPase to tryptic cleavage, is also sensitive to conformational states related to  $\text{Ca}^{2+}$ , nucleotide (Saito et al., 1984) and  $\text{K}^+$  binding (Nowak 1976). However, direct evidence for a conformational change associated with  $\text{Ca}^{2+}$

translocation across the membrane is lacking (deMeis and Vianna, 1979), although  $\text{Ca}^{2+}$  binding sites undergo a marked decrease in affinity for  $\text{Ca}^{2+}$  following phosphorylation (Ikemoto 1976).

The  $\text{Ca}^{2+}$ -ATPase of skeletal muscle sarcoplasmic reticulum, involved with the signaling ion  $\text{Ca}^{2+}$ , is a relatively well characterized and probably the most experimentally accessible coupled vectorial systems available (deMeis and Vianna, 1979). The requirement for osmotic energy storage is the realization of barriers, that prevent dissipation of catalysed energy fluxes.

Jencks has proposed certain rules for coupled vectorial systems that prevent one process, such as ATP hydrolysis from taking place without the other, such as work. The rules are formally independent of the thermodynamics of ligand binding, but are related to the affinity and mechanism of ligand binding (Jencks 1980, 1983).

The basic requirements for coupling are that there should be no hydrolysis of ATP without  $\text{Ca}^{2+}$  transport, and no leak of  $\text{Ca}^{2+}$  from the vesicle without ATP synthesis (Pickard and Jencks, 1984). The rules are :- a) ATP binds to the enzyme but is not catalysed to ADP and Pi (see Scheme I). This is defined as the  $E_1$  conformation and the site reacting to  $\text{Ca}^{2+}$  is exposed to the outer (cytoplasmic) side of the vesicle. b) The enzyme interconverts the sites for outside-exposed  $\text{Ca}^{2+}$  to inside-exposed  $\text{Ca}^{2+}$  only when phosphorylated. c) The conformation  $E_2$  catalyses the reaction with water and phosphate but cannot react with ATP. This prevents ATP hydrolysis occurring when the  $\text{Ca}^{2+}$  site is facing the inside of the vesicle. d) The enzyme interconverts the inside and outside exposed  $\text{Ca}^{2+}$  sites only when the site does not contain  $\text{Ca}^{2+}$ . This is the  $E_2$  to  $E_1$  transition and prevents  $\text{Ca}^{2+}$  efflux.

A matrix of four states is therefore possible. Certain reactions are confined to specific states of the enzyme.

Jencks, (1980) states that  $\text{Ca}^{2+}$  acts as a 'scalar' switch that tells the the enzyme whether to react with ATP or Pi, while covalently bound phosphate acts as a 'vectorial' switch that selects an external or internal  $\text{Ca}^{2+}$  reaction. The critical properties of a coupled system depend on correct behavior of all these rules, while changes in affinity of the ligands at optimal stages in the process will only accelerate the whole process. Isolated affinity changes in an uncoupled system will not perform work.

Catalysts involved in scalar/vectorial interconversions differ in their mechanisms from catalysts of ordinary chemical reactions. In the latter, interacting substrates undergo chemical transformations where matter is exchanged, requiring close physical proximity of interacting species. The rate of the reaction, which in principle occurs spontaneously, albeit slowly, is accelerated. Transport proteins do not require proximity of interacting species for free energy coupling, but are more likely to be involved in protein mediated-linkages operating at some distance (Tanford, 1983). Jencks (1980) has described the rate acceleration brought about by enzymes in terms of the binding energy of non reacting groups, to the enzyme in its transition state. For this binding energy to have a large effect on the rate, it is essential that it be manifest only in the transition state and not in the enzyme-substrate complex. This is necessary to prevent the formation of a tightly bound enzyme-substrate complex that will react and dissociate slowly. Mechanisms are utilized to prevent realization of the binding energy prior to transition state events.

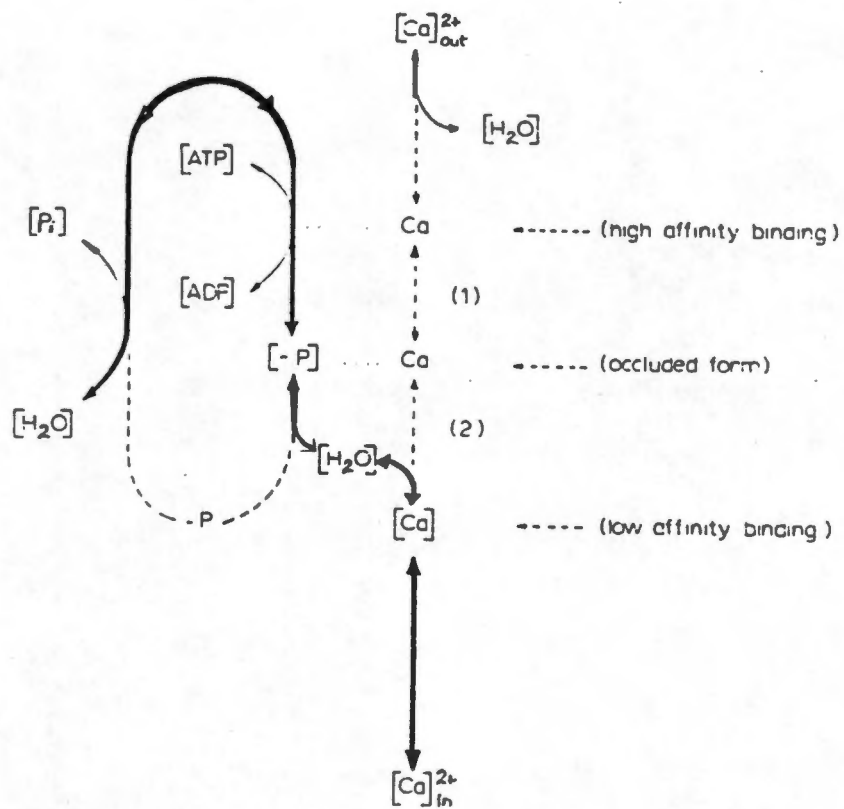
During the last decade the concept of the high energy compounds has been revised. It was originally thought that both the opposing resonance and electrostatic repulsion within the molecule were the main contribution to the large negative free energies of hydrolysis of ATP and other high

energy compounds (Hill and Morales, 1951). Subsequent analysis of the thermodynamics of hydrolysis of different forms of high energy molecules concluded that the effects of opposing resonance and electrostatic repulsion were of secondary importance. George et al.(1970) suggested that the differences in solvation energies of reactants and products were the predominant free energy contributors to the large negative free energies of hydrolysis of these compounds.

The destabilization and entropy losses that increase reaction rates and allow coupled vectorial systems to transform chemical into other forms of energy, are apparent as large changes in substrate specificities in different conformations of the enzyme.

There exist a number of energy transducing models of the  $\text{Ca}^{2+}$ -ATPase. This study selects a few, especially those incorporating water in catalysis. Singer has proposed a mobile pore mechanism in which a rocking motion of polypeptide chains acts to reorientate charges that constitute binding sites as well as to change the affinity of this site for the ligand. Tanford (1983) has developed this concept further described as the alternating access model (For review, see Tanford, 1983). Since antibodies specific for the  $\text{Ca}^{2+}$ -ATPase of rabbit skeletal muscle have failed to inhibit ATPase activity (Martonosi and Fortier, 1974; Sumida and Sasaki, 1975; Dutton et al., 1976), large conformational changes, such as rotation of large domains, have been shown unlikely. A rotary mechanism fulfills orientational aspects but cannot explain affinity changes and also appears thermodynamically unfavourable.

Wiggins (1982) has proposed a mechanism for vectorial ion transfer based on the organization of water structure within the ion channel spanning the lipid bilayer. Water structure is determined by the geometry of proton donor and acceptor groups on the protein channel surface to achieve ice-like water structures that excluded  $\text{Ca}^{2+}$  ions in the



**Scheme IV** Water pump hypothesis for the  $\text{Ca}^{2+}$ -ATPase as proposed by Dupont (1983). Transfer of water molecules from the catalytic site to  $\text{Ca}^{2+}$  ions is represented by darker line.

forward pumping mode and prevent reverse flux.

Phosphorylation of the enzyme requires minor conformational change in the peptide for alteration of water structures.

Alternatively, Dupont (1983) proposed that the  $\text{Ca}^{2+}$ -ATPase operates primarily as a water pump. Water molecules are excluded from the catalytic site following phosphorylation, and rehydrate two  $\text{Ca}^{2+}$  ions bound with high affinity at the  $\text{Ca}^{2+}$  site (Scheme IV). In effect this decreases the site affinity for  $\text{Ca}^{2+}$  ions as well as prevents their reverse flux.

Low and Somero (1975) have proposed a group transfer hydration model of enzyme action that may perform an energy storage reservoir in any of the above models. The model involves the hydration properties of amino acid side groups into or out of the protein interior during partial reactions of the catalytic cycle. The energy requirements depend on size and relative hydrophobicity of these side chains in relation to the energy required to disturb the structure of water.

#### 1.2.5 CHARACTERISTICS AND ROLE OF THE REGULATOR NUCLEOTIDE BINDING SITES

The  $\text{Ca}^{2+}$ -ATPase activity of the sarcoplasmic reticulum is modulated by ATP in a complex manner. ATP stimulation occurs over two ranges. ATP concentration dependence of the initial enzyme phosphorylation is limited to the micromolar range (Kanazawa et al., 1971; Froelich and Taylor, 1976; Verjovski-Almeida and Inesi, 1979; Scofano et al., 1979), but the hydrolytic cleavage of the phosphoenzyme formed in the initial part of the reaction is activated by high ATP concentrations (deMeis and deMello, 1973; Froehlich and Taylor, 1975; deSouza and deMeis, 1976) resulting in enhanced catalysis in the millimolar ATP range. The observed ATP dependence cannot be fitted according to simple Michaelis-

Menten kinetics. It has been established that the effect of ATP activation is related to acceleration of partial reactions of the catalytic cycle. Pang and Briggs (1977) and Dupont (1977) have detected nucleotide binding sites on the  $\text{Ca}^{2+}$ -ATPase in the  $10^{-5}$  M range and have postulated the existence of low affinity sites. The regulatory effects of ATP in this range have been evidenced by the fact that nonhydrolysable ATP analogues, such as AMP-CPP (Dupont, 1977) and AMP-PCP (Taylor and Hatton, 1979), activate ATPase activity.

Various partial reactions that are modulated by ATP have been implicated in the regulatory role of ATP: these are the activation of the  $E_2$  to  $E_1$  transition (Froehlich and Taylor, 1975; Scofano et al., 1979), activation of the rate of conversion of the ADP-sensitive and insensitive phosphoenzyme intermediates, and the acceleration of phosphoenzyme hydrolysis and liberation of  $\text{P}_i$  (Yamamoto and Tonomura, 1967; Froehlich and Taylor, 1975; McIntosh and Boyer, 1983).

Two possibilities exist for the nature of the effector site involved. The  $\text{Ca}^{2+}$ -ATPase may possess discrete regulatory sites separate from the catalytic site operating through an allosteric interaction (Dupont, 1977; Verjovski-Almeida et al., 1979), or the catalytic site may be able to bind a second ATP molecule after phosphorylation and ADP liberation (McIntosh and Boyer, 1983; Cable et al., 1985). A partial monomeric preparation in TX-100 has been shown to possess regulatory sites, eliminating the possibility of a dimeric interaction of regulatory and catalytic sites on separate polypeptide chains (McIntosh and Boyer, 1983; Taylor and Hattan, 1979; Moller et al., 1980). In support of these findings, the linear dependence of FITC inhibition of the ATPase is not in favour of a site-site effector model (Cable et al., 1985). However, a recent study proposes that an allosteric regulatory site exists on the basis of the lack of

competition by ADP for ATP bound to the E<sub>2</sub>-P conformation, assuming that all E-P intermediates are formed prior to Ca<sup>2+</sup> transport (Coll and Murphy, 1985).

The stoichiometry of one mol/mol for ATP or AMP-PCP binding on the phosphoenzyme eliminated the possibility of two sites simultaneously existing on a single polypeptide chain (Cable et al., 1985). These authors have concluded that a single site on the ATPase chain is able to produce the effects of acceleration observed. A similar conclusion was reached in studies on the Na<sup>+</sup>/K<sup>+</sup> ATPase using the ATP analogue TNP-ATP. In this case, the non-Michaelian ATP concentration dependence is entirely explained by one single ATP site on the ATPase (Moczydlowski and Fortes, 1982).

### 1.3 ASPECTS OF WATER STRUCTURE RELEVANT TO PROTEIN FUNCTION

#### a) The structure of water and protein hydration

The stability of biomembrane systems is largely dependent on their hydrophobic and hydrophilic interactions with the ambient solvent. The constraints imposed by water structure are diverse and have formed the basis of many studies. Interpretation of data is often complicated by the problems of a multicomponent system, in which many types of water interaction exist. There is no widely accepted theory for the structure of water. The central difficulty appears to be that while the interactions between water molecules are sufficiently strong to couple a large number of motions, they are not sufficiently strong to permit "solid state models", (Cooke and Kuntz, 1974). Scatchard, (1949) advised that "the best advice which comes from years of study of liquid structures, is to use any model insofar as it helps, but not to believe that any moderately simple model corresponds very closely to any real mixture".

In recent studies, general patterns based on high resolution NMR techniques, partial molar entropies, viscosity B coefficients, calorimetric studies and vapor pressure studies, have emerged. Cooke and Kuntz (1974) suggested the following brief characterization of three water systems, involved in the solvation of macromolecules:-

Type I "Bulk water", whose properties are independent of solvated macromolecules;

Type II " Bound water" associated with surface or solvent accessible surface of macromolecules;

Type III "Irrotationally bound water" molecules, essentially site bound to the macromolecules, have no solvent properties.

Type I "bulk water" has a transient structure similar to ice I. Each water molecule is in an approximate tetrahedral arrangement for short periods ( $10^{-10}$  to  $10^{-11}$  sec) with four neighbours, forming quasicrystalline structures (Norton and Levy, 1969). There is some short range disorder, such that each water molecule has a slightly higher number of near neighbours (ca 4.4) and somewhat fewer hydrogen bonds (90% of possible) in water near  $0^{\circ}\text{C}$ , as compared to ice at the same temperature. The non-random arrangement of 2 to 3 water molecules, forming 'flickering clusters', as initially described by Frank and Wen (1957) involve 21 to 91 water molecules (at  $100$  to  $0^{\circ}\text{C}$ , respectively) in any direction and exist with a half-life of  $10^{-11}$  sec (Nemethy and Sheraga, 1962). Alternatively, small aggregates, as well as extended or isolated chains with a random network of hydrogen bonds, have been postulated to form pentagonal or hexagonal rings (Bernal, 1964). Water is unique in that simpler liquids do not exhibit such local ordering. The dynamic state is a result of local energy fluctuations, tending towards a state of equilibrium, in which free energy will be a minimum. The strongly electronegative oxygen will form as many hydrogen bonds as is possible, without bending unduly from the H-O-H

bond angle of  $104.5^\circ$  to that required for a tetrahedron,  $109.5^\circ$ .

The extent of water structure has been studied in relation to the effects of hydrophobic interfaces, showing transient structures ranging up to  $10^4$  Å (Drost-hansen, 1973). Molecular dynamic simulation methods show oscillations of perturbed water structure penetrating 10 Å from a structureless (hydrophobic) wall (Lee *et al.*, 1984) and 7 Å from a phosphorylcholine wall, by the Monte Carlo technique for the simulation of water structure (Scott, 1984).

Type II 'bound water' forms a loosely defined hydration shell of 1 to 2 monolayers around macromolecules. Measurements show that 0.3 to 0.6 g H<sub>2</sub>O per polymer do not freeze for geometric reasons. NMR and low frequency dielectric dispersion techniques agree with predictions of short range water structuring effects imposed by the surfaces of macromolecules (Cooke and Kuntz, 1974). These water molecules explore the surfaces for relatively short periods ( $10^{-9}$  sec).

Tertiary and quaternary protein structure is largely dependent on solvent polarity. Hydrophobic groups fold into the protein interior to avoid unfavourable polar interactions, at the cost of burial of polar groups that might have formed hydrogen bonds (Kausmann, 1959). The consequence of these rearrangements is to subtend water across exposed polar groups and to impose certain water structures. Klotz *et al.* (1959) proposed that hydrophobic residues would organise surface water into five-membered ring arrays analogous to the water clathrate (cage) hydrate structures. Water forms pentagonal arrays of upto 16 water molecules, linking polar groups by chains to other polar groups on the surface of the hydrophobic protein, Crambin (Mr= 4720) (Teeter, 1984). Water forms extensive hydrogen bond networks bridging crevices on the molecular surfaces and

between adjacent molecules of the Iron-sulphur protein, Rubredoxin. The protein holds 127 water molecules that merge with the bulk medium at 5 -6 Å (Waughtenpaugh, 1978). High resolution X-ray studies on bovine pancreatic phospholipase A2 demonstrates two layers of "bound water " that merge with water in the active site (Dijkstra et al., 1981).

Solvent accesible surface mapping techniques, originally computed by Lee and Richards, (1971), have recently been used to map protein folding, using the primary sequence in computer simulations (Connoly, 1983). Water is less densely spaced at clefts where active sites of enzymes appear to be situated (Wolfenden, 1983). During the first event in enzyme function, the formation of the enzyme-substrate complex, water presumably is stripped from the substrate and the enzyme at points where they make contact. Small molecules are often bound by an enzyme with affinities inversely related to their affinities for water.

Whereas the cooperative structure of water is destroyed by cosolvents, the chemical reactivity is scarcely affected. Enzyme reactions that depend on water structure, such as the hydrolysis of phosphate compounds, change markedly with cosolvent addition (deMeis et al., 1985). It is proposed that the differences in energies of hydrolysis between reactants in solution and those bound with high affinity, can be accounted solely by changes in water structure on the surface of enzymes (George et al., 1970; Haynes et al., 1978; deMeis et al., 1985).

Type III water is irrotationally bound water. These water molecules are site bound to the macromolecule. Rotational correlation times ( $T_r = 0.1$  to 10 usec) from NMR studies are similar to rotational times of the protein (Cooke and Kuntz, 1974). Type III water is not clearly differentiated from active site water described by Dijkstra et al. (1981) (above). Approximately 10 to 20 water molecules are randomly spaced about the protein interior and form

structural links by hydrogen bonding to the polypeptide chain (Bickroft, 1972). Raskin et al.(1986) have developed an algorithm that predicts internal cavities in proteins and associated buried water molecules. Cavities ranging in volumes from 10 to 180 Å exist in most proteins. Multidomain proteins have a higher probability of cavities at interdomain surfaces, and most of these contained water.

Muscle cell studies show that 25% of intracellular water is osmotically inactive (Henke, 1970). Total intracellular K<sup>+</sup> concentrations are 150 mM, whereas actual intracellular measurements show 232 mM at the electrode tip. Henke, (1970) concluded that protein bound water cannot readily participate as a solvent.

#### b) The effects of salts on water structure

The structure of water is profoundly effected by polar and apolar solutes alike (for review see Klotz, 1962; Amis and Hinton, 1973). These interactions are relayed to bulk water (type I) and surface accesible water of macromolecules (Type II), as mentioned above. The interactions of polar and apolar solutes differ according to the structure imposed on water.

Polar solutes, such as the alkali metal group, are small highly charged ions that form a firm hydration sphere, which holds water molecules in a highly ordered pattern in the vicinity of the ion (Frank and Wen, 1957). Theoretically, a pinpoint charge of minimum volume creates a tetracoordinated structure similar to ice. The water molecules are held with high energy for periods of 1 to 100 usec (Klotz, 1962). Numerous studies on hydration numbers have been performed, with no general agreement. The hydration of K<sup>+</sup> is 5 ±2, but values range from 0.6 to 10, according to the experimental protocol employed (for comprehensive review see Amis and Hinton, 1973). The intermediate region, outside the

immediate hydration sphere, consists of highly disorganized water, resulting from two competing forces; those of the organization of water, imposed by the ion, versus those of water structure attempting to realign to the hexagonal arrays of tetra-coordinated water in flickering clusters (Nemethy and Schegara, 1962; Klotz, 1962; Frank and Wen, 1957; Jencks, 1969).

Predictably, the ionic strength effects of monovalent cations ( $\text{Cs}^+ > \text{Rb}^+ > \text{K}^+ > \text{Na}^+ > \text{Li}^+$ ) follows the inverse of their ionic radii (Amis and Hinton, 1973). Smaller cations present a higher charge density and have a larger range of their hydration spheres.  $\text{Na}^+$  and  $\text{Li}^+$  are more structure forming and increase viscosity, while  $\text{Cs}^+$  and  $\text{Rb}^+$  are large and break water structure to decrease fluidity.  $\text{Li}^+$ , the smallest cation has the lowest mobility of the series, whereas protons diffuse rapidly and have diffusion coefficients  $10^6$  -fold higher than  $\text{Li}^+$  in ice. Protons migrate on the immobilized crystal lattice in ice by replacing near neighbours, so producing a 'proton wire' of conductance unrestrained by hydrogen bonding (Klotz, 1962).

Exposure of the solvent accesible surface of proteins to various ion dependent solvent environments may therefore have more powerful effects than those of ion binding to specific charged groups comprising binding sites. Cation binding sites impose specificity on the order of effectiveness of cations on the biosystem. The sequence of effectiveness has been classified by Eisenman et al., (1957), according to the Gibbs free energies of binding versus those of hydration. Curiously, of the 120 combinations of effectiveness of cations excluding Francium, only 11 Eisenman sequences exist in biosystems. This may be the result of the constraints imposed on evolving biosystems by the relative abundance of group I cations in nature (Phipps, 1976).

- c) The interaction of chaotropes and anti-chaotropes with water and proteins

Hydrophobic interactions provide the major contribution to the stability of most membranes and to the native conformations of soluble and membrane bound proteins. The interactions of chaotropic agents with biosystems is largely attributable to their profound effect on water structure. The disordered structure of water therefore lowers the thermodynamic barriers, and weakens hydrophobic interactions, resulting in a net destabilization of most biosystems (Hatefi and Hanstein, 1969).

Chaotropic agents are usually monovalent and have a relatively large radius. These two factors account for their low charge density. The order of efficacy of chaotropic anions is as follows: tribromacetate > trichloracetate >  $\text{SCN}^-$  >  $\text{I}^-$  >  $\text{ClO}_4^-$  >  $\text{NO}_3^-$  >  $\text{Br}^-$  >  $\text{Cl}^-$  (Aviram, 1973).

Several lines of evidence have indicated that chaotropes decrease the organization of water structure. These include negative entropies of aqueous ions, proton NMR shifts to higher field strength, facilitated water self-diffusion, negative viscosity B coefficients (decreased viscosity) and diminution of surface tension (Hatefi and Hanstein, 1974). Insertion of a large ion of low charge density into water results in the occupation of a volume with few compensatory hydrogen bonds and is endergonic by 26 kcal/mol (Hatefi and Hanstein, 1959). Water molecules reorientate to the maximum number of energetically favourable interactions, and form a sphere of hydration that is poorly captured by the diffuse charge of the chaotrope. The water molecules adjacent to the hydration sphere are highly disordered and the magnitude of the interference in water structure exceeds that of the structure forming ions. The lipophilicity of water is significantly increased by anion concentrations exceeding 1 M (Hamabata and von Hippel, 1973). Mutual repulsion between

chaotropes prevents the type of packing that occurs with hydrophobic (uncharged) molecules that constitutes the hydrophobic interaction observed in lipid behaviour (Tanford, 1980).

Antichaotropes increase the structure of water and therefore impart increased stability to biological macrostructures. Thus, water forming ions, such as  $\text{SO}_4^{2-}$ ,  $\text{HPO}_4^{2-}$  and  $\text{F}^-$ , have strong salting out effects on nonelectrolytes, and tend to strengthen hydrophobic interactions in proteins and multicomponent systems (Hatefi and Hanstein, 1974). In contrast to chaotropes, the water structuring ions have high charge density, very small, often negative entropies of aqueous ions, positive viscosity B coefficients (increased viscosity) and retard water self-diffusion. The properties of antichaotropes may be intrinsically imitated by the use of deuterium oxide ( $\text{D}_2\text{O}$ ). Liquid  $\text{D}_2\text{O}$  is considered more structured than  $\text{H}_2\text{O}$  (Arnett and McKelvey, 1969).  $\text{D}_2\text{O}$  has a 1.23-fold higher viscosity than  $\text{H}_2\text{O}$ , whereas dielectric constants are similar (77.9 and 78.3, respectively) (Wiberg, 1955). Self-diffusion of  $\text{D}_2\text{O}$  is slower than for  $\text{H}_2\text{O}$  with equilibrium constants of  $1.54 \times 10^{-15}$  and  $1 \times 10^{-14}$ , respectively.  $\text{D}_2\text{O}$  is therefore an ideal substitute for water in experiments where water structure and viscosity factors are explored.

d) The effects of chaotropes on the SR

Initial studies showed that  $\text{Ca}^{2+}$  binding capacity is decreased by chaotropic anions in the series mentioned above (Ebashi, 1962). Chaotropes also decrease  $\text{Ca}^{2+}$  transport,  $\text{Ca}^{2+}$ -dependent ATPase, EP formation and ATP binding (The and Hasselbach, 1975). The effect was found to operate mainly through decreased ATP binding.

Chaotropes decreased ATP binding in the series and with half maximal effects : trichloracetate =  $\text{ClO}_4^-$  (.09 M), >

SCN<sup>-</sup> (0.15 M), > NO<sub>3</sub> (0.25 M), > Cl (0.5 M). Since water structure is disturbed only at high chaotrope concentrations, it is suggested that the mechanism of action is by preferential binding of chaotropes to hydrophobic pockets that are sites of nucleotide binding on the Ca<sup>2+</sup>-ATPase (The and Hasselbach, 1975). An inhibitory effect of KCl on dephosphorylation of EP by ADP has recently been reported (Yamada and Ikemoto, 1980). In support of this finding, Shigekawa and Kanazawa (1982) report that the apparent affinity of E<sub>1</sub>-P for ADP is decreased by KCl by an 11-fold acceleration of the "off" rate of ADP. The mechanism of action was found to operate through the anion Cl<sup>-</sup>, rather than the cation, as evidenced by the stronger inhibition by KSCN over KCl. Compounds and cosolvents that alter the structure of water provide a useful method for analysis of protein active site-water interactions as monitored by micro-environmental-sensitive fluorescent probes, such as TNP-ATP.

#### 1.4 USE OF TNP-ATP AS A PROBE OF REGULATORY AND CATALYTIC NUCLEOTIDE SITES

Chemical probes have been beneficial not only to our understanding of the topography of membrane-spanning ATP-ase complexes, but also for determination of different possible mechanisms in the function of these proteins. Chemical probes can be divided into two groups, depending on whether their binding is covalent or noncovalent. Generally, the use of covalent probes, while helpful in mapping sites, is an invasive technique that leads to ultimate inactivation of the protein under scrutiny. Noncovalent probes, such as nucleotide analogues, do not in general inactivate, but rather provide functional information of conformational change and other parameters of their binding site. Noncovalent fluorescent probes can provide 'realtime'

information of site status, because of their short fluorescent lifetimes (0.01 to 1 nanoseconds), if they do not compete for any natural ligand and alter the observation by their presence. The ideal fluorescent probe is the intrinsic fluorophore that is naturally associated with the protein, such as the tryptophan residues in the  $\text{Ca}^{2+}$ -ATPase (Dupont 1977). A problem encountered in the use of extrinsic probes that compete with ligands for sites is that the natural ligand is replaced and only a photoselective account of events is observed in the absence of the ligand (Lakowicz, 1983).

In order to probe the catalytic sites and associated conformational change in ATP-utilizing energy transducing systems, ATP analogues have been synthesized to elucidate the roles of the adenine base, ribose and triphosphate. In general, ribose modified ATP analogues at the 2' and 3' positions show decreased substrate specificity and catalytic activity (Anderson and Murphy, 1983). Trinitrophenylation of the ribose residue of ATP by 2,4,6 trinitrobenzene-1-sulphonate (TNBS) yields 2'3'-O-(2,4,6-trinitrophenyl) adenosine 5'-triphosphate (TNP-ATP), (Fig. 1.1) (Hiratsuka and Uchida, 1973). The microenvironmental sensitivity and ATP like properties make TNP-ATP a powerful tool for probing the ATP sites of ATPdependent enzymes. The chromophoric properties of TNP-ATP are similar to the Meisenheimer complex with absorption maxima at 408 and 470 nm that disappear at low pH ( $\text{pK} = 5.1$ ). TNP-ATP is sensitive to solvent polarity and viscosity, with high fluorescence quantum yield and blue shifted emission maxima in solvents of low polarity such as dimethylformamide (quantum yield = 46; emission maximum = 529 nm), but low quantum yield (= 1) and red shifted emission maxima (= 560 nm) in water (Moczydlowski and Fortes, 1981).

The interactions of TNP-ATP vary for different enzymes types. TNP-ATP is hydrolysed at a similar rate to ATP in heavy meromyosin, adenylate kinase and alkaline phosphatase,

but more slowly by adenosine deaminase (Hiratsuka and Uchida, 1973) and the  $\text{Ca}^{2+}$ -ATPase of SR (Dupont et al., 1982b). TNP-ATP inhibits mitochondrial  $\text{F}_1$ -ATPase (Grubmeyer and Penefsky, 1981), the  $\text{Na}^+/\text{K}^+$ -ATPase (Fortes et al., 1977), and heavy meromyosin (Hiratsuka and Uchida, 1973), by competition for the catalytic site, and may even enhance catalysis in SRV (Dupont et al., 1985).

TNP-ATP binds with high affinity to the  $\text{Ca}^{2+}$ -ATPase (Watanabe and Inesi, 1982), with a  $[\text{TNP-ATP}]_{0.5} = 0.1$  to  $0.3$   $\mu\text{M}$  (Dupont et al., 1982; Nakamoto and Inesi, 1984). The small increase in fluorescence and the absorbance changes of TNP-ATP when bound to the non-phosphorylated enzyme, has been used to generate TNP-ATP binding isotherms showing saturation with  $5.9$  to  $7.1$   $\text{nmol/mg}$ , (Dupont et al., 1982b). A useful spectroscopic property is the composite difference absorption spectrum of TNP-ATP bound to SR with respect to free TNP-ATP with a trough at  $455$   $\text{nm}$  and a peak at  $510$   $\text{nm}$ . Titration with increasing TNP-ATP shows a linear increase in the difference, and a sharp inflection at site saturation, ( $7.1$   $\text{nmol/mg}$ ), (Watanabe and Inesi, 1982; Dupont et al., 1982).

However, the stoichiometry of TNP-ATP sites is uncertain. Values range from  $5$  to  $8$   $\text{nmol/mg}$ , depending on the method used (Watanabe and Inesi, 1982; Dupont et al., 1982). TNP- $[\gamma\text{-}^{32}\text{P}]\text{ATP}$  binding, measured by the minicolumn centrifuge method of Penefsky, yields a value of  $5$   $\text{nmol/mg}$  (Watanabe and Inesi, 1982). Scatchard plots showed two populations of binding sites, with apparent dissociation constants of  $1.5$  and  $160$   $\mu\text{M}$ . These authors stated however, that "the population of low affinity sites is poorly resolved and its saturation cannot be demonstrated unambiguously." It is surprising that only half of this bound TNP-ATP was displaced by saturating millimolar  $[\text{ATP}]$  in their study. Dupont et al., (1985) described two classes of site that are sensitive to  $\text{H}^+$  and  $\text{Mg}^{2+}$  under turnover conditions. At acid pH or in the absence of  $\text{Mg}^{2+}$ , a single family of sites exists

of ( $K_d = 20 \mu\text{M}$ ). This splits into two classes of sites of high ( $K_d = 2$  to  $4 \mu\text{M}$ ) and low ( $K_d = 1 \text{ mM}$ ) affinity, at pH values higher than neutral in the presence of  $\text{Mg}^{2+}$ . A stoichiometry of 6.6 to 7.1 nmol/mg by filtration binding, supports these findings (Dupont et al., 1982b). In view of the values of 8 nmol/mg for  $\text{Ca}^{2+}$  (Watanabe and Inesi, 1982), and 3.2 nmol/mg for ATP bound (Dupont et al., 1982), there is uncertainty as to the relative stoichiometries of 1 or 2 mol/mol.

Phosphoenzyme formation from [ $\gamma$ - $^{32}\text{P}$ ]ATP is slowed down 100-fold if TNP-ATP is bound to the enzyme before ATP addition, consistent with the forward reaction limited by the "off" rate of TNP-ATP (Bishop et al., 1984). The monoexponential rate of E-P formation is consistent with TNP-ATP leaving a single site. It was concluded that TNP-ATP forms a low, fluorescent dead-end complex which must decompose before enzyme turnover can proceed (Bishop et al., 1984). TNP-ATP is displaced from this site by millimolar ATP (Bishop et al., 1984).

Watanabe and Inesi (1982), first demonstrated that the fluorescence intensity of bound TNP-ATP is increased several-fold upon formation of the phosphoenzyme intermediate from ATP in the presence of  $\text{Ca}^{2+}$ . Subsequently, a large fluorescence enhancement was also found upon phosphorylation from  $\text{P}_i$  in the absence of  $\text{Ca}^{2+}$  (Dupont et al., 1983). TNP-ATP displays a high quantum yield, with a blue shifted emission maximum (525 nm), that is consistent with decreased polarity of the site (Dupont and Pougéois, 1983; Nakamoto and Inesi, 1984). The binding affinity of highly fluorescent TNP-ATP has not been directly measured, but titration of the enzyme with TNP-ATP during steady state turnover shows an apparent high affinity ( $[\text{TNP-ATP}]_{0.5} = 1 \mu\text{M}$ ), (Nakamoto and Inesi, 1984). The three nucleotide analogues, TNP-ATP, TNP-ADP and TNP-AMP were shown to respond qualitatively similarly for both these conditions (Nakamoto and Inesi, 1984).

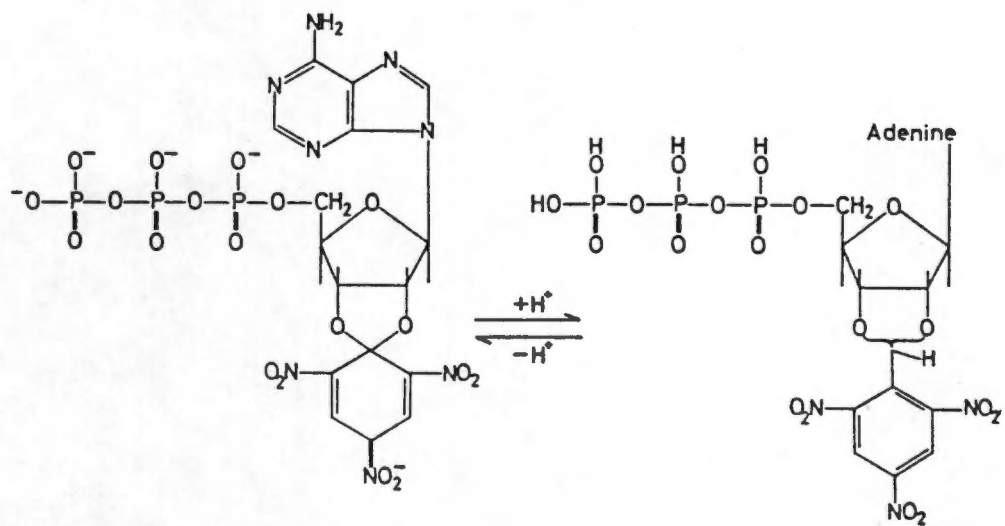


**Figure 1.1** Structure proposed for TNP-ATP at acidic and basic pH (Hiratsuka and Uchida, 1973)

The fluorescence enhancement from Pi, in the absence of Ca<sup>2+</sup>, was initially reported to much higher than that produced in the forward reaction of the cycle. Differences in the levels of this fluorescence in the forward and reverse reactions have led to a hypothesis that there are two sequential forms of the enzyme, differing in their H<sub>2</sub>O activity, and that extrusion of water from the catalytic site, following phosphorylation, is the driving force for Ca<sup>2+</sup> translocation (Dupont and Pougeois, 1983; Nakamoto and Inesi, 1984). However, varying amounts of KCl, that decrease fluorescence (Bishop *et al.*, 1984; Davidson and Berman, 1985), were employed in the experiments. In addition, the relative fluorescence levels were found to be related to differences in phosphoenzyme levels and the use of subsaturating ATP levels.

The qualitative relationship between phosphoenzyme subspecies and enhanced TNP-ATP fluorescence is uncertain. Enhanced TNP-ATP fluorescence parallels phosphoenzyme levels (Nakamoto and Inesi, 1984; Bishop *et al.*, 1984). Fluorescence increases at the same rate as acid-stable phosphoenzyme formation ( $k_{obs} = 110 \text{ sec}^{-1}$ ) (Bishop *et al.*, 1984). It is uncertain as to which phosphoenzyme intermediates support the enhanced fluorescence state of bound TNP-ATP. In a recent study, manipulation of phosphorylation conditions that alter relative levels of phosphoenzyme subspecies by variations of pH, Ca<sup>2+</sup>, and K<sup>+</sup> levels did not alter the ratio of fluorescence to E-P (total), for the same amount of TNP-ATP bound (Bishop *et al.*, 1986). The fluorescence lifetimes of highly fluorescent TNP-ATP did not change. It was concluded that all phosphoenzyme species cause enhanced fluorescence, and a K<sub>d</sub> of the phosphoenzyme for TNP-ATP has been calculated; [TNP-ATP]<sub>0.5</sub> = 0.4 μM. However, direct measurements of ADP-insensitive phosphoenzyme levels, at pH 8.0 and 2°C, show a parallel increase in TNP-ATP fluorescence, suggesting a close relationship between

$E_2$ -P and the enhanced fluorescence state, and a single step mechanism for energy transfer between the catalytic site and the  $Ca^{2+}$  transport sites (Andersen et al., 1985). Uncoupling of the enzyme during EGTA treatment has a similar effect in that enhanced TNP-ATP fluorescence is decreased parallel to the degree of uncoupling, under conditions that do not alter total EP levels (Berman, 1986).

KCl decreases phosphoenzyme induced TNP-ATP fluorescence (Bishop et al., 1984) at concentrations that modify a number of partial reactions of the catalytic cycle ( $[K^+]_{0.5} = 50$  mM) (Davidson and Berman, 1985). The decreased fluorescence has been attributed to  $K^+$  induced changes in the affinity of the fluorescent site for TNP-ATP ( $[TNP-ATP]_{0.5} (+K^+) = 3.6$   $\mu$ M), (Bishop et al., 1986).

Enhanced TNP-ATP fluorescence is  $Mg^{2+}$  -dependent (Dupont et al., 1985). In the absence of  $Mg^{2+}$ , phosphorylation by CaATP yields normal phosphoenzyme levels without enhanced fluorescence, conditions under which,  $E_1$ -P accumulates (Shigekawa and Dougherty, 1978), while TNP-ATP binding to the  $E_1$  conformation is unaltered ( $[TNP-ATP]_{0.5} = 0.2$   $\mu$ M), (Dupont et al., 1982b). Bishop et al., (1986) propose that bound TNP-ATP requires bound  $Mg^{2+}$  to achieve enhanced fluorescence in the  $E_1$ -P conformation.

The existence of regulatory sites has been proposed (see above). The relationship of the TNP-ATP site to the regulatory and catalytic sites is uncertain. The effector site may be a separate regulatory site (Dupont, 1977), or a modified catalytic site with low affinity for ATP after ADP liberation (McIntosh and Boyer, 1983). Dupont et al. (1985) have proposed from studies of TNP-ATP binding that two discrete sites, a regulatory and a catalytic, exist on the same polypeptide chain. Results of kinetic studies, however, show evidence for interaction of TNP-ATP with a single site (Bishop et al., 1984), as have studies with FITC binding (Nakamoto and Inesi, 1984).

Three important questions crucial to the understanding of the interaction of TNP-ATP with nucleotide binding sites remain unresolved; (I) The precise stoichiometry of TNP-ATP sites to ATP sites, (II) The relationship of enhanced TNP-ATP fluorescence to phosphoenzyme species,  $E_1-P$  and  $E_2-P$ , and (III) The relationship of the TNP-ATP site to the catalytic site.

### 1.5 INTERACTION OF IONOPHORES WITH ENERGY TRANSDUCING MEMBRANES

The generic term 'ionophore' (ion bearer) was introduced by Pressman to emphasise the dynamic aspects of several classes of antibiotics that form organo-soluble complexes with alkali cations, and facilitate their transport across lipid bilayers (Pressman, 1967). Although this term is widely accepted, Ovchinnikov *et al.* (1974) choose the term 'complexone' to emphasise the nature of the association between the carrier and the cation.

Ionophores have provided valuable tools for studies on the coupling between metabolism and ion transport. Ionophores are compounds of moderate molecular weight ( $M_r = 200$  to  $2000$ ), and form lipid soluble complexes with polar cations, of which  $K^+$ ,  $Na^+$ ,  $Ca^{2+}$ ,  $Mg^{2+}$  and the biogenic amines are the most biologically significant (for review, see Pressman, 1976; Painter and Pressman, 1982). The first indication of their unique biological and physical properties was the uncoupling of mitochondrial oxidative phosphorylation by valinomycin (McMurray and Beggs, 1959). Valinomycin differed from classical protonophore uncouplers in that its mode of action is by increased  $K^+$  conduction that it imparts to the membranes (Moore and Pressman, 1964). Physical studies indicate that the complexation-decomplexation kinetics and diffusion rates of ionophores and their

complexes are so favourable that their transport turnover numbers across biomembranes attain values of thousands per second, exceeding the turnover of most macromolecular enzymes (Haynes et al., 1974).

The ion selectivity of ionophores together with their electrometric effects on artificial thick membranes have provided the technological basis for a novel series of ion-selective electrodes. The in vivo effects of ionophores, however, are complex and toxicity has limited their clinical use.

The general architectural features of ionophores require specifically oriented polar and non-polar groups that simultaneously provide an interface compatible with polarity of the ion and that of the medium. The polar groups function as ligands and focus inward to surround the ion and replace the solvent molecules in the primary solvation sphere. The nonpolar groups insulate the ion for passage of the complex within media of low dielectric constant, such as the lipid bilayer. A compromise between ion affinity and ion exchange kinetics must exist for complexation and decomplexation to proceed at sufficiently rapid rates (Painter and Pressman, 1979).

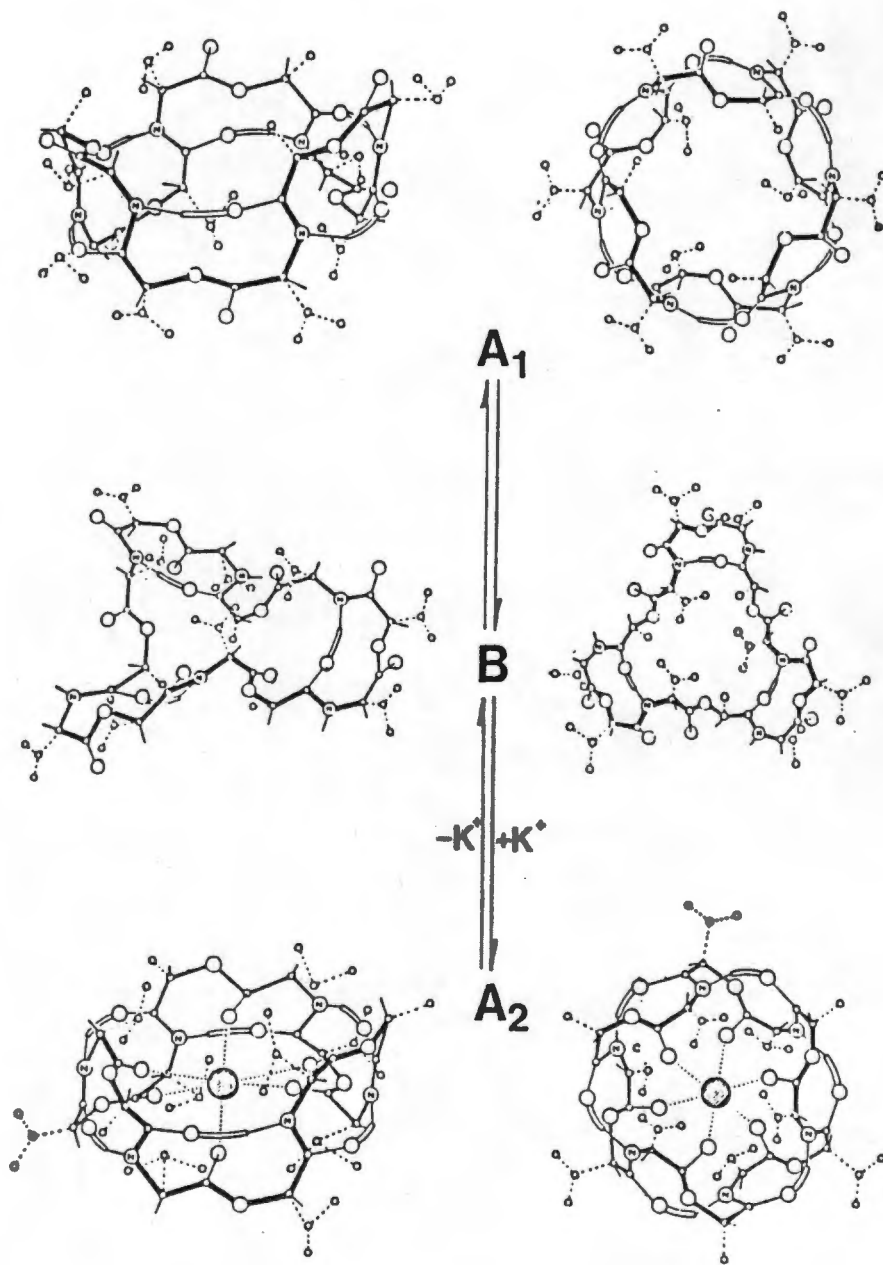
The transport mechanism facilitated by ionophores, functions either through a mobile carrier action or by channel formation within the lipid bilayer. Channel formers, such as gramicidin have been termed 'quasi ionophores', since they span the membrane and remain relatively immobile during ion conduction (Pressman, 1976), whereas mobile carriers proceed through a series of consecutive reactions which, taken in sum, constitute the overall transport cycle.

Mobile carrier ionophores are classified as i) neutral or ii) carboxylic, depending on a charge related mechanism during transport. The neutral ionophores, such as the valinomycin group, are devoid of ionizable or other functional groups and the complex acquires the charge of the

ion; they return across the membrane after decomplexation in a neutral form.

Neutral ionophores are either "electrophoretic", if they carry ions under the driving force of a constant imposed potential, or "electrogenic" if they alter pre-existing membrane potential. Carboxylic ionophores, on the other hand, such as monensin, nigericin, A23187, and X537A, contain a single carboxyl group and form cationic complexes as electrically neutral zwitterions only in their deprotonated form. All carboxylic ionophores carry protons in their protonated form on the return cycle. Since both the protonated and zwitterionic forms are electrically neutral, the final ionic equilibrium is pH sensitive and independent of electrical potential.

Carboxylic ionophores have been extensively used as tools in  $\text{Ca}^{2+}$  pump studies. The  $\text{Ca}^{2+}$  ionophores, A23187 and X537A, impart increased  $\text{Ca}^{2+}$  conductance to lipid bilayers of the SR and are useful in experimental design to remove product inhibition by dissipation of the energy linked  $\text{Ca}^{2+}$  gradient formed (Caswel and Pressman, 1972). They complex divalent cations in a 2 : 1, ionophore :  $\text{Ca}^{2+}$  ratio, and select  $\text{Ca}^{2+}$  over  $\text{Mg}^{2+}$ . A23187 differs from X537A in its high selectivity of divalent over monovalent cations, but both transport monovalent cations as 1:1 complexes (Pfeifer et al., 1974). The spectroscopic properties of X537A have been exploited in determining distances from tryptophans by fluorescence energy transfer studies (Verjovski-Almeida, 1981).



• C O O N ⊙ K — H-bond

**Figure 1.2** Conformations of valinomycin in the presence and absence of  $K^+$  (Ovchinnikov et al., 1974).

### 1.5.1. ANOMALOUS EFFECTS OF VALINOMYCIN

Valinomycin, a neutral monovalent cation ionophore, was originally isolated from *Streptomyces* fermentation (Brockman, 1955). Independent NMR (Ivanov *et al.*, 1969) and X-ray crystallographic studies (Pinkerton *et al.*, 1969) showed valinomycin to be a cyclic dodecadepsipeptide, constructed of a bracelet of three repeating units of the sequence, D-hydroxyisovalerate, L-valine, L-lactate, and D-valine, and forming a castellated ring structure 8 Å in diameter and 4 Å high.

Various solvent-dependent conformations have been discovered (Ovchinnikov, 1972). These are A1, B and A2 (Fig. 1.2). Conformation A1 is predominant in the absence of  $K^+$ , and the ester carbonyls face outward. Conformation A2 has the carbonyl esters focused to the centre, and the amide groups and hydrogen bonds are rearranged, giving the conformation an opposite chirality. Chelated  $K^+$  ions stabilize conformation A2 and are held by six ester carbonyls. The external hydrocarbon groups are compatible with media of low dielectric constant, and favour entry of the complex into hydrophobic areas. The transition from A1 to A2 is rapid, but requires that six intramolecular hydrogen bonds are broken. Conformation B is the intermediate and exists in non-polar solvents.

Valinomycin shows a strong discrimination between alkali cations on the basis of Gibbs free energy lost from dehydration versus that gained by complexation with ester carbonyls. The specificity therefore is a function of non-hydrated ionic radius and there is a 10000 : 1 preference for  $K^+$  (1.33 Å) over  $Na^+$  (0.95 Å). The sequence of specificity follows,  $Rb^+ > K^+ > Cs^+ \gg Na^+ > Li^{2+}$ , (Moore and Pressman, 1964). Valinomycin can also complex divalent cations such as  $Ca^{2+}$ , by forming 2 : 1 sandwich complexes (Vishwanath and Easwarin, 1982).

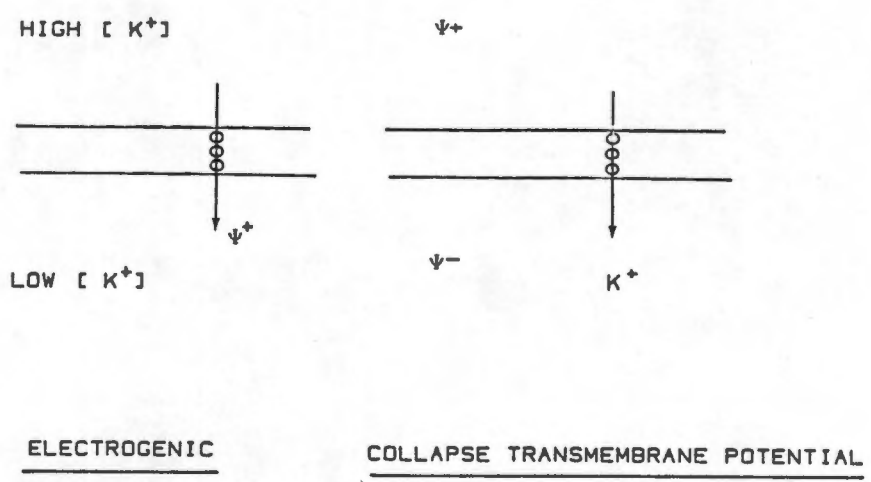


Figure 1.3 Uses of valinomycin in biomembrane studies

Valinomycin has been usefully applied in biochemistry studies for the interconversion of chemical and electrical potentials. Dissipation of a an osmotic gradient of KCl results in a selective  $K^+$  transport-dependent redistribution of charges, whereas a strong electrical gradient will reequilibrate to form an osmotic gradient (Fig 1.3). Most of the effects of valinomycin on whole cells and on isolated subcellular particles and lipid bilayers appear to depend on its ionophoric properties alone.

There have been recent reports, however, of valinomycin effects that cannot be entirely attributed to increased ion permeability. Valinomycin ( $10^{-7}$  M) depolarizes mitochondria in intact lymphocytes (Felber and Brand, 1982), and inhibits mitogenesis by concanavalin A, under conditions in which there are no increases in  $K^+$  membrane fluxes (Negendank and Schalter, 1982). The ionophore also inexplicably inhibits atractyloside binding to heart mitochondria (Vignais et al., 1983). This inhibition is reversed at  $K^+$  concentrations greater than 300 mM.

Anomalous effects have also been demonstrated on the  $Ca^{2+}$ -ATPase of SR. Louis et al. (1980) have shown that valinomycin stimulates the time-dependent reuptake of  $Ca^{2+}$  ions into partially filled SRV by a mechanism that involves modification of unidirectional  $Ca^{2+}$  fluxes operating near equilibrium. Since these phenomena were observed in the absence of  $K^+$  or proton gradients, it was suggested that valinomycin might act by modifying lipid-protein interactions (Louis et al., 1980).

The use of 1-anilino-8-naphthalene sulfonate ( $ANS^-$ ) has recently been demonstrated as a probe of conformation of the  $Ca^{2+}$ -ATPase (Arav et al., 1983). The method of equilibration of the negatively charged  $ANS^-$  anion into SRV includes the use of valinomycin and KCl to facilitate charge redistribution (Chiu and Haynes, 1980). Valinomycin ( $3 \times 10^{-7}$

<sup>6</sup> M) inhibited both ATPase activity and Ca<sup>2+</sup>-uptake over a range of KCl concentrations (20 - 120 mM) by 30% (Arav et al., 1983). Since preincubation conditions appeared to eliminate any K<sup>+</sup> gradient across the SR membrane, the inhibitory effects of valinomycin could not be readily explained.

In the present study we have characterized the monovalent cation sensitivity of phosphoenzyme-dependent TNP-ATP fluorescence and show that this phenomenon is a novel and useful parameter for the study of binding of monovalent cations to the Ca<sup>2+</sup>-ATPase. The ionophore valinomycin is shown to interact directly with the enzyme, independently of its transmembrane ion conductance effects. The effect is essentially to lower the affinity of the site for K<sup>+</sup> ions.

## 2.0 EXPERIMENTAL PROCEDURES

### 2.1 MATERIALS

Valinomycin, ATP (vanadate free), and diadenosine pentaphosphate were obtained from Sigma. A23187, nigericin and monensin were from Calbiochem-Behring. KCl, RbCl, NaCl, CsCl and LiCl were of analytic grade from BDH Chemicals (England). Creatine phosphate (salt-free, from rabbit muscle) and creatine phosphokinase were supplied by Boehringer Mannheim. [ $^{32}\text{P}$ ]Pi, (3000 Ci/mmol) was from New England Nuclear (NEN) and was purified by the method of deMeis and Tume (1977). [ $\gamma$ - $^{32}\text{P}$ ]ATP, (4 Ci/umole) was from NEN, or was synthesised from  $^{32}\text{P}$ i by the method of Glynn and Chapell (1964). [ $8$ - $^{14}\text{C}$ ]ATP (1 uCi/umol), N-[ethyl-2- $^3\text{H}$ ]maleimide (53 mCi/umol), and  $^{45}\text{CaCl}_2$  were from NEN. [ $6,6(\underline{n})$ - $^3\text{H}$ ]sucrose (15 mCi/umol) was from Amersham.

### 2.2 PREPARATIVE METHODS

#### 2.2.1. ISOLATION AND PURIFICATION OF SARCOPLASMIC RETICULUM VESICLES

SRV were prepared according to the method of Eletr and Inesi (1972), with minor modifications. White skeletal muscle was removed within 15 minutes post-mortem from the hind legs of a New Zealand White, crossed with a commercial hybrid strain male rabbit. Extracted tissue (200g) was homogenized in 800 ml medium A: 10 mM Histidine, 0.3 M Sucrose, 0.1 mM EDTA, pH 7.0, for 15 minutes every 5 minutes for a total of one hour at 0 - 4 °C with the pH adjusted to 7.0 with 5% (w/v) NaOH. The homogenate was centrifuged at 15000 x g (9500 rpm) for 20 min in rotor no. JA 14 in a Beckman J2-21 centrifuge. The supernatent was filtered through glass wool

and washed with medium A to remove low-density lipid aggregates. The filtrate was then centrifuged at 40 000 x g (1900 rpm) for 90 min in rotor no. 19 in a Beckman model L4 ultracentrifuge. The sediment was resuspended in 100 ml medium B : 10 mM histidine, pH 7.0, 0.6 M KCl for 40 min to solubilize contaminating actomyosin. The incubate was centrifuged at 15000 x g (14000 rpm) for 20 min in rotor no. JA 20 in a Beckman J2-21 centrifuge. The supernatant was recentrifuged at 27800 rpm for 60 min in rotor no. 30 in a Beckman model L4 ultracentrifuge. The final pellet was resuspended in 5 ml buffer C: 10 mM imidazole pH 7.4, 0.3 M sucrose, giving a concentration of 10 to 20 mg/ml SRV. Aliquots of the preparation were frozen in liquid nitrogen and stored at -70 °C for periods of up to 6 months. Calcium transport activity at pH 7.0, 25°C, measured in the presence of 100 mM KCl, was 2 to 3 umol/mg/min.

#### 2.2.2 DETERMINATION OF PROTEIN CONCENTRATION

Protein concentration was determined by the Lowry method (Oosta et al., 1978). Standards, using BSA (Sigma) in the range of 2.5 to 25 mg/ml and SR (in triplicate), 10 ul of approximately 10 mg/ml were incubated with 10 ul 10% sodium deoxycholate for 10 min and diluted to a concentration of approximately 100 ug/ml. Color was developed with Biuret reagent (38 parts 4 g NaOH + 20 g Na<sub>2</sub>CO<sub>3</sub>/1 ; 1 part 2.5 g CuSO<sub>4</sub>/250 ml and 1 part 2g Na/K tartrate/100 ml) was developed for 10 min followed by a 1/20 dilution of Folin-Ciocalteu phenol reagent for a further 30 min. The calibration curve was fitted by a binomial equation, to allow for non-linear calibration curves. Purity of the isolated protein is shown in Fig. 2.1.

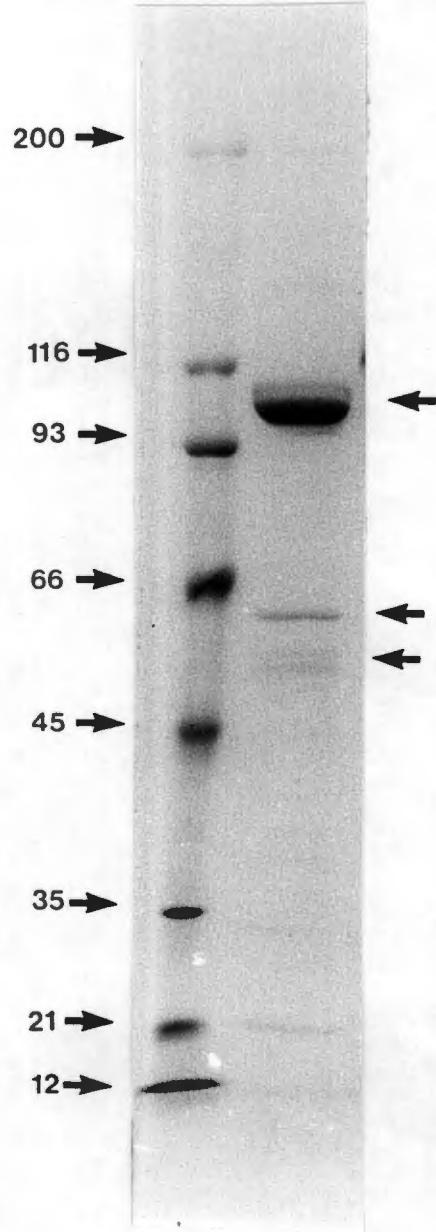


**Figure 2.1** Protein composition of isolated SR vesicles

Sodium dodecylsulphate gel electrophoresis was performed according to Laemmli (1970) (4 - 16 % gradient gel) and stained with Coomassie blue. SR protein (8 ug) run on the right lane showed ATPase ( $M_r = 110$  k), calsequestrin ( $M_r = 63$  k) and a glycoprotein ( $M_r = 53$  k), as indicated by arrows. The markers (left lane) were myosin (200 k),  $\beta$ -galactoside (116 k), phosphorylase (93 k) and bovine serum albumin (66 k), ovalbumin (45 k), Lactate dehydrogenase (35 k), Soybean trypsin inhibitor ( $M_r = 20$  k) and cytochrome C (12 k), where indicated.

### 2.2.3 TNP-ATP SYNTHESIS

TNP-ATP was synthesized and purified according to the method of Hiratsuka (1982). Thin layer chromatography showed a single orange spot with  $R_F = 0.08$ , consistent with the  $R_F$  values obtained for TNP-ATP on PEIE-cellulose plates, developed with 2 M Formic acid and 0.5M LiCl (Grubmeyer and Penefsky, 1981). ATP contamination was not detected under UV examination of the TLC, and also was considered negligible as evidenced by the stable fluorescence signal obtained upon addition of TNP-ATP to SRV in 50  $\mu$ M  $\text{CaCl}_2$  in the absence of added ATP. Concentration of the nucleotide in 0.1 M Tris-Cl, pH 8.0, was determined by absorbance measurements at 408 nm, using  $E_{408} = 26.4 \text{ mM}^{-1} \text{ cm}^{-1}$  (Hiratsuka and Uchida, 1973).

### 2.2.4 [ $^{14}\text{C}$ ]TNP-ATP SYNTHESIS

Labelled TNP-ATP was essentially synthesized as above with minor modifications. [ $^{14}\text{C}$ ]ATP ( $\text{Na}^+$  salt), (15  $\mu$ mol, 50  $\mu\text{Ci}/\mu\text{mol}$ ) was buffered with 1 ml of 0.091 g  $\text{Na}_2\text{CO}_3$  and 0.06  $\text{NaHCO}_3$ , pH 9.5, and reacted with 1 ml of 0.27 mmole 2,4,6-trinitrobenzene sulphonic acid for 8 hours under continuous stirring at 37°C. A dark yellow granular precipitate was observed after 3 hours. The reaction mixture was centrifuged at 4000 rpm for 5 min to remove unreacted precipitated components. The supernatant was chromatographed on an LH 20 column (2.5 x 17 cm) and eluted with water at a flow rate of 15 ml/min at room temperature. Fractions were collected at a rate of 4 min/fraction. Absorbance at 260, 360 and 408 nm of elution components was determined (Fig 2.2) and 5  $\mu$ l aliquots assayed for radioactivity. A separation profile (Fig. 2.3) was obtained, showing elution of [ $^{14}\text{C}$ ]ATP, [ $^{14}\text{C}$ ]TNP-ATP and picrate/trinitrobenzene sulphate, respectively. Fractions were assayed by thin

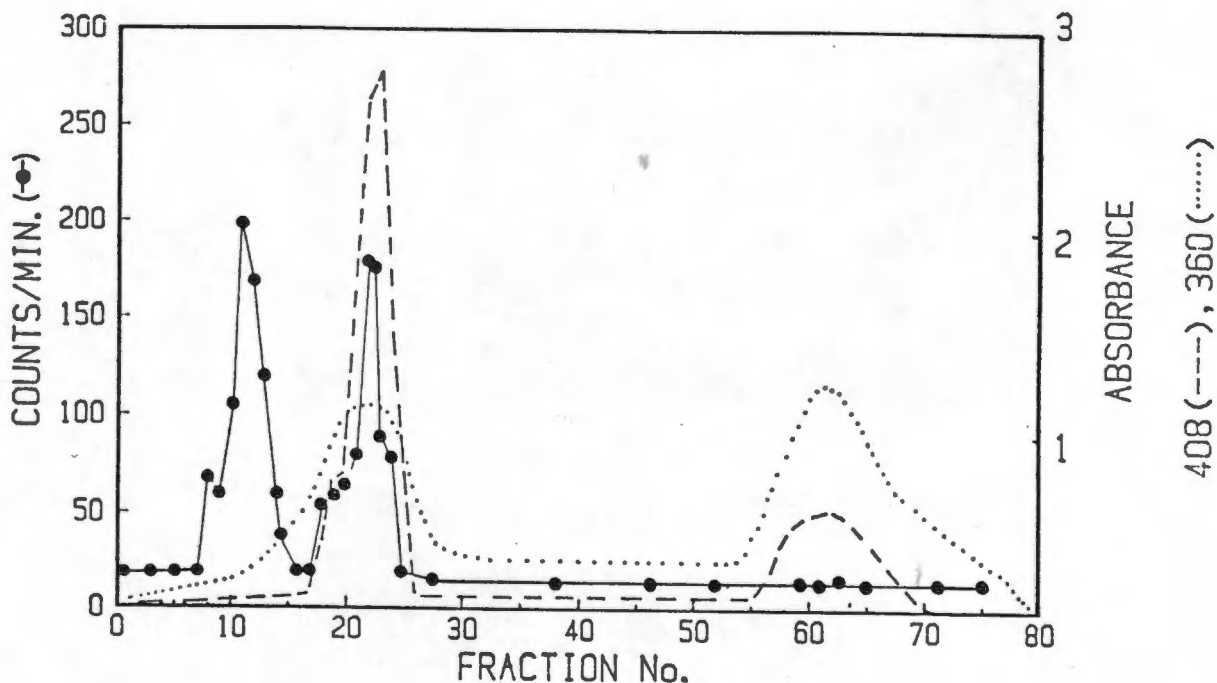


**Figure 2.2** TNP-ATP elution profile from LH 20 column

<sup>14</sup>C]TNP-ATP, reactants and reaction products were eluted from a 2.5 x 17 cm LH 20 column with water at a flow rate of 15 ml/min at room temperature.

Fraction collection was initiated 50 minutes after layering the TNBS/TNP-ATP reaction mixture onto the column. The eluent was directed through a flow cell (path-length = 2 mm) for absorbance readings at 360 (...) and 408 nm (---). Aliquots (5 ul) were taken for radioactive determination (●).

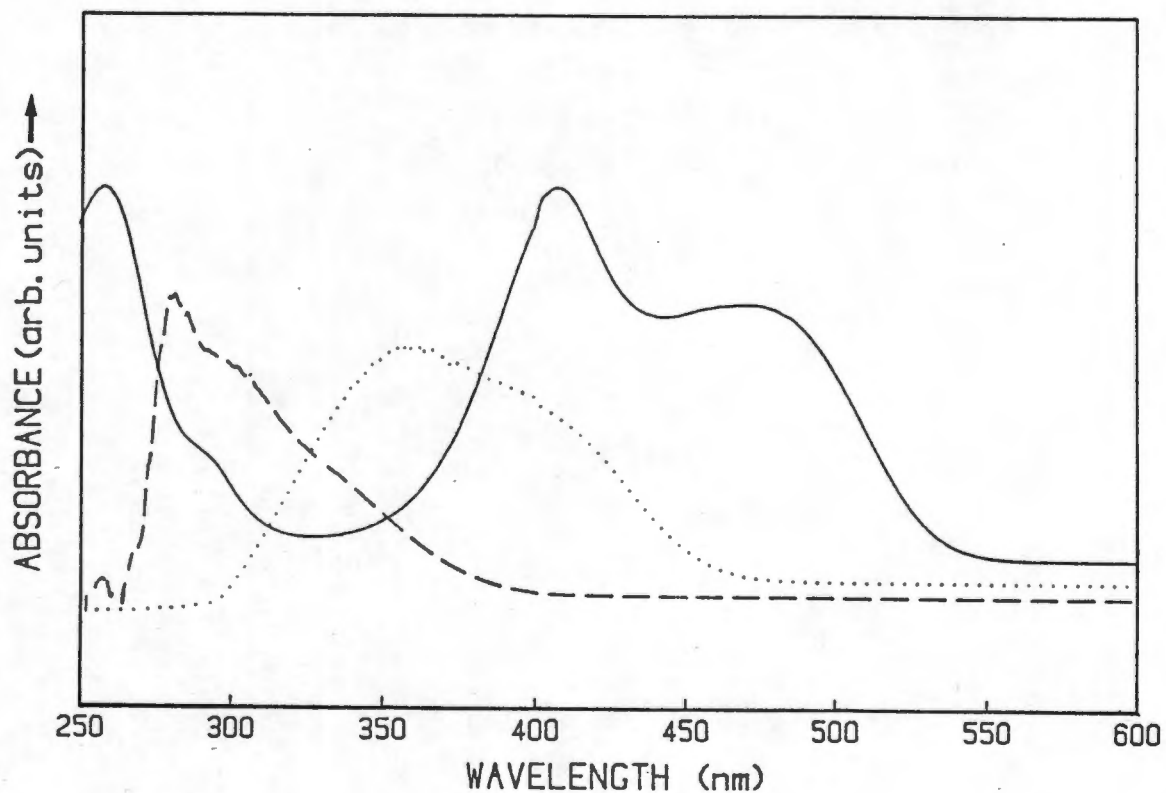


**Figure 2.3** Absorbance profiles of reactants and reaction products during synthesis of TNP-ATP

Absorption scans in 100 mM Tris-Cl, pH 8.0 were: TNBS (dashed line); picrate (dotted line); and TNP-ATP (solid line).

layer chromatography on DEAE-cellulose plates with 2 M formic acid and 0.5 M LiCl, and then scanned for radioactivity on a gas-flow proportional counter (Dunnschicht-scanner II).

Fractions containing [ $^{14}\text{C}$ ]TNP-ATP ( $R_F = 0.08$ ), and absorption profiles resembling those of [ $^{14}\text{C}$ ]TNP-ATP in the 300 to 500 nm range, were pooled and freeze-dried. Water-free [ $^{14}\text{C}$ ]TNP-ATP was reconstituted in acetone at 0 to 4°C, and centrifuged at 3000rpm for 5 min to remove picrate. This procedure was repeated 5 to 10 times until the supernatant was clear of the yellow stain of picrate. Radioactivity of aliquots of the supernatant was virtually undetectable, confirming the poor solubility of [ $^{14}\text{C}$ ]TNP-ATP in acetone. Acetone was removed from the [ $^{14}\text{C}$ ]TNP-ATP pellet by evaporation under a weak jet of nitrogen gas. [ $^{14}\text{C}$ ]TNP-ATP was reconstituted in 1 mM Mops-Tris, pH 7.0, and its identity confirmed on TLC (Fig. 2.4). Scans showed contamination with less than 5% TNP-ADP and less than 0.5% [ $^{14}\text{C}$ ]ATP.

Concentration of the nucleotide was determined as above. Aliquots of [ $^{14}\text{C}$ ]TNP-ATP, pH 7 were stored at -20°C and remained stable for periods of 3 to 6 months. [ $^{14}\text{C}$ ]TNP-ATP was repurified after accumulation of breakdown products during storage, by elution from a 2.5 x 12 cm LH20 column. The dehydration and acetone-wash steps were then omitted.

Unreacted [ $^{14}\text{C}$ ]ATP was reclaimed from the initial 15 fractions by the same procedure for purification of [ $^{14}\text{C}$ ]TNP-ATP above. This was then reutilized for further synthesis of [ $^{14}\text{C}$ ]TNP-ATP.

## 2.3 ANALYTICAL METHODS

### 2.3.1 RADIOACTIVE LIGAND BINDING

Binding was performed by filtration, according to the method of Guillain et al.(1982). SRV were diluted into buffers containing varying concentrations of isotope and filtered under vacuum (220 -400 mm Hg) through Millipore HA 0.45 micron paper or GF/F glass-fibre filters, where stated. Controls showed that more than 98% of SRV adsorb to these filters, when filter surface area is subsaturated (SRV < 0.5 mg). Filters were removed under vacuum to prevent isotope back flow from the surface of the sintered glass filter holder. [<sup>3</sup>H]Sucrose (250 cpm/nmol) was used at low concentrations (1 mM) to determine filter wet volumes, required for determination of the amount of unbound ligand present on the filter. Radioactivity on the filters was quantitated by liquid scintillation counting, using Insta-Gel (Packard Instruments International). Counts were determined separately in the ranges for tritium and <sup>14</sup>C or <sup>45</sup>Ca<sup>2+</sup>. Correction of overflow from the <sup>14</sup>C and <sup>45</sup>Ca<sup>2+</sup> ranges into the <sup>3</sup>H range, caused by quenching of scintillant emission by TNP-ATP, and salt containing buffers, was performed by calibrating these ranges with known samples of <sup>3</sup>H and <sup>14</sup>C (Beckman), containing various quenching agents to obtain true disintegrations per minute.

Filter volume was calculated according to equation 1,

$$\text{Residual volume (R)} = D \times B / C \quad \dots\dots\dots 1$$

where D = experimental <sup>3</sup>H cpm, corrected for overflow of <sup>14</sup>C cpm into the <sup>3</sup>H range as described above, B = volume (in microliters) <sup>3</sup>H taken from buffer containing [<sup>3</sup>H]sucrose, and C = cpm <sup>3</sup>H in B. Filter volumes were found to be approximately 30 ul for paper, and 90 ul for glass fibre

filters.

Binding to the SRV on the filter was determined according to equation 2,

$$\text{Bound} = (I - (R \times H \times A / (E \times F)) \times 1000 \times E \times F / (M \times H)..2.$$

where bound isotope is expressed in nmol/mg,

I = experimental  $^{14}\text{C}$  cpm, R = residual volume in ul from equation 1, A = final concentration of  $^{14}\text{C}$  in each buffer, M = mg SRV, F = stock  $^{14}\text{C}$  concentration (uM), E = volume of stock  $^{14}\text{C}$  taken from F, and H = cpm of stock  $^{14}\text{C}$  of volume E and concentration F. Essentially,  $H / F \times E$ , is the specific activity of the isotope used in nmol/ml, but calculations were more easily used by keeping the terms separate.

a)  $^{14}\text{C}$ TNP-ATP binding

SRV (0.5 mg) were added to preparations of [ $^{14}\text{C}$ ]TNP-ATP from 0.01 to 10 uM, in volumes of standard buffer, ranging from 20 to 1 ml respectively, equilibrated for 30 seconds at 25°C and filtered on Gf/F filters. Non-specific filter binding was observed for Millipore 0.45 micron filters, and gave 50% higher TNP-ATP binding. Glass-fibre filters showed virtually no non-specific TNP-ATP binding.

$^{14}\text{C}$ ATP binding was performed by the same method as above. SRV were added to preparations of varying concentrations of [ $^{14}\text{C}$ ]ATP in 0.5 mM EGTA and standard buffer at pH 7.0 and 25°C, and filtered on millipore 0.45 micron filters after 30 sec.

$^{45}\text{Ca}^{2+}$  binding was performed with preparations of  $^{45}\text{Ca}^{2+}$  buffered with EGTA for various free [ $\text{Ca}^{2+}$ ], according to the calculations of Schwartzbach (1957), at 5 mM  $\text{MgCl}_2$  and pH 7.0.

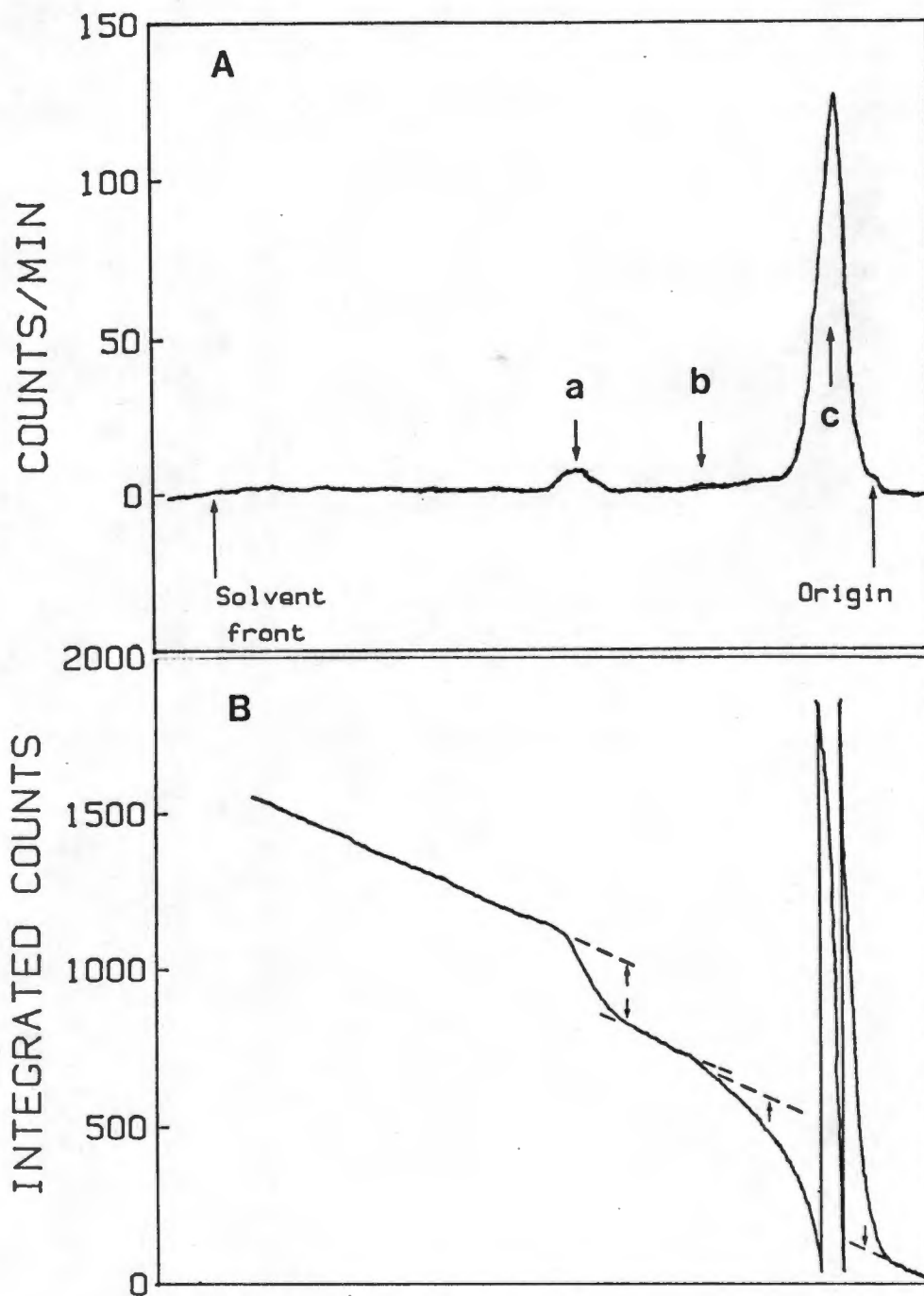


**Figure 2.4** Radioactivity scans of TNP-ATP by thin layer chromatography

TNP-ATP (approx. 5 nmol) was spotted on to TLC plates, and developed in 2 M formic acid and 0.5 M LiCl. Dried plates were scanned for total counts/min (A) where a is TNP-ADP; b is ATP ; and c is TNP-ATP. Integrated counts/min (B) were measured on the same plate. Arrows represent the integrated range of counts/min for a, b, and c.

b) [<sup>14</sup>C]TNP-ATP COLUMN BINDING METHOD

TNP-ATP binding stoichiometry was measured by passing SRV (mg/ml) in the presence of excess TNP-ATP, through a 5 x 0.5 cm Sephadex G 25 column, and eluted with 20 mM Tris-maleate, pH 8.0, were collected and assayed for protein content by the Lowry method (Oosta et al, 1978), and for radioactivity as above.

2.3.2 FLUORESCENCE MEASUREMENTS

FLUORIMETER CALIBRATION Wavelength calibration of the Aminco-SPF 500 spectrofluorimeter was performed by scanning the excitation transmission profile of Holmium Oxide Standard (Hewlett Packard) (Fig. 2.5). The emission wavelengths were matched to the excitation grating wavelengths through a front-face mirror placed at 45° in the cuvette holder. Wavelengths were found to be consistent in the ultraviolet range, but 2 to 3 nanometers red-shifted in the range 400 to 500 nm, and were corrected accordingly.

Fluorescence titrations were performed at 25°C under continuous stirring in 100 mM Mops-Tris, pH 7.0, 5 mM MgCl<sub>2</sub>, 100 uM CaCl<sub>2</sub>, using 0.1 mg/ml SRV, and 2 uM TNP-ATP, unless otherwise stated. Excitation and emission wavelengths were 415 and 525 nm respectively at 10 nm bandpasses. Fluorescence binding titrations were corrected for the attenuation of the excitation light intensity by unbound TNP-ATP, by standard correction for inner filter effects as described by Lakowicz (1983). Changes in absorbance for the addition of other ligands were negligible.

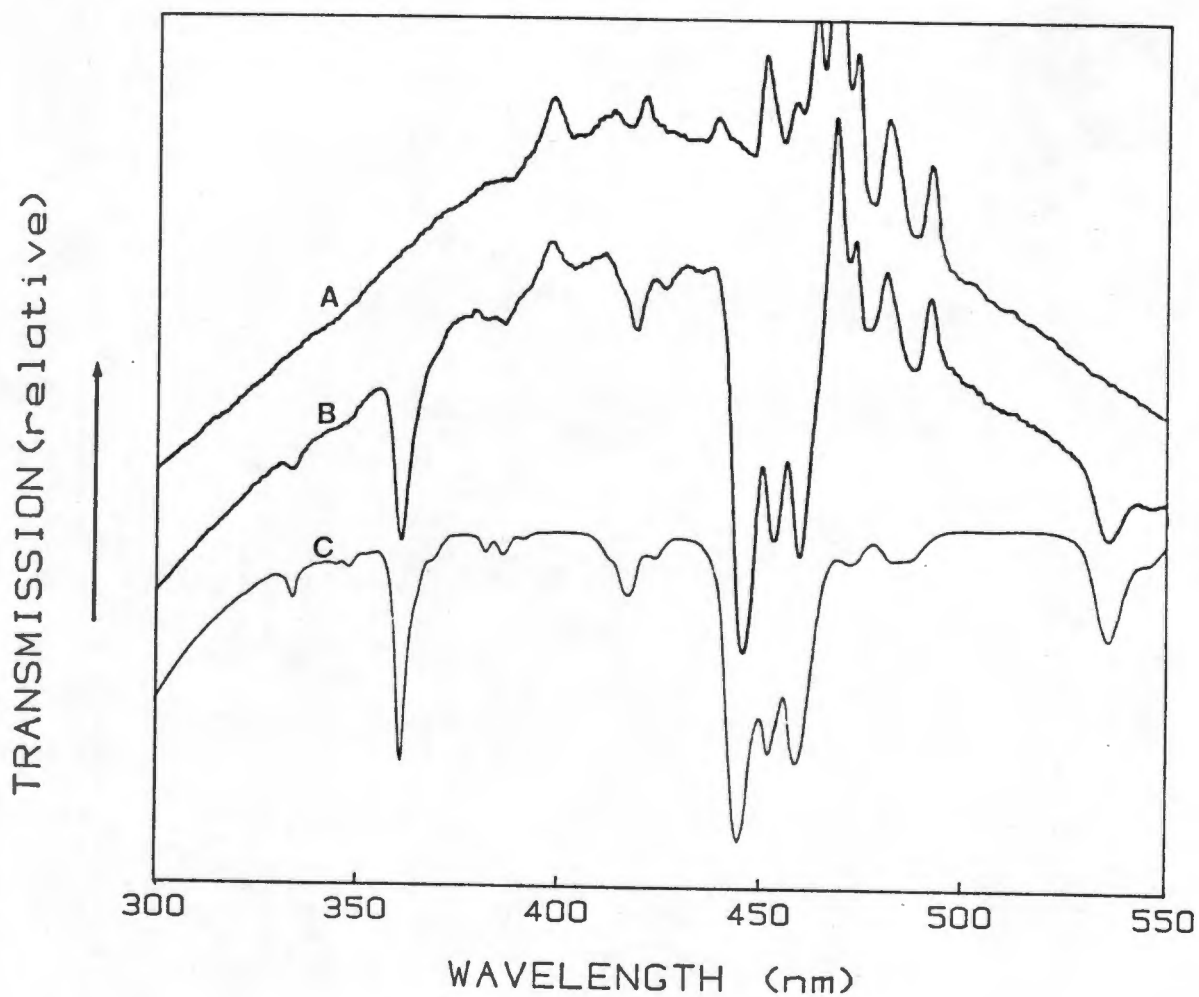


Figure 2.5 Spectrofluorimeter wavelength calibrations

Trace (A) represents the transmission scan output of the SPF-500 spectrofluorimeter Xenon lamp. Wavelength calibration was performed by placing a Holmium Oxide filter across the excitation lightpath (B). Trace (C) is the transmission spectrum of the Holmium oxide filter as measured on a HP 8450A spectrophotometer.

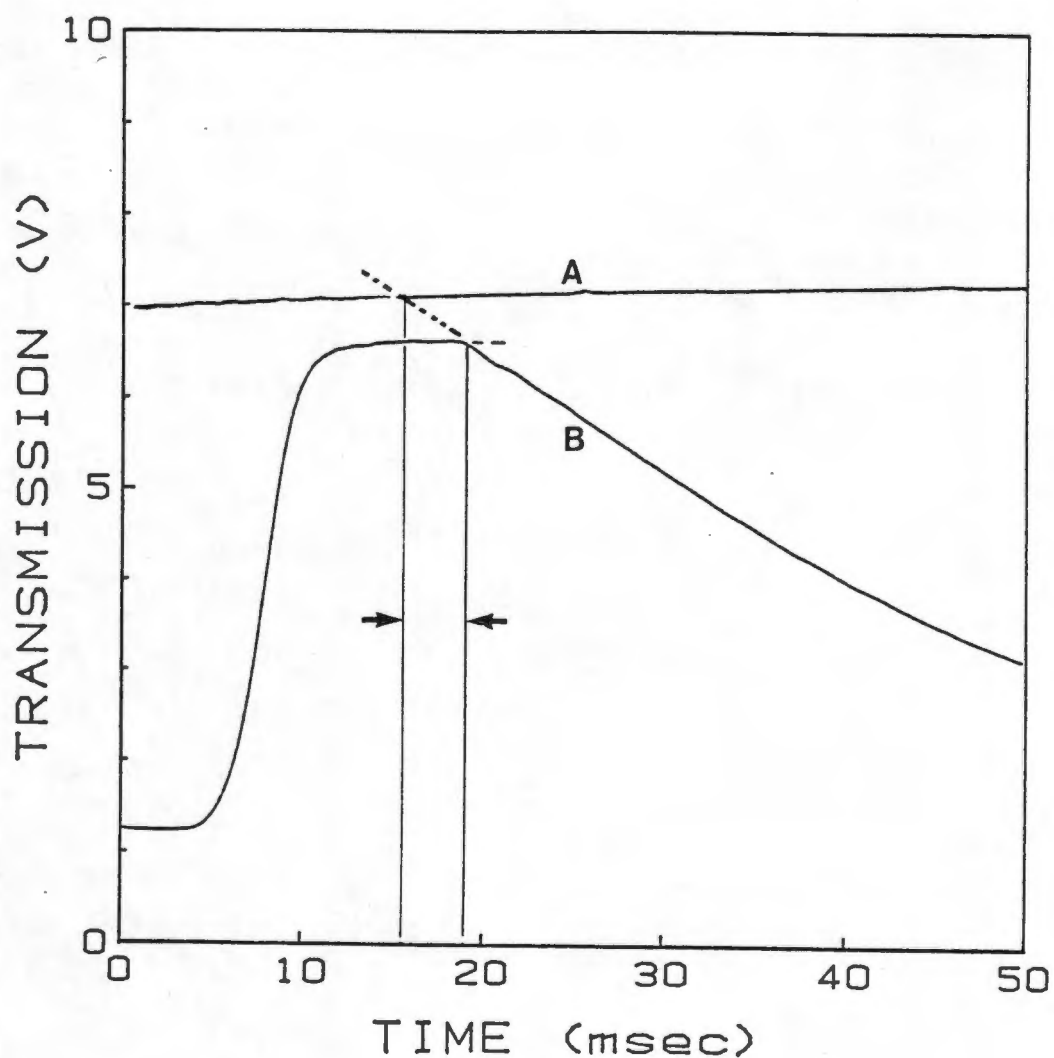


Figure 2.6 Calibration of the dead time of the stopped flow fluorimeter

Contents of syringe A, containing 0.1 M KSCN, were mixed with those of syringe B containing 0.01 M  $\text{Fe}(\text{NO}_3)_3$  in 0.1 N  $\text{H}_2\text{SO}_4$ . Transmission was monitored at 450 nm at room temperature. Trace A represents transmission of either of the components of syringe A and B, alone and represents 100% transmission. Extrapolation of the linear portion of the descending trace B back to A (dotted line) gave the mixing time (between arrows).

2.3.3 KINETIC MEASUREMENTS were performed on a Dionex D-110 stopped-flow fluorimeter equipped, with a 375 W Tungsten lamp. Excitation wavelengths were selected at 418 nm through the standard Durrum grating, and further filtered through a 405 nm cut-on filter. Emission wavelengths were selected through a 530 nm cut-on filter. The dead time of the instrument was measured to be 3.44 msec (Fig. 2.6).

The photomultiplier tube output voltage was stored on a Hewlett Packard HP 7090 storage voltmeter, capable of a high frequency resolution of 3 KHz. The time constant response on the Dionex apparatus was set to approximately 0.1 of the reaction time constant. Two hundred data points were transferred to an HP 85 computer, and fitted to an single exponential equation of the form, fluorescence =  $A + Be^{(-kt)}$ , where A and B are constants, by an iterative nonlinear least squares procedure, programmed in Basic. The observed first order rate constants from this fit are referred to as  $k_{obs}$ .

2.3.4 ABSORBANCE MEASUREMENTS were performed on an HP 8450 Diode Array spectrophotometer, using wavelength calibration of a Holmium Oxide sample,  $Ho_2O_3$  (Hewlett Packard) (trace C, Fig. 2.5). Binding of TNP-ATP was measured by differential spectroscopy, using an Aminco-DW2 dual wavelength spectrophotometer, by the absorbance difference at 460 and 510 nm, according to the method of Watanabe and Inesi (1982).

2.3.5 ATPase ASSAYS were performed by two methods.

a) pH STAT measurements were performed using a Radiometer PHM 82 standard pH meter, with standard pH electrodes, ABU 80 Autoburette, TTT 60 titrator, and TTA 80 titration assembly, which were interfaced to an Apple II computer. The medium, 4 ml, contained 0.25 M sucrose, 5 mM  $MgCl_2$ , 0.1 mg/ml SR, 3.2  $\mu M$  A23187, 100  $\mu M$   $CaCl_2$ , 50  $\mu M$  diadenosine pentaphosphate (to inhibit myokinase activity), and various concentrations of KCl, NaCl and valinomycin. The medium at

25°C was maintained at pH 8 by titration with NaOH (final  $[Na^+] < 2$  mM). Calculations of ATPase activity were based on a calibrated value of 0.96 mol of  $H^+$  released per mol ATP hydrolysed at pH 8.0. Calibration of the titrator and NaOH were performed with standard 0.1 M HCl. Basal ATPase activity was not effected by the addition of 100 mM KCl or of up to 15  $\mu$ M valinomycin.b) NADH coupled ATPase assays were performed on an Aminco-DW2 spectrophotometer. NADH disappearance was monitored at 340 nm in a coupled enzyme assay including phosphoenolpyruvate, pyruvate kinase and lactate dehydrogenase according to the method of Horgan et al., (1972). The reaction mixture (2.5 ml) contained 20 mM Mops-C1 pH 7.0, 100 mM KCl, 5 mM  $MgCl_2$ , 0.5 mM EGTA 2.6 mM PEP, 0.1 mM NADH, 8 U/ml pyruvate kinase, 8 U/ml lactate dehydrogenase and 10 to 20  $\mu$ g SRV, with 4% (w/w) A23187 to Ca-ATPase. The reaction was initiated by the addition of ATP (100  $\mu$ M) and basal activity measured, followed by the addition of 0.5 mM  $CaCl_2$  (free  $Ca^{2+} = 11.2$   $\mu$ M) for Ca-ATPase activity. ATPase activity was calculated using the molar extinction coefficient of 6.22 for NADH. SRV previously incubated in NEM in the presence of AMP-PNP, were diluted into the above assay medium giving a  $[AMP-PNP]_{final} = 100$   $\mu$ M.

2.3.6  $^{45}Ca^{2+}$  UPTAKE measurements were performed by millipore filtration using a transport medium of 100 mM Mops-Tris pH 7.0, 0.05 to 0.1 mg/ml SRV, 5 mM  $MgCl_2$ , 5 mM Tris-oxalate (pH 7.0), 0.5 mM EGTA, 0.5 mM  $^{45}CaCl_2$  (3000 cpm/nmol). The free  $Ca^{2+}$  concentration was calculated to be 11.2  $\mu$ M, using a stability constant,  $K_{CaEGTA}$ , of  $10^{11}$  (Schwartzbach et al., 1957). The reaction, at 25°C was initiated by the addition of ATP (250  $\mu$ M), terminated at 10 and 20 seconds by filtering an aliquot (300  $\mu$ l) through a Millipore filter (HA 0.45 micron) (Martonosi and Feretos, 1964) and washed with 20 mM imidazole, pH 6.0 and 5 mM  $CaCl_2$ .

Fluorescence Ca<sup>2+</sup> uptake measurements were performed as for <sup>45</sup>Ca<sup>2+</sup> uptake above. These results were compared to times taken to decrease TNP-ATP (2 uM) fluorescence under the same conditions using 0.1 mg/ml SRV, to which were added 150 nmol CaCl<sub>2</sub> in 5 mM Tris-oxalate in the absence of EGTA (see fluorescence methods above).

### 2.3.7 [<sup>32</sup>P]EP LEVELS

Phosphoenzyme levels were measured with [ $\gamma$ -<sup>32</sup>P]ATP or [<sup>32</sup>P]Pi by phosphorylation, acid quenching and filtration as previously described (Lacapere *et al.*, 1981). The reactions were initiated by the addition of [ $\gamma$ -<sup>32</sup>P]ATP (100 uM) (500 to 1500 cpm/nmol), to the medium containing 0.4 mg/ml SRV in 100 mM Mops-Tris pH 7.0, 50 uM CaCl<sub>2</sub>, 5 mM MgCl<sub>2</sub>, at 25°C for 5 min. Alternatively, the enzyme was phosphorylated with [<sup>32</sup>P]Pi (5 mM, 2000 x cpm/nmol) in 10% Me<sub>2</sub>SO, 0.5 mM EGTA, as above for 30 sec. The reaction mix (400 ul) was quenched by adding 2 ml 0.25 M PCA with 15 mM Pi, incubated at room temperature for 15 min, and washed with 50 volumes of 0.125 M PCA and 15 mM Pi on GF/C glass-fibre filters. The filters were further washed directly after removal of the funnel apparatus to remove any unbound <sup>32</sup>Pi. Radioactivity was determined by liquid scintillation counting in 6 ml Instagel (Packard). Background radioactivity was less than 10% of total radioactivity.

Kinetic measurements were performed on a Dionex d-133 multimix apparatus equipped with three reaction syringes. One volume each of syringe A and B containing SRV and [ $\gamma$ -<sup>32</sup>P]ATP (3000 to 5000 dpm/nmol) were mixed and aged in a 450 uL reaction coil for 4 seconds. The third syringe (C), containing 2 volumes of 10 mM Mg.ADP and 1 mM EGTA, was mixed with the 4 second-aged A plus B mixture, and 400 to 600 uL was collected in the sample collect syringe, containing 500 uL PCA quench solution (Fig. 2.7).

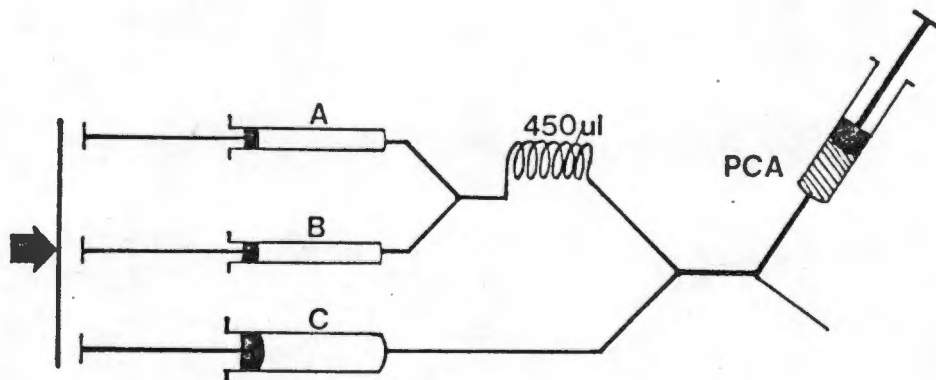


Figure 2.7 Configuration of the Dionex rapid mix apparatus.

A Dionex D-133 three syringe multimixing instrument was effectively used as a 4 syringe rapid mixing device. PCA (0.5 ml), usually placed in syringe C to quench reactants of mixed A and B, was instead placed in the take-up syringe and quenched the mixture of A, B and C within 40 msec. The flow rate was 5 ml/sec and the volume displaced between mixing A, B and C was 0.10 ml. The apparatus in this configuration was utilized for reactions with a time resolution of greater than 200 msec.

### 2.3.8 NEM modification

SRV (2 mg/ml) were derivitized under standard conditions of 400  $\mu$ M NEM, 50  $\mu$ M  $\text{CaCl}_2$ , 1 mM AMP-PNP, 100 mM Mops-Tris, 5 mM  $\text{MgCl}_2$ , pH 7.0 at 25°C. The reaction was stopped by 1 in 20 dilution into fluorescence,  $\text{Ca}^{2+}$  uptake and ATPase assays, the final NEM concentrations (20  $\mu$ M) was too low to further derivitise -SH groups for the duration of the assays.

Control studies of SRV, incubated under the same conditions for 50 minutes in the absence of NEM, showed a maximal loss of 5 % activity. KCl was omitted from incubations and has previously been shown to alter neither the extent nor specificity of NEM modification (Yamada and Ikemoto, 1978).

[ $^3\text{H}$ ]NEM modification was determined as above, and the reaction was stopped by a 10-fold (v/v) addition of 0.25 M PCA, followed by filtration on GF/F glass-fibre filters, and washed with 0.125 M PCA. Radioactivity was determined by liquid scintillation counting in 6 ml Instagel.

2.3.9 Binding parameters were calculated by an iterative non-linear least squares procedure according to the method of Wilkinson (1961).

### 3.0 RESULTS

#### 3.1 THE INTERACTION OF TNP-ATP WITH THE $\text{Ca}^{2+}$ -ATPase

Fluorescence of the ATP analogue, TNP-ATP, is strongly polarity dependent. TNP-ATP has a high extinction at 408 nm (Fig. 2.3). TNP-ATP fluoresces with a low quantum yield, and a emission maximum = 560 nm, in buffer at pH 7.0. The emission peak is blue shifted to 535 nm on the addition of non-phosphorylated SRV, with a moderate increase in quantum yield consistent with the finding that TNP-ATP binds to a relatively hydrophobic site on the enzyme (Watanabe and Inesi, 1982; Dupont et al., 1982; Bishop et al., 1984), that has a dielectric constant equivalent to that of glycerol ( $D = 42.5$ ) (Moczyldowski and Fortes, 1981). Phosphorylation of the enzyme by ATP further blue-shifts the emission maximum to 528 nm, with a 3.5-fold increase in fluorescence quantum yield (Fig. 3.1). The identical blue-shift also occurs upon phosphorylation by  $\text{P}_i$  in the absence of  $\text{Ca}^{2+}$ . The dielectric constant of the probe microenvironment is equivalent to that of a dimethylformamide solution ( $D = 24$ ), (Moczyldowski and Fortes, 1981).

The above results are consistent with previous findings of the interaction of TNP-ATP with sites on the phosphorylated enzyme (Watanabe and Inesi, 1982; Dupont et al., 1982b). The ATP-dependent enhanced fluorescence decayed relatively slowly, and was restored by re-addition of ATP, (Fig. 3.2 a) consistent with the previously reported phosphoenzyme-dependence of TNP-ATP fluorescence (Watanabe and Inesi, 1982; Nakamoto and Inesi, 1984; Bishop et al., 1984). The fluorescence level induced by the second ATP addition did not return to the initial levels as the first for a number of possible reasons. ATP and/or ADP may be competing with TNP-ATP for the nucleotide binding site.

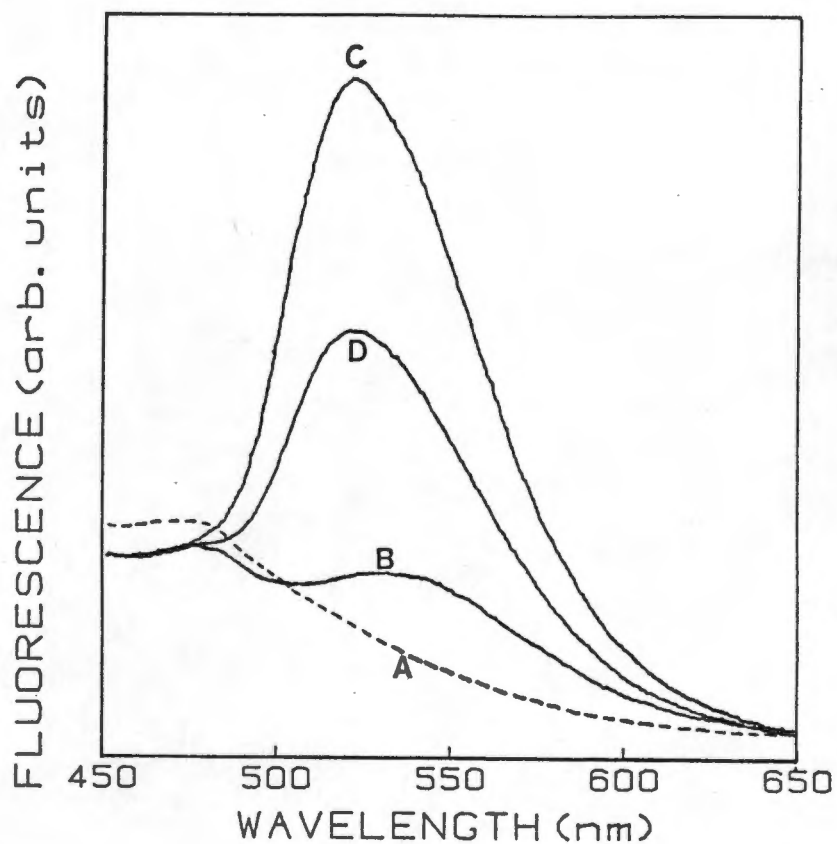


**Figure 3.1.** Fluorescence emission spectra of TNP-ATP bound to phosphorylated and non-phosphorylated enzyme

Fluorescence emission scans of 0.1 mg/ml SRV in 0.1 M Mops/Tris, pH 7.0, 50  $\mu\text{M}$   $\text{Ca}^{2+}$ , 5 mM  $\text{MgCl}_2$  at 25°C, (broken line) at an excitation wavelength of 418 nm and bandpasses = 10 nm. Additions were: (E), 2  $\mu\text{M}$  TNP-ATP; (C), 250  $\mu\text{M}$  ATP; or (D), 5 mM Pi, with 1 mM EGTA added to A. Wavelengths for excitation and emission gratings were calibrated as described under "Methods".

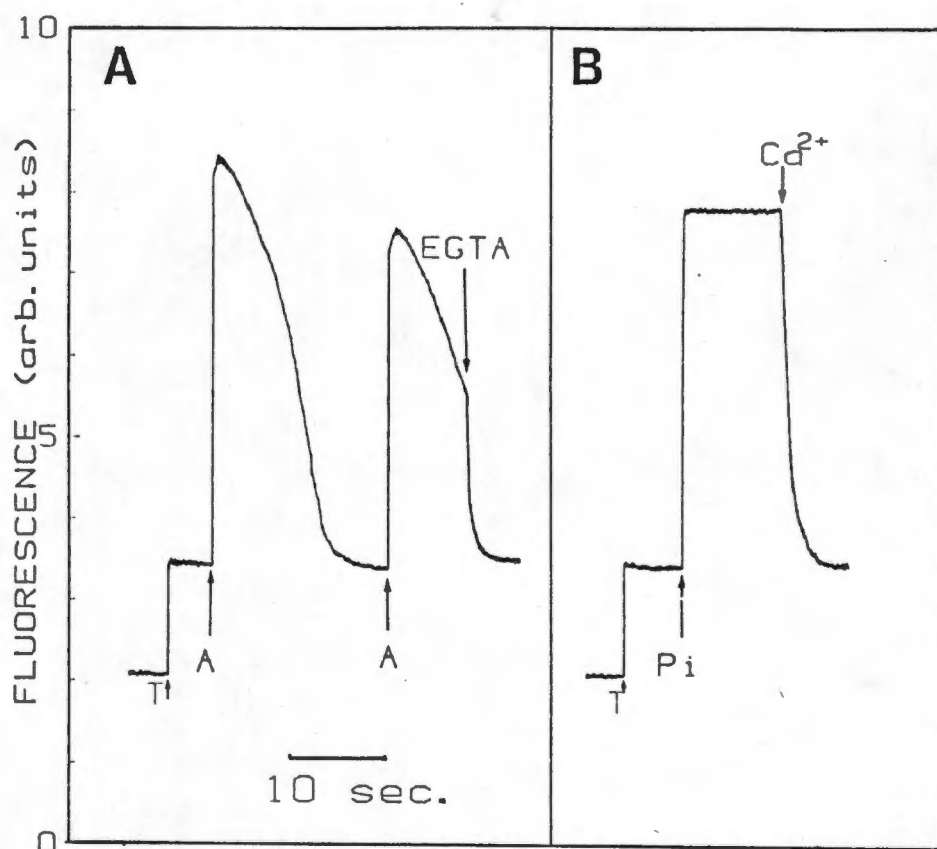


**Figure 3.2.** ATP and Pi-dependent TNP-ATP fluorescence

Fluorescence measurements were initiated in (A) by the addition of 0.1 mg/ml SRV to the cuvette containing 0.1 M Mops/Tris, pH 7.0, 50  $\mu\text{M}$   $\text{Ca}^{2+}$ , 5 mM  $\text{MgCl}_2$  at 25°C, followed by additions of 2  $\mu\text{M}$  TNP-ATP, (T); 66  $\mu\text{M}$  ATP, (A); and 1 mM EGTA. (B): SRV were added to 0.1 M Mops/Tris pH7.0, 10% (v/v) Me<sub>2</sub>SO, 100  $\mu\text{M}$  EGTA, 5 mM  $\text{MgCl}_2$ , followed by 5 mM Pi and 200  $\mu\text{M}$   $\text{Ca}^{2+}$ . Excitation and Emission wavelengths were 418 and 525 nm with bandpasses at 10 nm each.

Catalytic conditions have been altered in that free external  $\text{Ca}^{2+}$  levels are lower, due to sequestration inside vesicles. The vesicles have reached maximum  $\text{Ca}^{2+}$  capacity, and ADP and Pi levels have risen significantly. The latter factors may be termed 'product inhibition' for the forward reaction, according to deMeis and Vianna, (1979).

There was no observed enhanced TNP-ATP fluorescence in the presence of ATP and the absence of  $\text{Ca}^{2+}$  (in the presence of EGTA), consistent with the phosphoenzyme-dependence of enhanced fluorescence, as initially described by Watanabe and Inesi, (1982).

Phosphorylation of the enzyme by Pi maintains high TNP-ATP fluorescence from the equilibrium condition existing between Pi and  $\text{E}_2\text{-P}$  (deMeis *et al.*, 1980). The fluorescence is diminished to initial levels by the addition of  $\text{Ca}^{2+}$  (Fig. 3.2 b), due to dephosphorylation of the enzyme in the forward reaction (steps 6 and 7, Scheme I).

### 3.2 TNP-ATP BINDING AFFINITY AND STOICHIOMETRY

TNP-ATP binding affinity and site stoichiometry have previously been measured by spectrophotometric methods in studies that assume that the optical signals obtained are proportional to the fraction of TNP-nucleotide that is bound (Watanabe and Inesi, 1982; Dupont *et al.*, 1982). Since accurate stoichiometric measurements are crucial for attempts of model formulation, we have synthesised [ $^{14}\text{C}$ ]TNP-ATP for use in direct determination of TNP-ATP binding.

Fluorescence levels increase with the addition of increasing amounts of TNP-ATP to the non-phosphorylated enzyme (Fig. 3.3), with an apparent  $[\text{TNP-ATP}]_{0.5} = 0.35 \mu\text{M}$ , similar to previous findings (Watanabe and Inesi, 1982; Dupont *et al.*, 1982b). Corrections for the small contribution of fluorescence of soluble TNP-ATP and from non-specific TNP-ATP binding to phospholipids, were not applied.

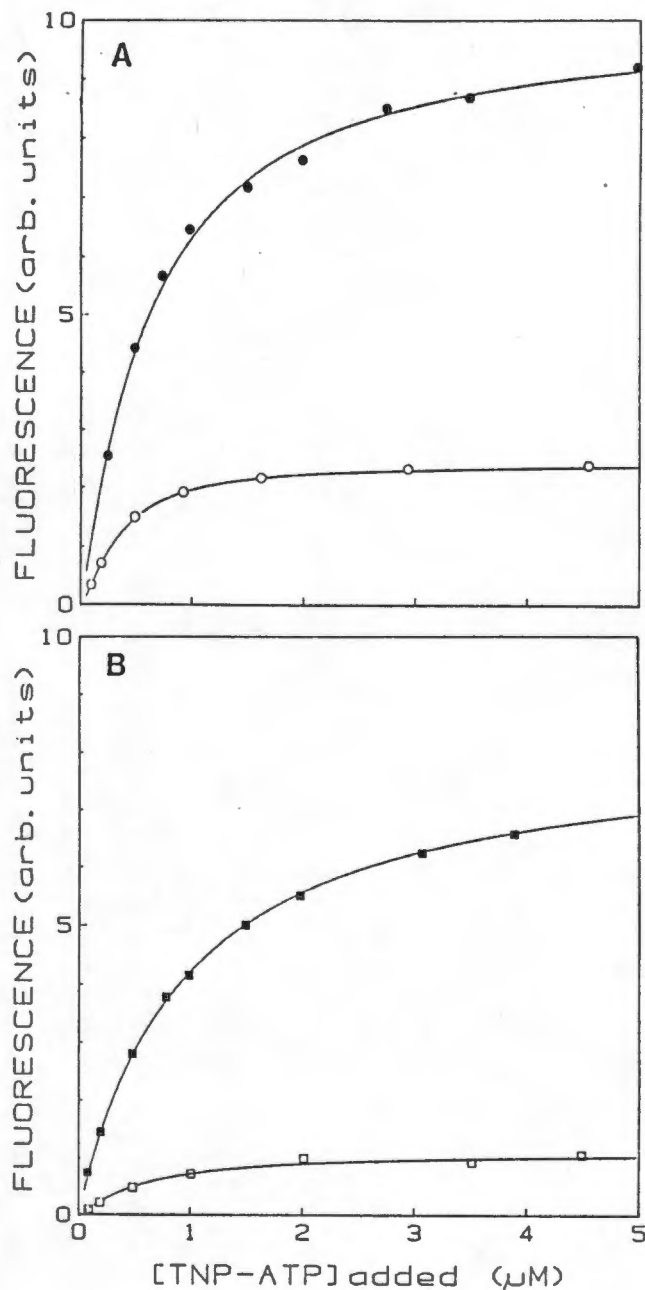


**Figure 3.3** Fluorescence measurements of TNP-ATP binding

Serial additions of TNP-ATP to 0.1 mg/ml SRV in 100 mM Mops/Tris, pH 7.0, 50  $\mu\text{M}$   $\text{Ca}^{2+}$ , 5 mM  $\text{MgCl}_2$ , in the absence, (open circles) or presence of 10  $\mu\text{M}$   $\text{ATP}^2$  (closed circles) with 20  $\mu\text{g/ml}$  creatine phosphokinase and 800  $\mu\text{M}$  creatine phosphate. The ATP regenerating system did not contribute to background fluorescence. B, fluorescence titrations were as above, using 10% (v/v)  $\text{Me}_2\text{SO}$  and 500  $\mu\text{M}$  EGTA, in the absence (open squares) or presence of 5 mM Pi (solid squares), added as a Tris salt, pH 7.0. Corrections for inner filter effects caused by increasing [TNP-ATP], were performed by measurement of absorbance at 418 and 528 nm after each TNP-ATP addition (see "Methods"). Fluorescence levels were not corrected for the contribution of unbound TNP-ATP. Excitation and emission wavelengths were 418 and 528 nm with 10 and 20 nm bandpasses respectively.

The apparent affinity of the enzyme site for TNP-ATP = 0.61  $\mu$ M under phosphoenzyme conditions initiated by low concentrations of ATP ( $< 10 \mu$ M) (Fig. 3.3).

Binding titrations on the Pi-induced phosphoenzyme showed a similar affinity, with  $[TNP-ATP]_{0.5} = 0.95 \mu$ M (Fig. 3.3b). The latter experiments were performed in the presence of 10% Me<sub>2</sub>SO in order to obtain high levels of E-P ( $3.05 \pm 0.16$  nmol/mg) from Pi at pH 7.0, consistent with findings of deMeis *et al.*, (1980). Cosolvents decrease the structure of water and decrease the Gibbs free energy of solvation of ligands (deMeis *et al.*, 1985). This may account for the small discrepancy that was found between  $[TNP-ATP]_{0.5} = 0.35$  and  $0.61 \mu$ M in the non-phosphorylated enzyme in the absence and presence of Me<sub>2</sub>SO respectively. These values differ from those reported in a recent study by Bishop *et al.*, (1986), in which TNP-ATP bound was expressed as a fraction of E-P total under the assumption that all phosphoenzyme species (E<sub>1</sub>-P and E<sub>2</sub>-P) induce fluorescence.

The stoichiometry of sites was measured by changes in the difference absorption spectrum at 460 and 510 nm for added TNP-ATP, (Fig. 3.4). Saturation of the absorbance changes occurred at 5.3 nmol/mg, consistent with previous findings (Watanabe and Inesi, 1982).

[<sup>14</sup>C]TNP-ATP binding was performed by equilibrium filtration studies. The accuracy of these titrations depends on measurement of the residual volume retained on each filter that allows a calculation of non-specific binding of TNP-nucleotides (see "Methods"). The affinity of the non-phosphorylated and the phosphorylated enzymes were found to be  $[TNP-ATP]_{0.5} = 0.12 \mu$ M and  $0.76 \mu$ M, respectively. The stoichiometry of TNP-ATP binding sites for the non-phosphorylated enzyme and phosphorylated enzymes were 5.2 and 5.6 nmol/mg respectively (Fig. 3.5), which is essentially in disagreement with previous studies of Dupont *et al.*, (1982

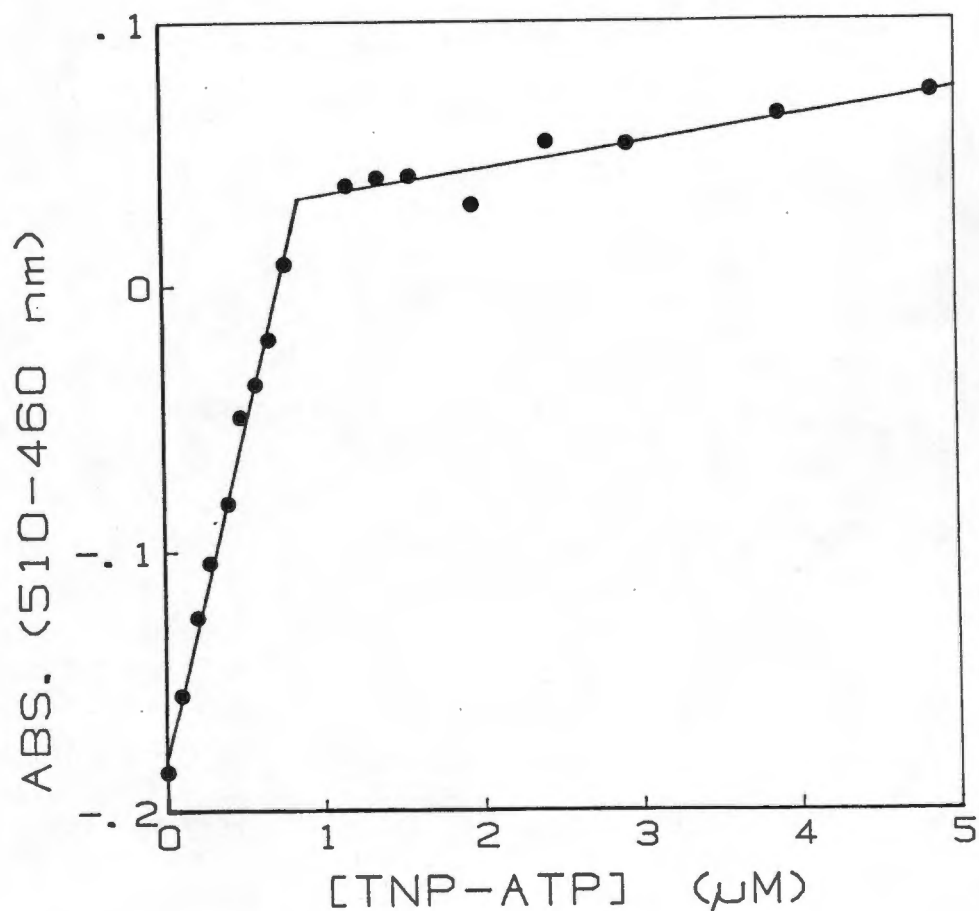


**Figure 3.4** Determination of TNP-ATP binding site stoichiometry by differential absorbance titration.

Difference spectra between the reference and sample were recorded from 450 to 520 nm in cuvettes of 5 cm pathlength. The difference between the peak at 520 and trough at 460 nm was plotted against the concentration of TNP-ATP added to both cuvettes. The buffer contained 20 mM Tris-maleate pH 8.0, 20 % (v/v) glycerol, 5 mM  $MgCl_2$ , 50  $\mu M$   $Ca^{2+}$  at 25°C and the sample cuvette contained 0.15 mg/ml SRV.

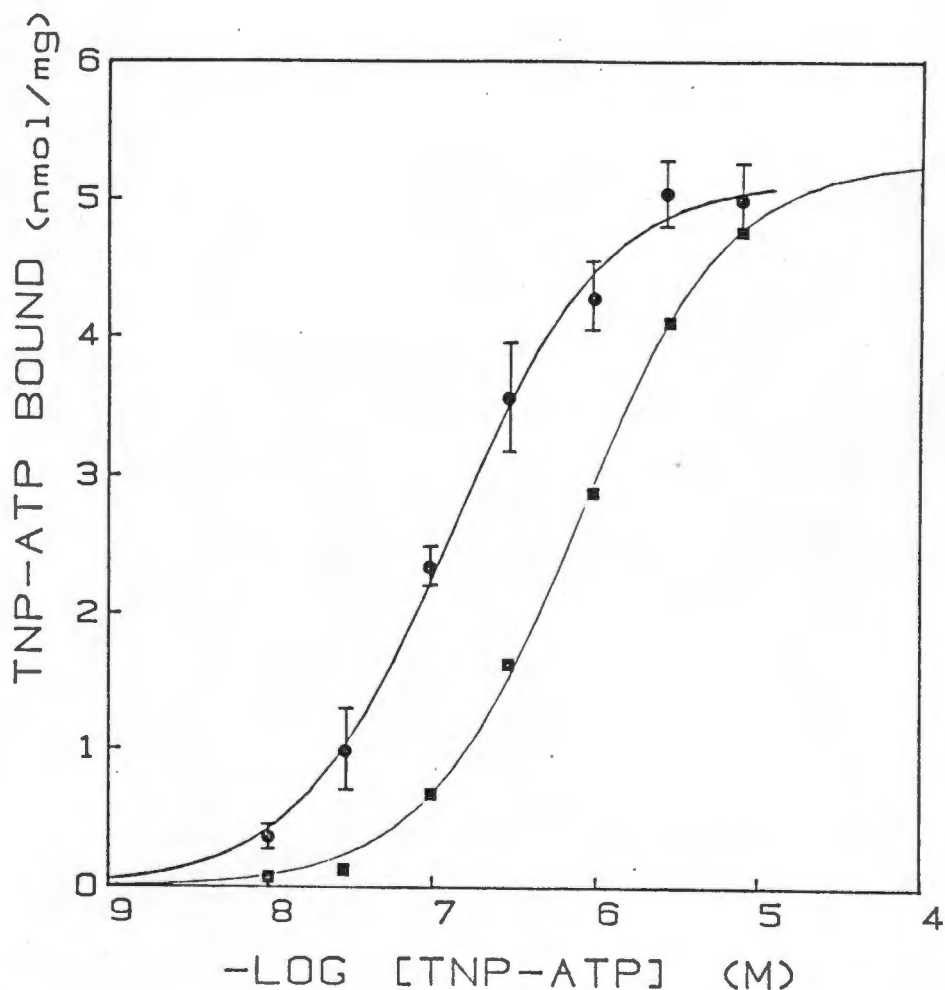


Figure 3.5 Binding of [<sup>14</sup>C]TNP-ATP to the phosphorylated and non-phosphorylated enzyme.

TNP-ATP binding was determined by filtration under the following conditions: 0.1 M Mops/Tris, pH 7.0, 5 mM MgCl<sub>2</sub>, 100 μM EGTA and 1 mM [<sup>3</sup>H]sucrose (250 cpm/nmol). SRV (0.3 mg) were added to the buffer preparations containing concentrations of 0.01 to 10 μM [<sup>14</sup>C]TNP-ATP (1 uCi/μmole) in buffer volumes of 20 to 1 ml respectively, and filtered under vacuum (closed symbols). Non-specific binding of [<sup>14</sup>C]TNP-ATP to the filter were corrected for blank values determined in the absence of SRV. Correction for buffer fluid, trapped on the filters, was calculated from <sup>3</sup>H counts of the labelled sucrose. Error bars represent standard deviations of 5 experiments. TNP-ATP binding to the phosphoenzyme in 10% Me<sub>2</sub>SO and 5 mM Pi, was determined under the same conditions (open symbols). Non-linear least squares fits for the non-phosphorylated and phosphorylated enzyme were: K<sub>d</sub> = 0.12 and 0.76 μM; Maximal binding = 5.2 and 5.6 nmol/mg and n<sub>H</sub> = 0.9 and 0.95 respectively.

and 1985), obtained by filtration of TNP- $[\gamma\text{-}^{32}\text{P}]\text{ATP}$  on millipore (HAWP 0.45 u) filters. In the present study, TNP-ATP has been shown to bind non-specifically to these filters to an extent equivalent to approximately 4 nmol/mg, which may account for the higher stoichiometries obtained in previous studies.

ATP and  $\text{Ca}^{2+}$  binding stoichiometries were measured on the same SRV preparation by filtration binding studies (Fig. 3.6).  $\text{Ca}^{2+}$  binds cooperatively,  $n_H = 1.74$  and with  $[\text{Ca}^{2+}]_{0.5} = 0.60 \text{ uM}$ , as found by Fernandes-Belda et al., (1984). ATP binding has a ten-fold lower affinity than TNP-ATP, ( $[\text{ATP}]_{0.5} = 1.72 \text{ uM}$ ) in agreement with previous studies (Guillain et al., 1984).

The stoichiometry for TNP-ATP is of the same order of magnitude as ATP binding (6.1 nmol/mg) and approximately half that for  $\text{Ca}^{2+}$  binding (11.2 nmol/mg), (Fig. 3.6), consistent with a stoichiometry of one mol/mol nucleotide binding in previous studies (Guillain et al., 1984; Cable et al., 1985). However, the above results were at variance with the stoichiometry found in previous studies (Dupont et al., 1982b) for ATP binding sites (3.2 nmol/mg) and which concluded that TNP-ATP binding stoichiometry is double that of ATP binding stoichiometry, and that two sites for TNP-ATP binding exist simultaneously on the non-phosphorylated enzyme. Table 3.1 shows a comparison of results obtained using labeled TNP-ATP and optical methods.

Values for stoichiometries fall into the range of 5 to 6 nmol/mg, that, in comparison to  $\text{Ca}^{2+}$  and ATP binding, are interpreted as one mol/mol binding. Bishop et al., (1984) have deduced, from kinetic studies, that TNP-ATP must leave its site before ATP can bind and phosphorylate. Our results confirm these conclusions that support the presence of only one family of nucleotide sites in the non-phosphorylated enzyme.

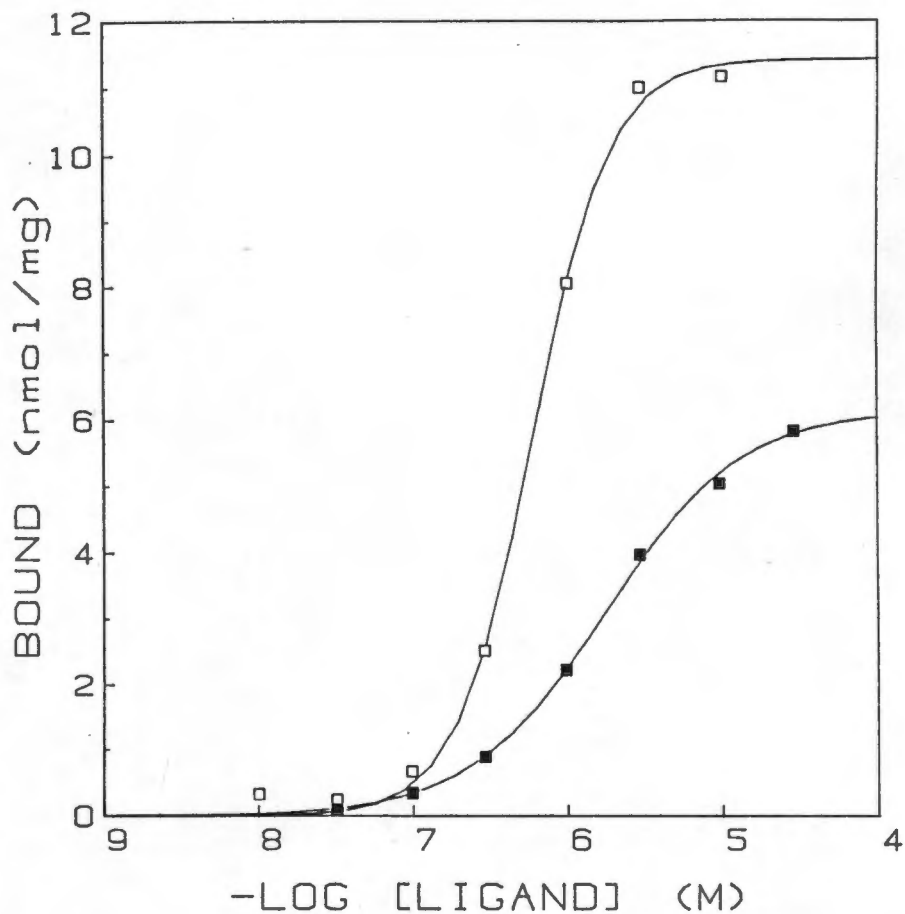


**Figure 3.6** Binding studies of  $\text{Ca}^{2+}$  and ATP to the non-phosphorylated enzyme

$^{45}\text{Ca}^{2+}$  (□) and  $[^{14}\text{C}]\text{ATP}$  (■) binding were performed under identical conditions and the same SRV preparation as in Fig. 3.5 Non-linear least squares fits for  $\text{Ca}^{2+}$  and ATP were: Maximal binding = 11.5 and 6.1 nmol/mg;  $K_{0.5} = 0.60$  and 1.72 uM and  $n_{-H} = 1.74$  and 0.90 respectively.

**TABLE 3.1**

Apparent Affinities ( $K_{0.5}$ ) and Stoichiometry (n) obtained for Ligands Binding by Various Experimental Techniques.

Ligand	Technique	$K_{0.5}$ (uM)	n (nmol/mg)
<u>Non phosphorylated enzyme</u>			
TNP-ATP <sup>a</sup>	fluorescence (EGTA)	0.35	-
TNP-ATP <sup>a</sup>	fluorescence (Me <sub>2</sub> SO)	0.61	-
TNP-ATP <sup>b</sup>	optical A. (EGTA)	-	5.3
[ <sup>14</sup> C]TNP-ATP <sup>c</sup>	filtration (EGTA)	0.12	5.2
[ <sup>14</sup> C]TNP-ATP <sup>d</sup>	column (EGTA)	-	5.4 ±0.07
<u>Phosphorylated enzyme</u>			
TNP-ATP <sup>a</sup>	fluorescence (ATP)	0.61	-
	fluorescence (Pi)	0.95	-
[ <sup>14</sup> C]TNP-ATP <sup>c</sup>	filtration (Pi)	0.76	5.6
[ <sup>14</sup> C]ATP <sup>e</sup>	filtration (EGTA)	1.72	6.1
<sup>45</sup> Ca <sup>c</sup>	filtration	0.60	11.2

Conditions were: a, as in Fig. 3.3; b, as in Fig. 3.4; c, as in Fig 3.5; d, as described under "Methods" ; e, as in Fig. 3.6. Hill coefficients ranged from 0.91 to 1.11 for all titrations except for Ca<sup>2+</sup> binding where  $n_H = 1.74$ .

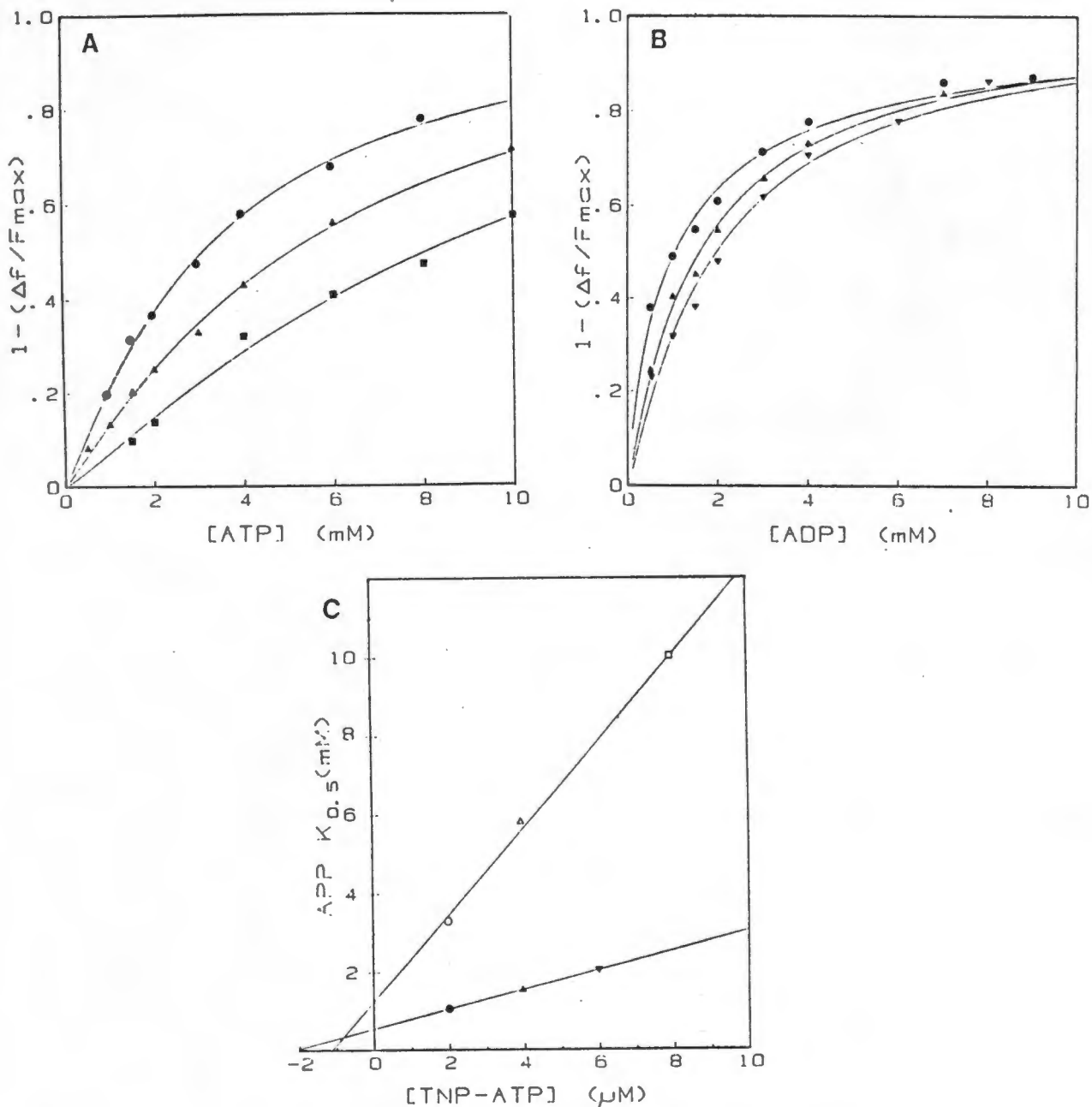


**Figure 3.7** Effects of millimolar ATP and ADP on TNP-ATP fluorescence

Experiments were initiated by addition of 20  $\mu$ M ATP to 0.1 mg/ml SRV in 20 mM Tris-maleate, pH 8.0, 20 % glycerol, and 2  $\mu$ M TNP-ATP, 50  $\mu$ M  $Ca^{2+}$ , 5 mM  $MgCl_2$ , 100  $\mu$ M creatine phosphokinase and 400  $\mu$ M creatine phosphate at 25  $^{\circ}$ C, followed by serial additions of  $Mg^{2+}$  salts of either (A), ATP or (B), ADP.  $\Delta f$  is the fluorescence change upon addition of the nucleotide and  $F_{max}$  is the total fluorescence that is inhibited by EGTA. Titrations were performed at various [TNP-ATP] : 2  $\mu$ M (●); 4  $\mu$ M (▲); 6  $\mu$ M (▼); and 8  $\mu$ M (■). In C, non-linear least squares fits of Mg.ATP (○) and Mg.ADP (●) were plotted against [TNP-ATP] and intercepted at  $K_m$  values of 1.25 and 0.54  $\mu$ M respectively, while  $K_i$ , on the abscissa, was 1.2 and 2.0  $\mu$ M respectively.

### 3.3 THE EFFECTS OF MILLIMOLAR ATP AND ADP ON TNP-ATP FLUORESCENCE

Previous studies have shown that the  $\text{Ca}^{2+}$ -ATPase possesses a regulatory site that is stimulated by ATP binding, with  $[\text{ATP}]_{0.5} = 1$  to 2 mM (McIntosh and Boyer, 1983). The phosphorylated catalytic site has a low affinity binding site for ADP in the  $\text{E}_1\text{-P}$  conformation, which supports covalent attachment of  $\text{P}_i$  to ADP to form ATP (deMeis and Vianna, 1979). Subsequent studies have implicated these sites as being responsible for enhanced TNP-ATP fluorescence (Watanabe and Inesi, 1982; Dupont *et al.*, 1982; Nakamoto and Inesi, 1984). In the present study, these proposals have been further explored by equilibrium binding and kinetic studies.

High concentrations ( $> 8$  mM) Mg.ATP and Mg.ADP decreased steady-state turnover TNP-ATP fluorescence signal by 90% (Fig. 3.7a and 3.7b). Phosphoenzyme levels are slightly decreased by these concentrations of ATP (Chaloub and deMeis, 1980), and decreased 60% by ADP (Shigekawa and Dougherty, 1978; Shigekawa and Akowitz, 1979). The  $[\text{ATP}]_{0.5}$  was found to be 3.4 mM at 2  $\mu\text{M}$  TNP-ATP. Increasing  $[\text{TNP-ATP}]$  from 2 to 8  $\mu\text{M}$  decreased the apparent affinity of ATP ( $[\text{ATP}]_{0.5} = 10$  mM), consistent with a competitive type of inhibition (Fig. 3.7a). A similar effect for ADP, with higher affinity, is seen in Fig. 3.7b. Linear regressions fitted through the apparent  $[\text{ATP}]_{0.5}$  and  $[\text{ADP}]_{0.5}$  extrapolated to 0  $\mu\text{M}$  TNP-ATP, intercepted at 1.25 and 0.54 mM respectively (Fig. 3.7c), and are consistent with previous values obtained for the low affinity nucleotide binding sites of the phosphorylated enzyme (McIntosh and Boyer, 1983; Pickard and Jencks, 1984, respectively). The apparent  $K_i(\text{TNP-ATP})$  was 1 to 2  $\mu\text{M}$  for inhibition of ATP and ADP effects, (Fig. 3.7c). Millimolar ATP and ADP concentrations also decreased  $\text{P}_i$ -induced TNP-ATP fluorescence in the absence of  $\text{Ca}^{2+}$  (data not shown), consistent with a competitive model

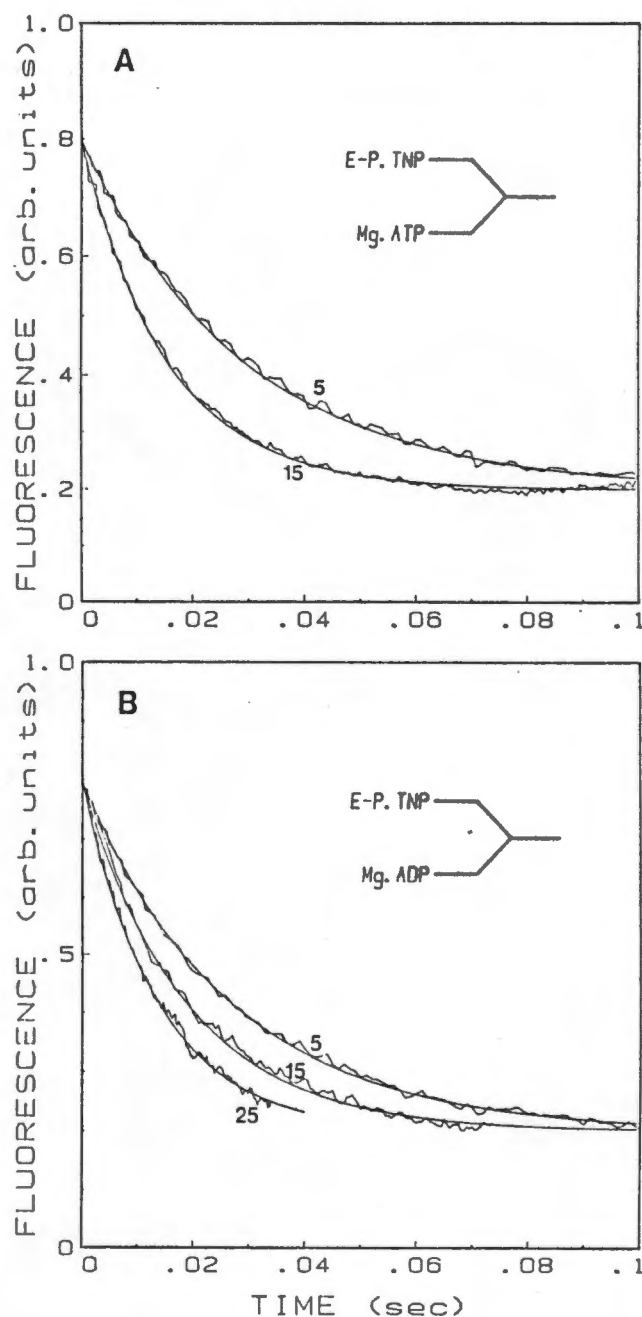


**Figure 3.8** Rates of decrease of TNP-ATP fluorescence upon the addition of Mg.ATP and Mg.ADP

Stopped flow measurements were performed under the same conditions as in Fig. 3.7. A: Syringe A contained 0.2 mg/ml SRV and 4  $\mu$ M TNP-ATP, and syringe B, 20 mM Mg.ATP, at 5 and 15°C, where indicated. In B, conditions were identical to A, except that syringe B contained 20 mM Mg.ADP at 5, 15, and 25°C, where indicated. The solid lines in both figures are the fit of a first-order equation for 200 data points, collected within 100 msec (see "Methods"). Traces are the average of three mixing cycles.

of nucleotides for the TNP-ATP site.

Attempts at model formation required a kinetic corroboration of the rates of decrease of fluorescence by ATP and ADP. Addition of ATP and of ADP to the phosphoenzyme causes a monoexponential decay in TNP-ATP fluorescence at 5°C ( $k_{obs} = 34$  and  $38 \text{ sec}^{-1}$ , respectively) (Fig. 3.8 a and b). The monoexponential nature of fluorescence decay in both cases is indicative of a single process occurring prior to the initiation of the effects of high nucleotide concentrations on the catalytic cycle. Addition of millimolar ADP to total E-P causes rapid disappearance of the ADP-sensitive phosphoenzyme with rapid formation of ATP at rates  $> 300 \text{ sec}^{-1}$  at 21°C (Froehlich and Heller, 1985). In this case ADP binding to a separate site would result in a biphasic decay in TNP-ATP fluorescence. The results of the present study are compatible with competition of nucleotides for TNP-ATP binding sites, in which the TNP-ATP "off" rate governs the nucleotide "on" rate at the same site. An allosteric linkage between two sites was considered as the alternative model. These sites would have to be coupled in such a manner that binding of nucleotide to one site immediately precludes binding to the second site. The observed stoichiometry obtained for both ATP and TNP-ATP of one mol/mol enzyme, excluded the possibility of such a model.

The "off" rate of TNP-ATP under the above conditions was therefore measured for comparison. Addition of varying concentrations of TNP-ATP to the turning over enzyme, already in steady state, resulted in  $k_{obs}$  values for fluorescence enhancement in the range 75 to  $200 \text{ sec}^{-1}$  (Fig. 3.9a), which were a linear function of [TNP-ATP] at 5, 15, and 25°C (Fig. 3.9b). The limitations of the dead-time of the stopped flow fluorimeter (3.2 msec, see Methods), preclude accurate measurements at higher rates.

The linear relationship between  $k_{obs}$  and [TNP-ATP] (Fig. 3.9b) is characteristic of a simple second order binding

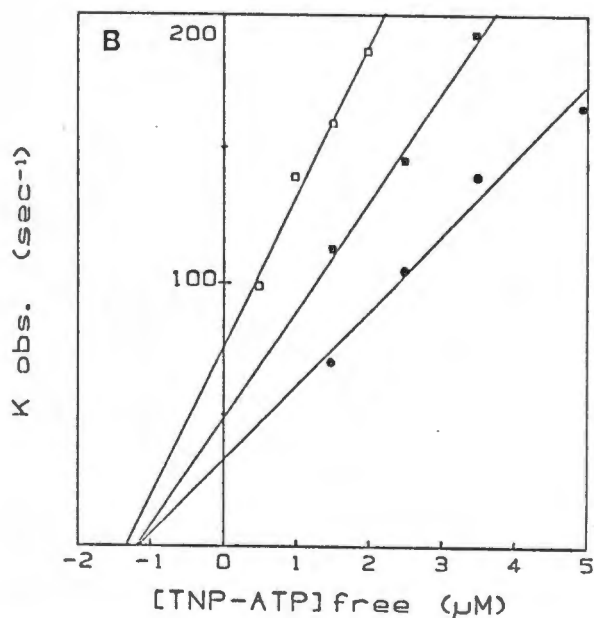
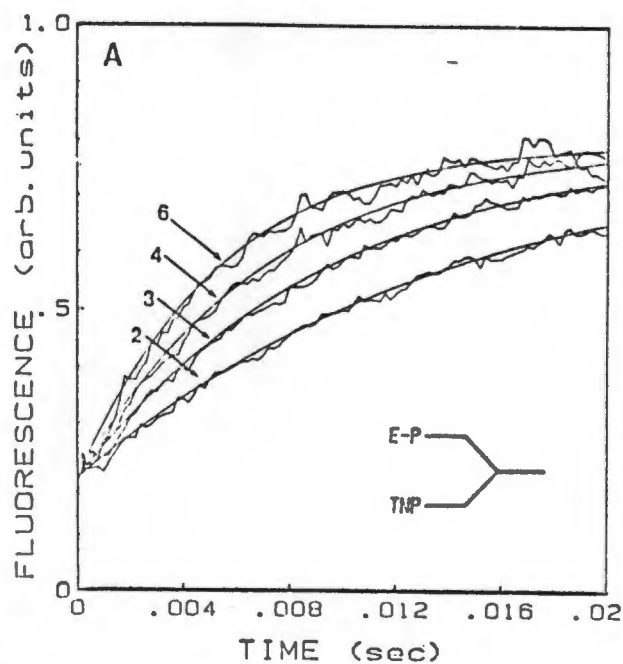


**Figure 3.9** Measurement of "off" and "on" rate constants of TNP-ATP

Stopped flow conditions were: Syringe A, 0.2 mg/ml SRV, 50  $\mu\text{M}$  ATP, 10  $\mu\text{g/ml}$  creatine phosphokinase, 500  $\mu\text{M}$  creatine phosphate, under the same buffer conditions as in Fig. 3.7 at 5  $^{\circ}\text{C}$ ; syringe B contained varying concentrations of TNP-ATP to give 2, 3, 4 and 6  $\mu\text{M}$   $[\text{TNP-ATP}]_{\text{final}}$ . B: Data from first order fits of varying  $[\text{TNP-ATP}]_{\text{final}}$  from A, and also from data at 15 and 25  $^{\circ}\text{C}$  (not shown in A) were plotted against  $[\text{TNP-ATP}]_{\text{free}}$ , calculated from a stoichiometry of 5.5 nmol/mg binding sites (see Table 3.1). Intercepts on the vertical axis were 32.7, 48.4 and 75.5  $\text{sec}^{-1}$  at 5 ( $\bullet$ ), 15 ( $\blacksquare$ ) and 25  $^{\circ}\text{C}$  ( $\square$ ), respectively.

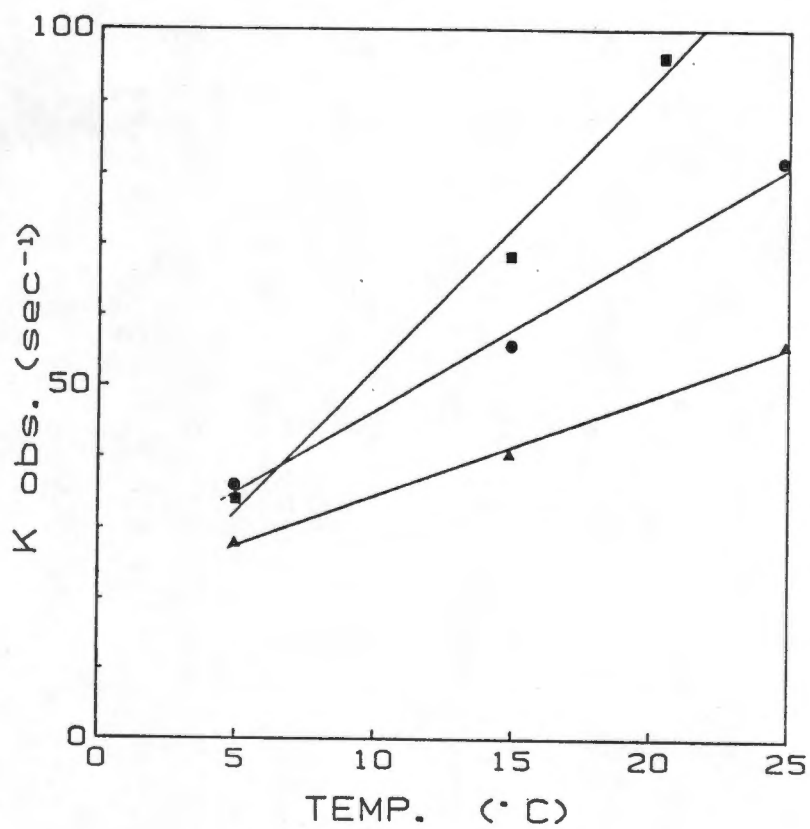


**Figure 3.10** Observed nucleotide-induced and derived "off" rate constants

Data for the apparent "off" rate constants by Mg.ATP (■), and Mg.ADP (●), of figs. 3.8 A and B, as shown together with data of derived "off" rate constants (▲) of Fig. 3.9 at the corresponding temperatures.

equilibrium between enzyme and ligand (Gutfreund, 1972). It follows that  $k_{obs} = k_{on} \times [TNP-ATP] + k_{off}$ . The slope and intercept gave values of  $k_{on} = 5 \times 10^7 \text{ M}^{-1} \text{ s}^{-1}$  and  $k_{off} = 72 \text{ sec}^{-1}$  respectively at 25 °C (Fig. 3.9b). Also of interest is the intercept on the abscissa ( $k_d = -k_{off} / k_{on}$ ). Slopes at 5, 15 and 25°C extrapolate to values ranging from 1.2 to 1.4  $\mu\text{M}$  (Fig. 3.9b), which correlate well with the affinity of the site for TNP-ATP.

The calculated  $k_{off}$  values are similar to the values obtained for  $k_{obs}$  for ADP quenching, but are 1.3-fold less than those for ATP at 25°C, (Fig. 3.10). The discrepancy in nucleotide-induced "off" rate constants and the "off" rate constants, extrapolated from the observed rates for TNP-ATP onto the enzyme, may be a result of TNP-ATP kinetics measured for two different equilibrium situations, i.e. that of phosphoenzyme decay, in which little new phosphoenzyme is formed after millimolar ADP addition, and that of a steady state of phosphoenzyme equilibrium, following millimolar ATP addition.

### 3.4 EFFECTS OF ALTERATION OF DISTRIBUTION OF E-P INTERMEDIATES ON ATP-INDUCED TNP-ATP FLUORESCENCE

#### 3.4.1 EFFECTS OF N-ETHYLMALEIMIDE ON PARTIAL REACTIONS OF THE CATALYTIC CYCLE

The effects of modification of sulphhydryl groups on the  $\text{Ca}^{2+}$ -ATPase on various functional activities of the enzyme have been studied. Kawakita *et al.* (1980) have shown that relatively specific derivitization of those thiol groups involved in the phosphoenzyme decomposition (SHd) can be obtained in the presence of  $\text{Ca}^{2+}$  and of the non-hydrolyzable analogue, AMP-PNP. The latter serves to protect those thiols involved in phosphoenzyme formation following nucleotide binding.

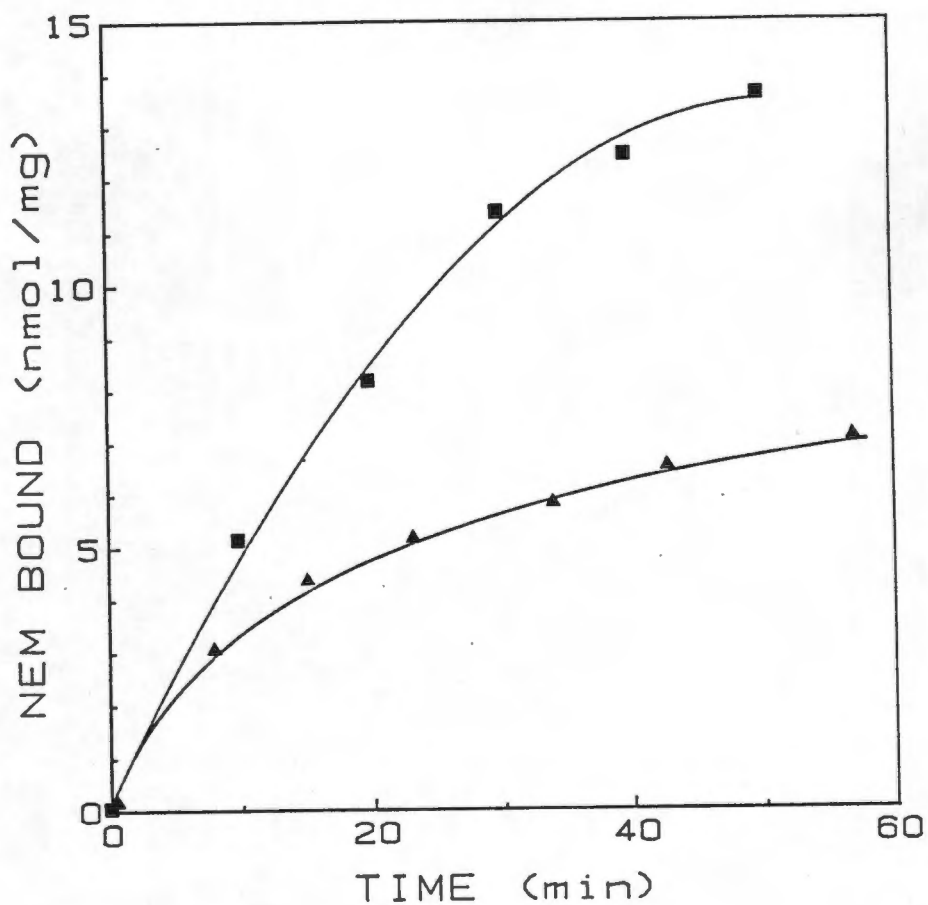


**Figure 3.11** Nem labelling of thiol groups of the  $\text{Ca}^{2+}$ -ATPase

SRV (2.0 mg/ml) were reacted with 40 uM ( $\blacktriangle$ ) and 400 uM ( $\blacksquare$ ) [ $^3\text{H}$ ]NEM in 100 mM Mops-Tris, pH 7.0, 50 uM  $\text{Ca}^{2+}$ , 1 mM AMP-PNP, at 25 °C. Radioactivity was determined as described under "Methods".

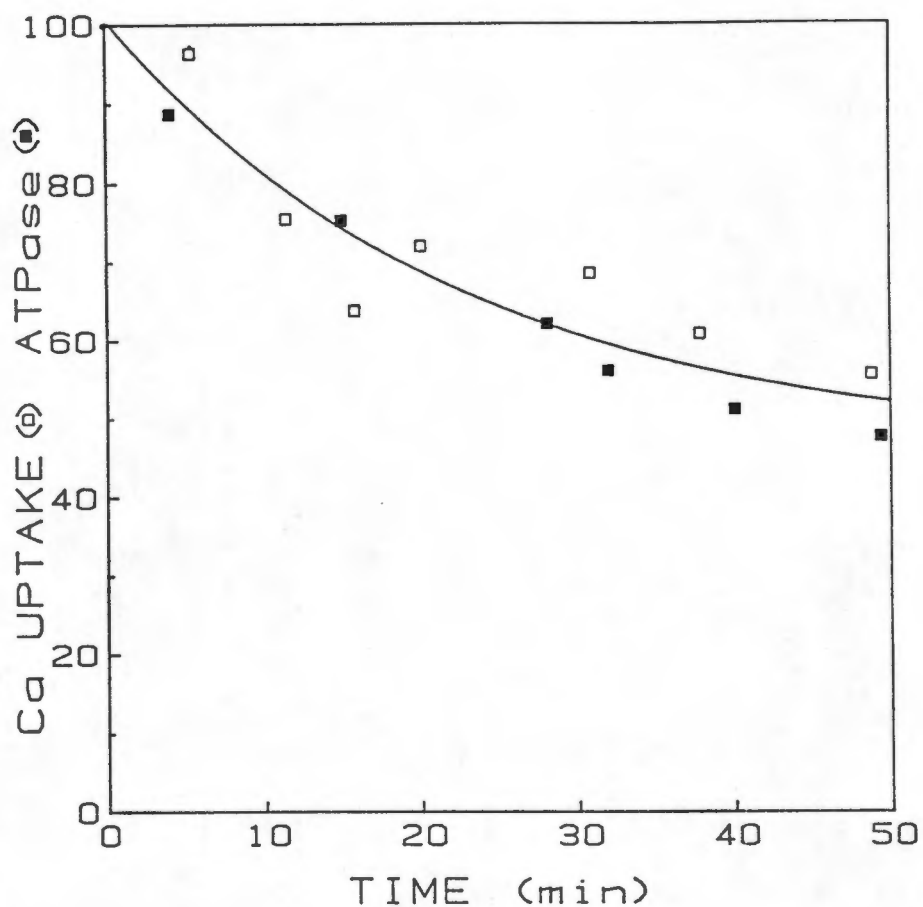


**Figure 3.12** Effect of -SH modification on Ca<sup>2+</sup>-uptake and ATPase

SRV were derivitized with 400  $\mu$ M NEM, under the conditions of Fig. 3.11. Aliquots were removed at various time intervals and assayed for Ca<sup>2+</sup>-uptake (□) and ATPase activity (■) as described under "Methods". The final [AMP-PNP] in these assays was 100  $\mu$ M. Values were corrected for the 5% loss of activity at 50 minutes for SRV incubated under the same conditions in the absence of added NEM.

The extent of modification with the reagent N-ethylmaleimide (NEM) depends on the time of the reaction and the concentration of the reagent employed (Fig. 3.11). Low concentrations (40  $\mu\text{M}$ ) of NEM rapidly label 4 - 5 -SH groups in 15 - 20 minutes, followed by a slower phase such that 6 - 7 groups are modified by one hour. At high (400  $\mu\text{M}$ ) concentrations, approximately 14 nmol/mg of NEM are bound by the enzyme. These data are essentially in agreement with those of Kawakita et al (1980) and Yamada and Ikemoto, (1978). The ATPase, modified by 400  $\mu\text{M}$  NEM for up to 50 minutes, has been used for further functional studies.

NEM modification results in a parallel decline of  $\text{Ca}^{2+}$  uptake and  $\text{Ca}^{2+}$ -dependent ATPase activity (Fig. 3.12), consistent with inhibition of the rate limiting step of phosphoenzyme decomposition. Derivatization had no apparent effect on coupling activity. It should be noted that data on thiol group modification and its effects on transport activity were obtained in the absence of  $\text{Ca}^{2+}$  in previous studies. EGTA, which has been shown to cause irreversible uncoupling of the  $\text{Ca}^{2+}$  pump (McIntosh et al., 1978), complicates interpretation of the data of those studies.

Original studies on TNP-ATP fluorescence, performed at pH 8.0 and 20% (v/v) glycerol showed  $\text{P}_i$ -induced fluorescence to be half of that induced by ATP (Bishop et al., 1984). In the present study (Fig. 3.13),  $\text{P}_i$ -induced fluorescence was assayed at pH 7.0 and in 10% (v/v)  $\text{Me}_2\text{SO}$ , which conditions maximise E-P levels. Under the circumstances, ATP- and  $\text{P}_i$ -induced fluorescence are equivalent. NEM modification diminished fluorescence enhancement from either source to approximately similar extents (compare fig. 3.13a and 3.13b at 16 and 40 minutes with fig. 3.13c). NEM modification did not alter the low TNP-ATP fluorescence in the non-phosphorylated enzyme prior to the addition of ATP or  $\text{P}_i$  (fig. 3.13a and b).

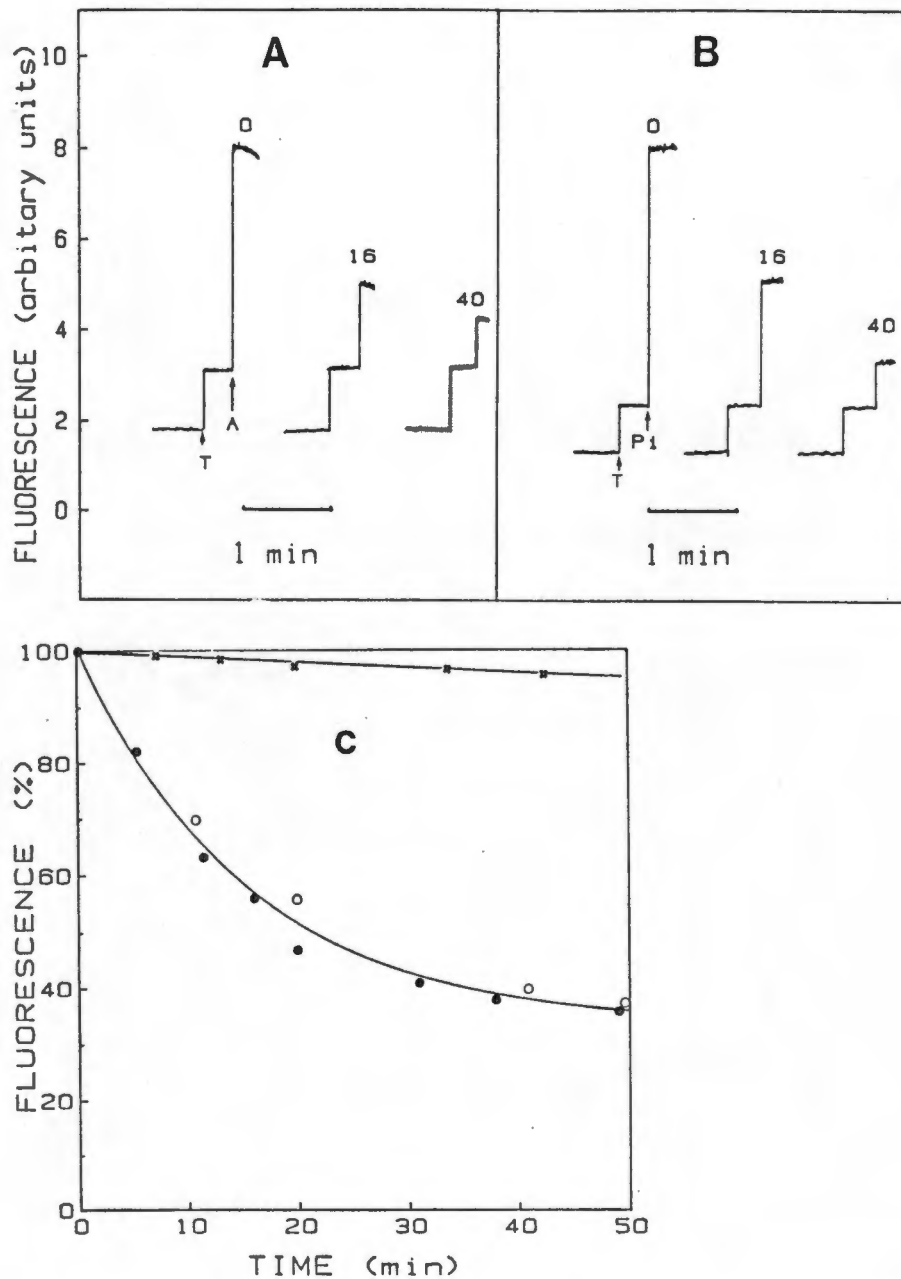


**Figure 3.13** The effects of NEM modification on ATP or Pi-dependent TNP-ATP fluorescence

TNP-ATP fluorescence was measured with 0.1 mg/ml, SRV derivitized under the same conditions as in Fig. 3.12. Fluorescence assays were performed in 100 mM Mops/Tris, pH 7.0, 2 μM TNP-ATP, 5 mM MgCl<sub>2</sub>, with (A) 100 μM ATP plus 50 μM Ca<sup>2+</sup>, or with (B) 5 mM Pi and 0.5 mM EGTA at times 0, 16 and 40 minutes as indicated. Corrections for inner filter effects were performed as described under "Methods".

(C) shows the time-dependence of ATP (●), Pi, (○)-dependent fluorescence of (A) and (B), respectively, and ATP-dependence of SRV derivitized by 40 μM NEM (×).

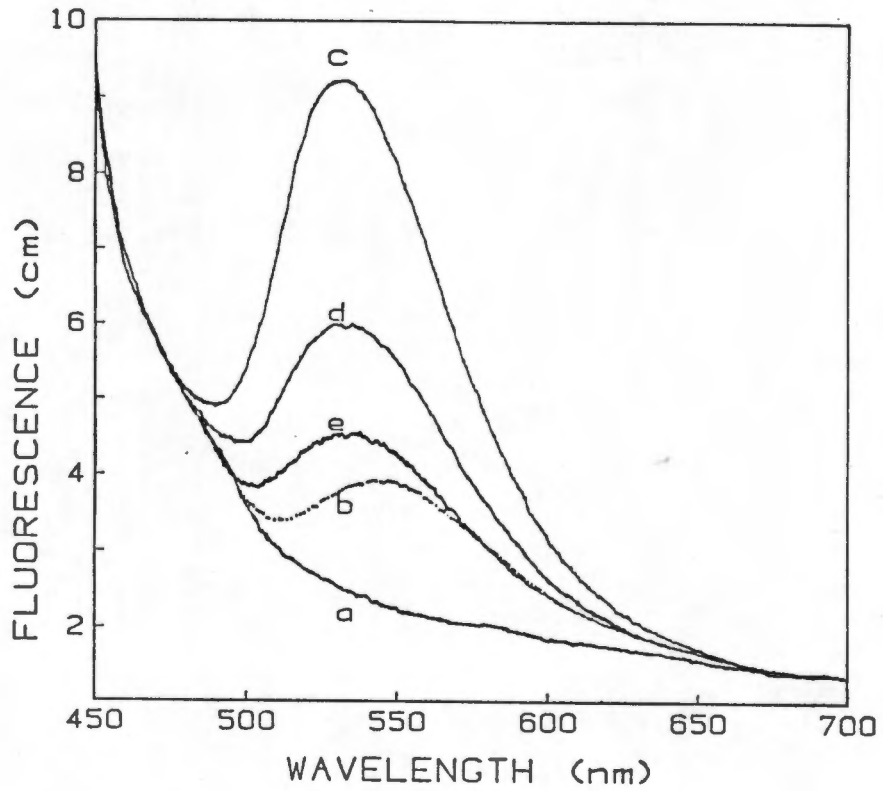


**Figure 3.14** Effect of NEM modification on TNP-ATP emission spectra

The emission spectra for Fig. 3.13 were scanned at an excitation wavelength of 418 nm, with 10 nm bandpasses. Additions were (a) 0.1 mg/ml SRV; (b) 2  $\mu\text{M}$  TNP-ATP; (c) 100  $\mu\text{M}$  ATP plus 50  $\mu\text{M}$   $\text{Ca}^{2+}$  at time 0; (d) 16 and (e) 40 minutes of NEM derivitization.

Fluorescence enhancement is accompanied by a blue shift in the emission spectrum of bound TNP-ATP (545 nm to 530 nm) (trace b and c, Fig 3.14), consistent with previous suggestions of increased hydrophobicity of the TNP-ATP binding site during turnover (Nakamoto and Inesi, 1984). NEM modification that resulted in decreased fluorescence had no effect on  $\lambda$  max of emission (530 nm) (curve d and e, fig. 3.14). The alteration in fluorescence does not appear to be a change in light scattering as a result of flocculation of vesicles since fluorescence emissions in the range 450 - 475 nm and 650 - 700 nm were unaltered. NEM modification also had little effect on the absorbance at 410 and 530 nm, causing negligible inner filter effects (data not shown), as described by Lakowicz (1982). Under conditions (40  $\mu$ M NEM) that have been reported to result in the modification of those thiol groups of unknown function SHn, the enhanced TNP-ATP fluorescence was unchanged (Fig. 3.13c).

TNP-ATP fluorescence has been related to E-P levels (Nakamoto and Inesi, 1984; Bishop et al., 1985) under static and dynamic conditions. Kawakita et al. (1980) have reported that inclusion of AMP-PNP protects a group of sulphhydryls, SHf, that are related to E-P formation, and thus NEM modification had no effect on ATP-dependent E-P levels. These findings are confirmed in Fig. 3.15. However, Pi-induced E-P levels were diminished by approximately 50% following derivitization. This suggests that the thiol groups that are modified and that are designated SHd, are involved in both the decomposition of E-P to Pi and H<sub>2</sub>O and, in the reverse reaction, of the formation of covalent E-P from Pi with the exclusion of water. Thus, under these conditions the decline in Pi-dependent TNP-ATP fluorescence is readily explained by decreased E-P formation. However, the decrease in TNP-ATP fluorescence from ATP plus Ca<sup>2+</sup> occurs when total E-P levels are unaltered.

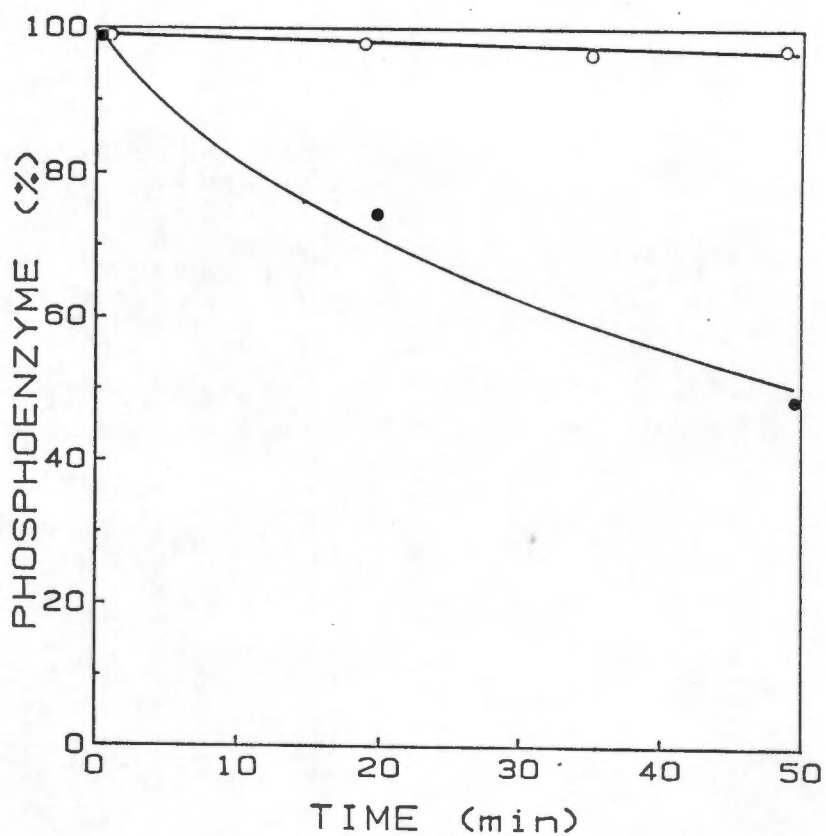


**Figure 3.15** Effects of NEM modification on E-P levels from ATP and Pi

Phosphoenzyme levels were determined from [ $\gamma$ - $^{32}$ P]ATP and  $^{32}$ Pi (see Methods) under identical conditions as for fluorescence assays in Fig. 3.13.

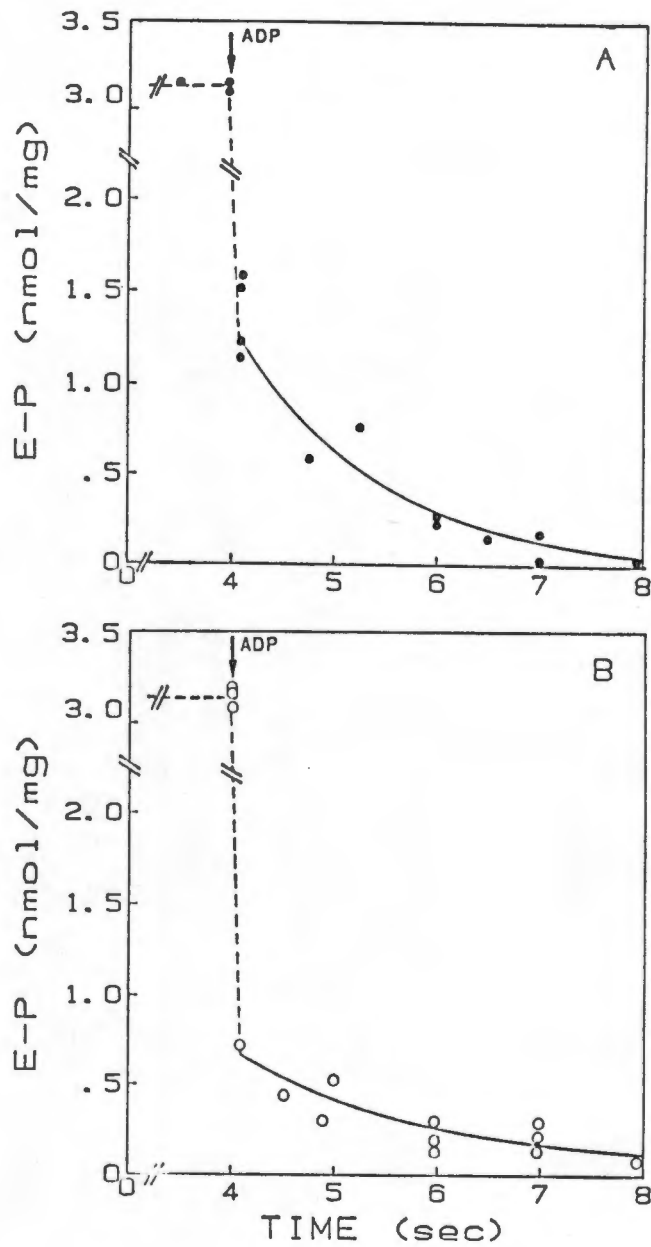


**Figure 3.16** Effects of NEM modification on phosphoenzyme ADP-sensitivity

NEM treated (O) and untreated (●) SRV were phosphorylated with 100  $\mu\text{M}$  [ $\gamma$ - $^{32}\text{P}$ ]ATP for 4 seconds followed by addition of 5 mM Mg.ADP plus 0.5 mM EGTA, where indicated. Mixing was performed on a Durrum 133 rapid mix device for data at 20 msec (see "Methods"). Non-linear least squares fits for phosphoenzyme decay showed rate constants of 0.71 and 0.60  $\text{sec}^{-1}$ , while extrapolation of the fit intercepted the rapid decay in E-P at 1.17 and 0.65 nmol/mg, before and after NEM modification, respectively.

Total E-P levels include both E<sub>1</sub>-P and E<sub>2</sub>-P intermediates. Pi-induced E-P, in the absence of Ca<sup>2+</sup>, is assumed to be predominantly E<sub>2</sub>-P, whilst during turnover, both E<sub>1</sub>-P and E<sub>2</sub>-P exist, with a ratio of approximately 2:1 (Froehlich and Heller, 1985).

The relative proportions of ADP-sensitive and insensitive E-P species have been determined following rapid quenching by millimolar ADP and EGTA (Fig. 3.16). This shows a rapid decay in E-P from 3.1 nmol/mg, complete within the mixing time, and was followed by a slower decay in the ensuing 5 seconds. The data yield a value of the ADP-sensitive fraction of 43 %, which is consistent with previous data of Shigakawa *et al.* (1978), and Shigekawa and Akowitz (1979). Similar experiments performed in NEM modified vesicles showed that ADP-sensitive E-P species was increased to 85% (Fig 3.16b), consistent with the previous findings (Nakamura and Tonomura, 1982; Yamaguchi and Kanazawa, 1984; Yasuoka-Yabe *et al.*, 1983). Exponential fits to the slow phase of E-P decay (Fig. 3.16a, b) following addition of ADP gave similar values of 0.71 and 0.60 sec<sup>-1</sup>, in the control and NEM modification vesicles respectively. These results are therefore consistent with a TNP-ATP fluorescence decrease parallel to that of E<sub>2</sub>-P.

#### 3.4.2 THE EFFECTS OF OXALATE

Oxalate is widely used for observation of rates of Ca<sup>2+</sup> accumulation by vesicles in studies on the Ca<sup>2+</sup>-ATPase in the absence of a Ca<sup>2+</sup> gradient (Hasselbach and Makinose, 1963; Newbold and Tume, 1979; Kometani and Kasai, 1978). Electron micrographs show the formation of Ca<sup>2+</sup>-oxalate precipitates in the vesicular lumen as electron opaque deposits (Deamer and Baskin, 1969). Oxalate effectively 'clamps' the free Ca<sup>2+</sup> concentrations at 4 uM at pH 7.0 and 25°C (Meltzer and Berman, 1984). Ca<sup>2+</sup> release from the low affinity Ca<sup>2+</sup>

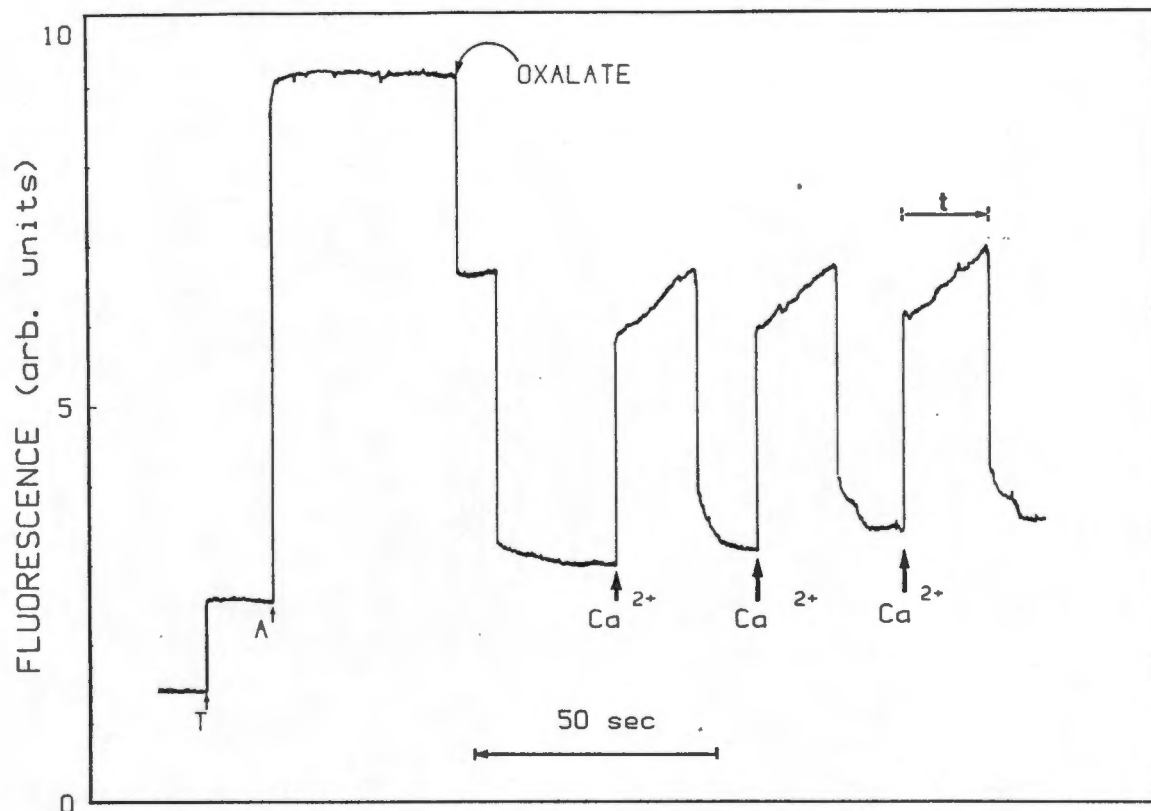


**Figure 3.17** The effects of oxalate on TNP-ATP fluorescence

TNP-ATP enhanced fluorescence was initiated by the addition of 2  $\mu\text{M}$  TNP-ATP (T) to 0.2 mg/ml SRV in 0.1 M Mops/Tris pH 7.0, 50  $\mu\text{M}$   $\text{Ca}^{2+}$ , 5 mM  $\text{MgCl}_2$ , phosphorylated by 66  $\mu\text{M}$  ATP (A), in a 3 ml cuvette at 25  $^{\circ}\text{C}$ . Oxalate was added (where indicated) as a Tris salt, pH 7.0 in 300  $\mu\text{L}$  to give a final concentration of 5 mM. Repeated additions of 150 nmol aliquots of  $\text{Ca}^{2+}$  were added where indicated. The duration of  $\text{Ca}^{2+}$ -induced fluorescence was 17 sec (t).

sites, oriented to the vesicle lumen, is the rate limiting step of the forward cycle at high (millimolar) [ATP] and high [KCl] (Pickart and Jencks, 1983). This step is accelerated by maintaining low free  $[Ca^{2+}]$  inside with the use of oxalate, while steady-state  $Ca^{2+}$ -uptake proceeds at rates equivalent to those of oxalate permeation into the vesicle (Kometani and Kasai, 1978). Oxalate has also been used in studies to determine coupling ratios at low external  $[Ca^{2+}]$ , using the "off" rate of  $Ca^{2+}$  from external  $Ca^{2+}$ -oxalate that is slower than the uptake rates of SRV. This effectively decreases external  $Ca^{2+}$  to levels lower than the  $K_d$  of the high affinity  $Ca^{2+}$  binding sites, resulting in  $Ca^{2+}$  transport stoichiometries of less than two (Gafni and Boyer, 1986).

Phosphoenzyme decomposition becomes rate limiting in the absence of  $K^+$  (Chaloub and deMeis, 1980). Steady-state levels of the  $E_2$ -P intermediate are significantly decreased. The present study employs this interaction for the comparison of levels of enhanced fluorescence to diminished  $E_2$ -P levels.

Steady-state turnover generates high levels of TNP-ATP fluorescence that are maintained over a period that allows near-maximal vesicle filling by  $Ca^{2+}$  (Fig. 3.17). The fluorescence decreases by 40% upon the addition of 5 mM oxalate (Fig. 3.17). Under these conditions the coupling ratios remain unchanged (1.78) (Gafni and Boyer, 1986), whereas decreasing external  $[Ca^{2+}]$  to 0.1 to 0.15  $\mu M$  alters pump stoichiometry (Meltzer and Berman, 1984), excluding low coupling ratios as a cause of decreased fluorescence.

Steady-state E-P levels from ATP $[^{32}P]$ , under identical conditions were 3.20 and 3.15 nmol/mg in the absence and presence of oxalate respectively. Since total E-P levels remain relatively unaffected, the decrease in fluorescence can only be attributed to a decrease in the relative levels of  $E_2$ -P.

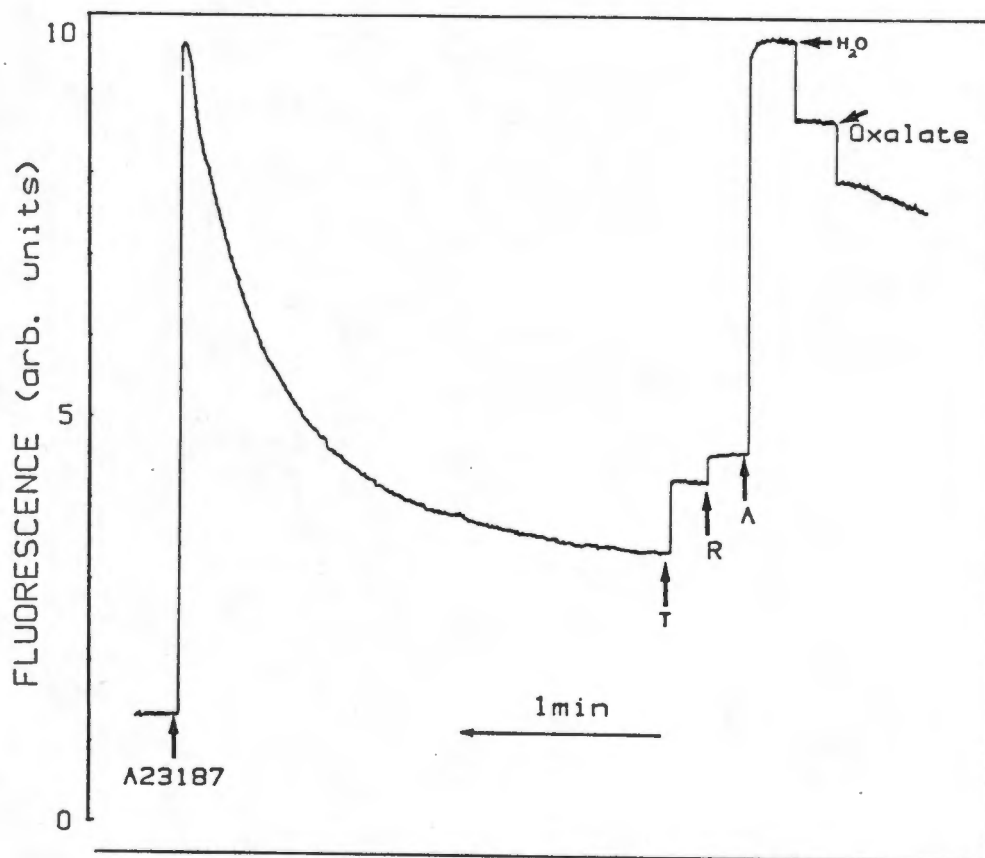


**Figure 3.18** The effect of A23187 on oxalate-induced changes in TNP-ATP fluorescence

Conditions of Fig. 3.17 were repeated, except that A23187 (4% w/w of SRV) was added to SRV, followed by TNP-ATP after the stabilization of the fluorescence signal. Further additions were: R, a regenerating system consisting of 800  $\mu$ M creatine phosphate with 20  $\mu$ g/ml creatine phosphokinase ; A, 20  $\mu$ M ATP, and where indicated, 300  $\mu$ L H<sub>2</sub>O and 300  $\mu$ L Tris-oxalate, pH 7.0, to a final concentration of 5 mM.

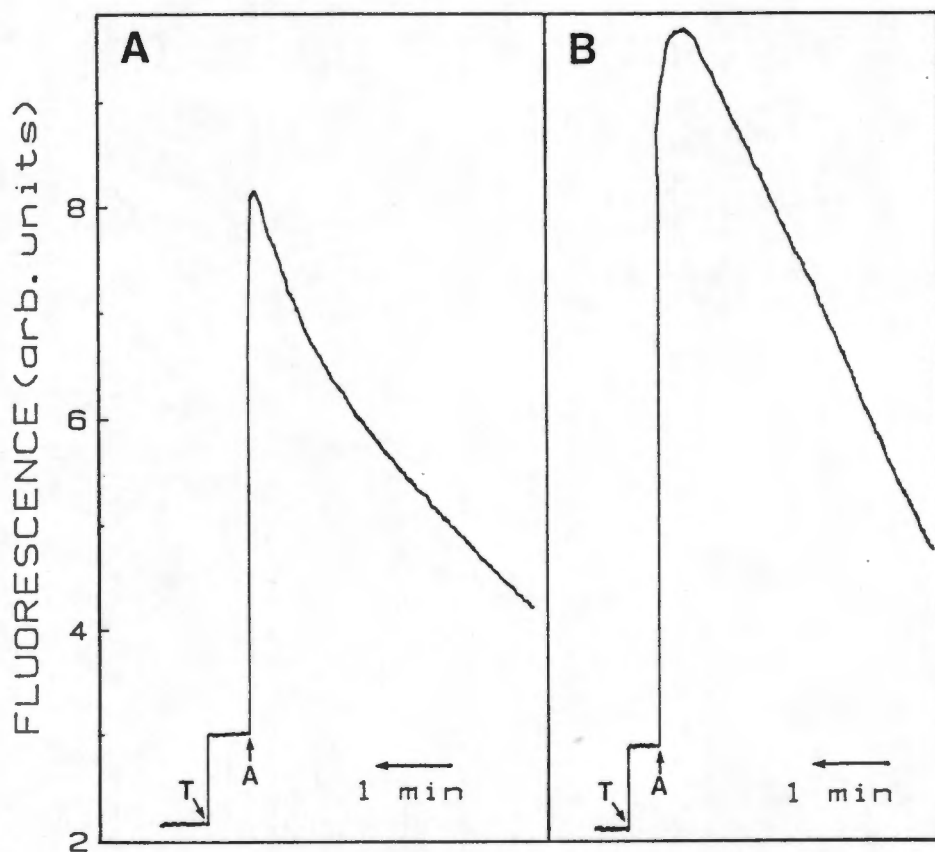


**Figure 3.19** The effects of  $\text{Sr}^{2+}$  transport on TNP-ATP fluorescence

Conditions were: A; 0.1 mg/ml SRV, 0.1 M Mops/Tris, pH 7.0, 5mM  $\text{MgCl}_2$ , at 25 °C, with 100  $\mu\text{M}$   $\text{CaCl}_2$ , and B; 100  $\mu\text{M}$   $\text{SrCl}_2$  replaced  $\text{CaCl}_2$ , on the same fluorescence scale. Additions were T, 2  $\mu\text{M}$  TNP-ATP and A, 66  $\mu\text{M}$  ATP, where indicated.

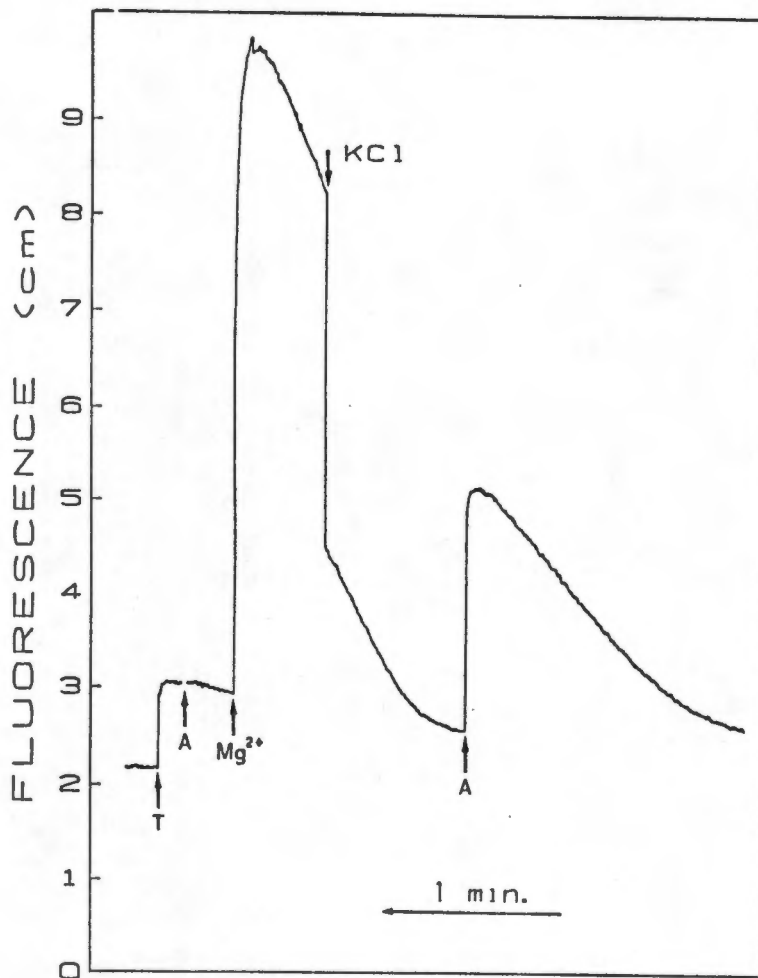


**Figure 3.20** The effects of  $\text{MgCl}_2$  and  $\text{KCl}$  on  $\text{Sr}^{2+}$ -dependent TNP-ATP fluorescence

Conditions were the same as for Fig. 3.19, except that  $\text{MgCl}_2$  was omitted. Addition of ATP (A), 25  $\mu\text{M}$  was followed by 5  $\text{mM}$   $\text{MgCl}_2$ , and 60  $\text{mM}$   $\text{KCl}$ , where indicated. Fluorescence was partially restored by further addition of 25  $\mu\text{M}$  ATP.

Further studies showed that the TNP-ATP fluorescence signal is sustained at 60% of maximal by oxalate for a finite period before rapidly decreasing to baseline levels (Fig 3.18). Readdition of  $\text{Ca}^{2+}$  (150 nmoles), restores the fluorescence to the 60% level for the same period. Repetitive  $\text{Ca}^{2+}$  additions resulted in similar fluorescence time courses. The sharp cut-off is presumably caused by depletion of external  $[\text{Ca}^{2+}]_{\text{free}}$  to levels less than those of the  $K_m$  of the enzyme (4  $\mu\text{M}$ ). A rate of transport of 150 nmoles  $\text{Ca}^{2+}$  by 0.2 mg SRV for 17 seconds was calculated to be 2650 nmol/mg/min. Rates of  $^{45}\text{Ca}^{2+}$  uptake under the same conditions (in the absence of  $\text{K}^+$ ) were in excellent agreement at 2500 nmol/mg/min (see "Methods"). This system, therefore, provides a convenient and rapid method of determining  $\text{Ca}^{2+}$  uptake rates in SRV. A future study may employ this phenomenon for  $\text{Ca}^{2+}$ -stat methodology to maintain  $\text{Ca}^{2+}$  at low (0.1  $\mu\text{M}$ ) levels that alter the pump stoichiometry.

Oxalate fails to decrease TNP-ATP fluorescence in vesicles pre-incubated with the  $\text{Ca}^{2+}$  ionophore A23187, which abolish the  $\text{Ca}^{2+}$  gradient and therefore prohibits  $\text{Ca}^{2+}$ -oxalate precipitation (Fig. 3.18). The addition of A23187 causes a transient increase in light scattering that decayed after 2 to 3 minutes. This was attributed to partitioning of the ionophore into the membranes. Oxalate decreased fluorescence levels by 10%, equivalent to the decrease observed for the addition of equal volumes of  $\text{H}_2\text{O}$ , indicating the absence of a direct quenching effect of the TNP-ATP fluorescence by the anion (Fig. 3.18). A23187 alone accelerates ATPase by removal of the rate limiting step of  $\text{Ca}^{2+}$  release, but interpretation of fluorescence changes is hampered by changes in light scattering caused by this ionophore.

### 3.4.3 EFFECTS OF STRONTIUM

Strontium ions can substitute for  $\text{Ca}^{2+}$  in vectorial transfer by the  $\text{Ca}^{2+}$ -ATPase (Mermier and Hasselbach, 1972).  $\text{Sr}^{2+}$ -induced turnover favours the formation of relatively higher levels of the ADP-insensitive phosphoenzyme (Guimares-motta et al., 1984). We have employed this phenomenon to test the hypothesis that the  $\text{E}_2$ -P intermediate is responsible for enhanced TNP-ATP fluorescence.

$\text{Sr}^{2+}$ -dependent enhanced TNP-ATP fluorescence is 10% higher than that with  $\text{Ca}^{2+}$  (Fig. 3.19). The decay in fluorescence levels after addition of a pulse of ATP was slower with  $\text{Sr}^{2+}$ , indicating of a lower rate of ATPase activity, as previously reported (McLennan, 1970). The emission spectrum shows an increased quantum yield, with no change in the emission maximum at 528 nm (data not shown), consistent with a quantitative increase in TNP-ATP enhanced fluorescence, without a change in the nature of the probe site. Strontium alone in the absence of  $\text{Mg}^{2+}$  is unable to increase TNP-ATP fluorescence (Fig. 3.20), similar to the inability of  $\text{Ca}^{2+}$  to stimulate TNP-ATP fluorescence in the absence of  $\text{Mg}^{2+}$  as shown below (Fig. 3.21). It has previously been reported that  $\text{Sr}^{2+}$  cannot substitute functionally for  $\text{Mg}^{2+}$  (McLennan, 1970). Phosphoenzyme levels, induced by  $\text{Sr}^{2+}$  and ATP (2.17 nmol/mg), are 10% lower than the Ca-dependent levels (2.4 nmol/mg), demonstrating that higher levels of  $\text{Sr}^{2+}$ -dependent enhanced fluorescence are supported by lower levels of total phosphoenzyme. The predominant E-P intermediate has previously been shown to be  $\text{E}_2$ -P under these conditions, in support of the hypothesis that  $\text{E}_2$ -P alone causes enhanced TNP-ATP fluorescence.

$\text{K}^+$  ions decrease  $\text{Sr}^{2+}$ -dependent fluorescence to the same extent as  $\text{Ca}^{2+}$ -dependent fluorescence (Fig. 3.20). The half maximal  $\text{K}^+$  effect occurs at 45 mM, in the range of inhibition for  $\text{Ca}^{2+}$ -dependent fluorescence ( $[\text{K}^+]_{0.5} = 48 \text{ mM}$ )

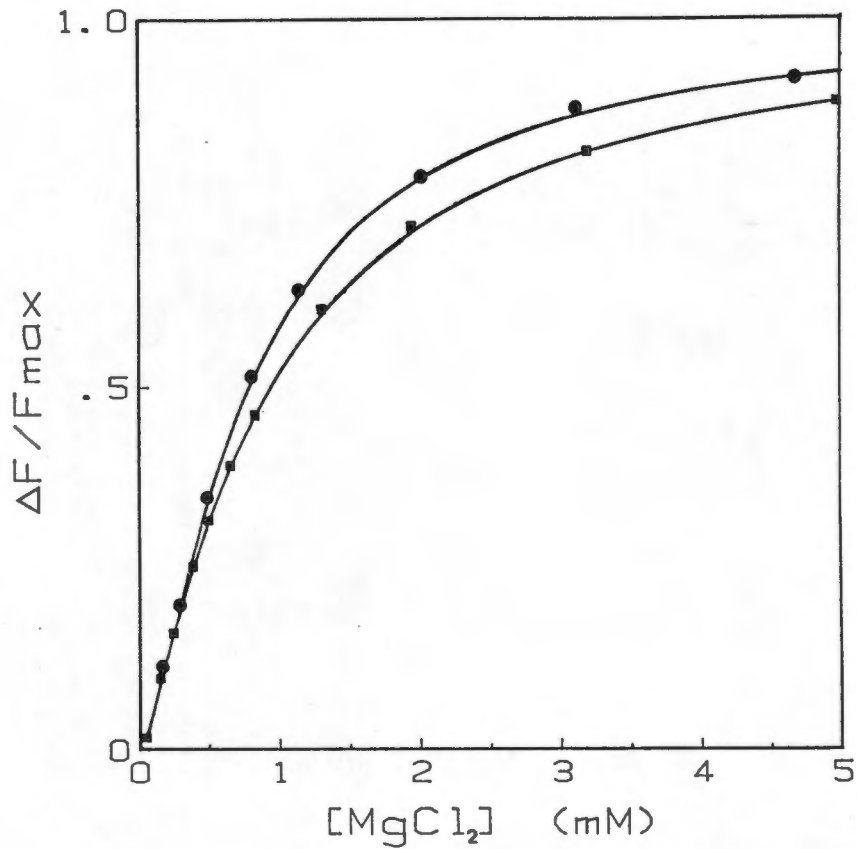


**Figure 3.21** The effect of  $Mg^{2+}$  on TNP-ATP fluorescence

Conditions were 0.1 mg/ml SRV, 2  $\mu$ M TNP-ATP, 0.1 M Mops-Tris, pH 7.0, 50  $\mu$ M  $CaCl_2$ , at 25 °C, in the absence of added  $Mg^{2+}$ .  $MgCl_2$  (1 M) was titrated against the phosphoenzyme formed either from 5 mM Pi, in the presence of 0.5 mM EGTA (■) or from 25  $\mu$ M ATP, with 20  $\mu$ g/ml creatine phosphokinase, 800  $\mu$ M creatine phosphate (●).

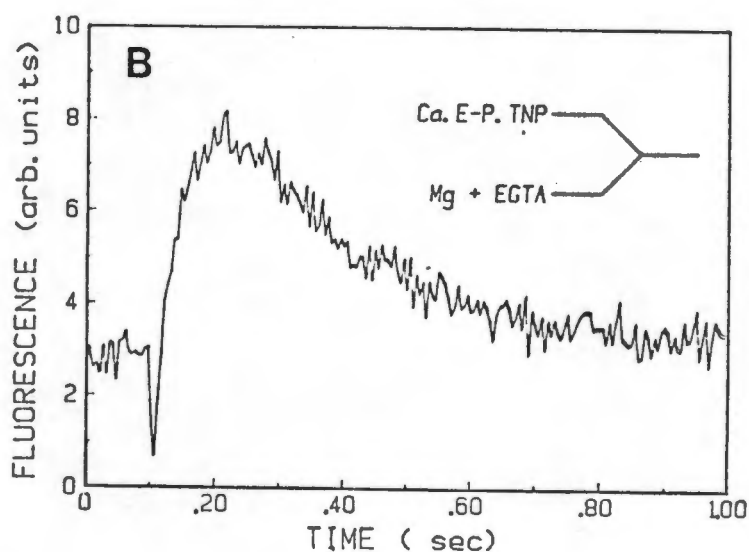
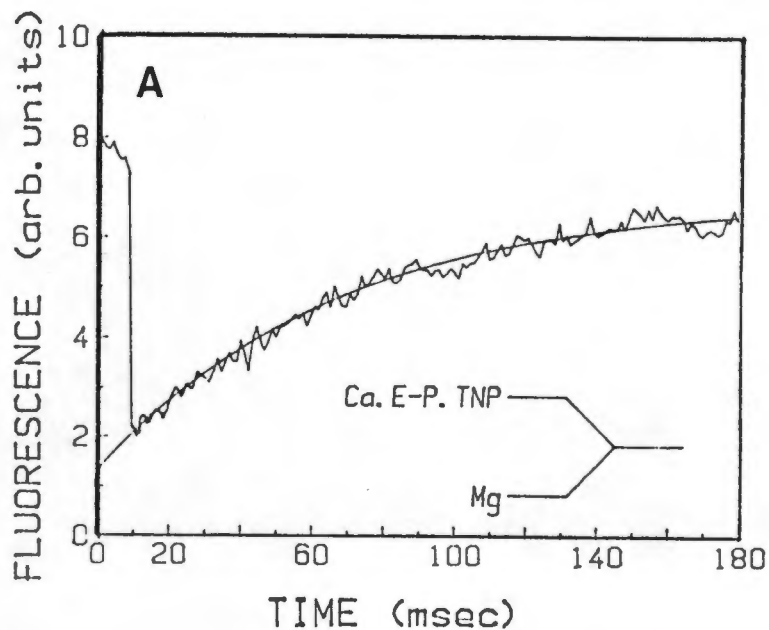


**Figure 3.22** The kinetics of the  $Mg^{2+}$ -induced change in TNP-ATP fluorescence

Stopped flow measurements were performed in the standard buffer conditions in Fig. 3.21 at 25°C. A: Syringe A contained 0.2 mg/ml phosphorylated SRV and syringe B contained 10 mM  $MgCl_2$  in standard buffer. B: Conditions were the same as in A, except that syringe B contained 0.5 mM EGTA in addition to 10 mM  $MgCl_2$  to prevent rephosphorylation following a completed pump cycle.

as shown below (Fig. 3.28). This finding is not consistent with the possibility that the acceleration of the  $E_2$ -P to  $E_1$ -P intermediate by  $K^+$  is operative as the cause of diminished fluorescence.

THE EFFECTS OF  $Mg^{2+}$  ON TNP-ATP FLUORESCENCE The enzyme was phosphorylated by  $Ca^{2+}$ -ATP in the absence of  $Mg^{2+}$ , showing E-P levels of 2.9 nmol/mg consistent with previous studies (Shigekawa et al., 1984). TNP-ATP, bound to the  $Ca^{2+}$ -substituted phosphoenzyme, did not show enhanced fluorescence. Bishop et al. (1986) suggested that TNP-ATP binds only as a  $Mg^{2+}$  complex, and that binding in the absence of  $Mg^{2+}$  is not conducive to a probe conformation that exhibits enhanced fluorescence.

Titration of  $MgCl_2$  onto the  $Ca^{2+}$ -dependent phosphoenzyme restores TNP-ATP fluorescence (Fig. 3.21). The apparent half maximal  $Mg^{2+}$  effect, in data uncorrected for TNP-ATP bound to the non-phosphorylated enzyme conformations (E), was calculated as  $[Mg^{2+}]_{0.5} = 0.7$  mM (Fig. 3.21). This value is lower than the  $K_{0.5}$  for  $Mg^{2+}$  binding previously shown (Shigekawa et al., 1984). The low affinity for  $Mg^{2+}$  implies that TNP-ATP binding was independent of  $Mg^{2+}$  as a cofactor, as a higher affinity for  $Mg^{2+}$  would have been expected.

The rate of increase of TNP-ATP fluorescence, following  $Mg^{2+}$  addition was measured ( $k_{obs} = 16$  sec $^{-1}$ , Fig. 3.22a) but was found to be too high to be related to turnover in the forward cycle ( $k_{cat} = 1$  to 3 sec $^{-1}$  at 25°C, data not shown), and too low to be limited by the "on" rate of TNP-ATP as a  $Mg$ .TNP-ATP complex ( $k_{on} = 180$  sec $^{-1}$ , Fig. 3.9b). Single cycle resolution experiments were performed by mixing E-P.TNP with  $Mg^{2+}$  plus EGTA. The latter component was included to chelate all  $Ca^{2+}$  required for a second cycle in the forward direction (Fig. 3.22b). These results showed that the "on" rate of  $Mg^{2+}$  was similar to that of  $Mg^{2+}$  under consecutive cycle conditions of Fig. 3.22a. In addition, the possibility that the slow "on" rate of  $Mg^{2+}$  occurred as a  $Mg$ .TNP-ATP

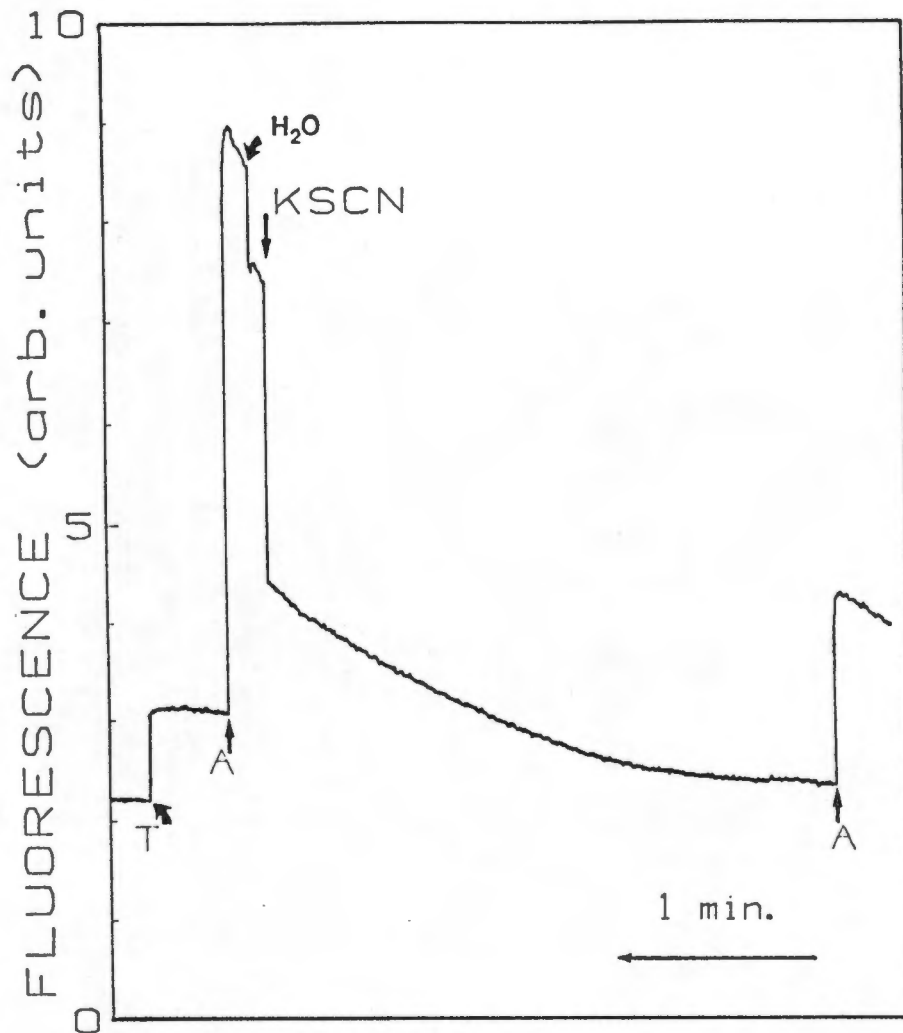


**Figure 3.23** The effect of KSCN on TNP-ATP fluorescence

SRV 0.1 mg/ml, in 100 mM Mops-Tris, pH 7.0, 5 mM  $MgCl_2$ , 50  $\mu M$   $CaCl_2$ , were reacted with 2  $\mu M$  TNP-ATP (T), 50  $\mu M$  ATP (A), followed by 300  $\mu l$  buffer for a dilution estimate and KSCN (300  $\mu l$ , final concentration = 10 mM). A final addition of ATP, (A), 50  $\mu M$ , restored fluorescence.

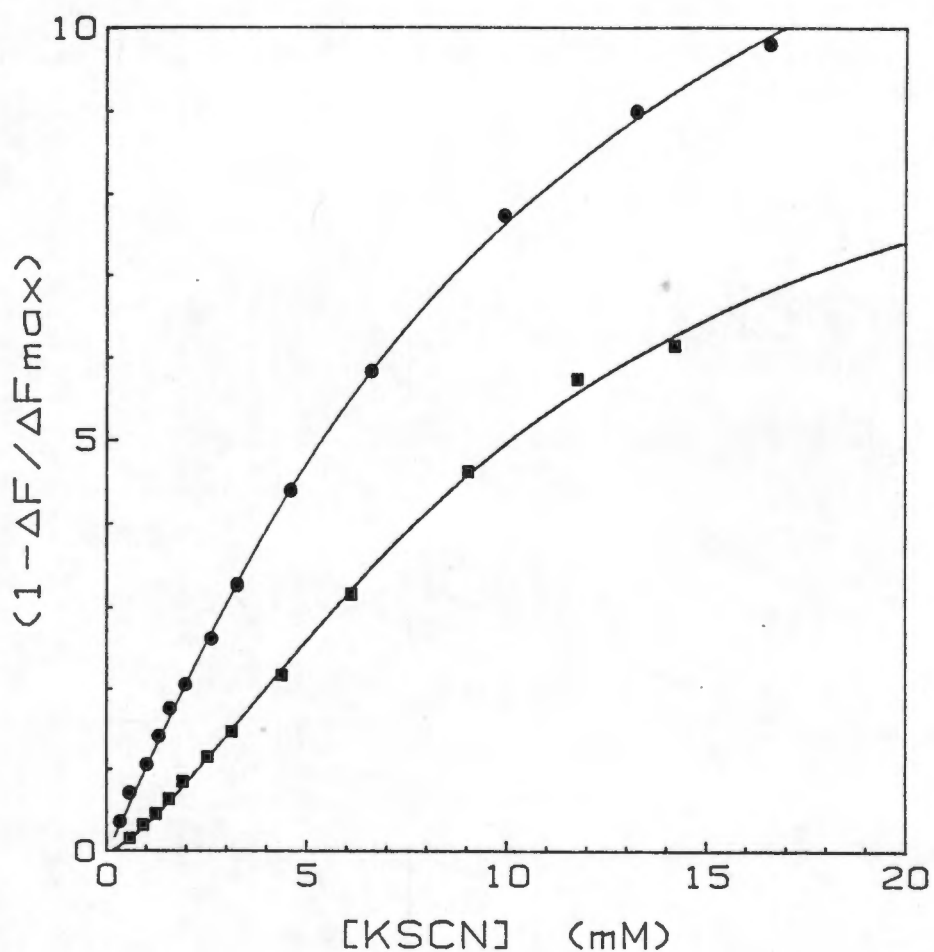


**Figure 3.24** The effects of TNP-ATP on the apparent  $k_{0.5}$  of KSCN

Fluorescence inhibition by KSCN at 2  $\mu\text{M}$  (■) and 10  $\mu\text{M}$  (●) TNP-ATP under conditions of Fig. 3.23, where  $\Delta F$  is the fluorescence decrease for added KSCN and  $\Delta F_{\text{max}}$  is the maximum TNP-ATP fluorescence that is inhibited by EGTA.

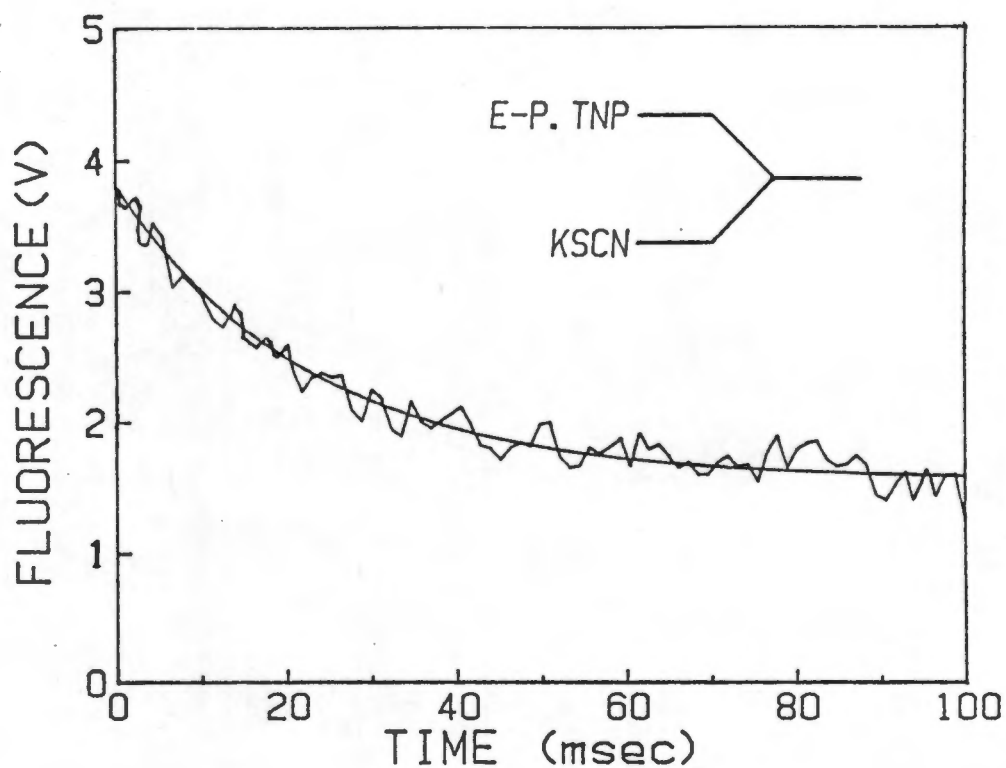


Figure 3.25 Rates of TNP-ATP fluorescence decrease by KSCN

Stopped flow measurements were performed under the conditions of Fig. 3.23 at 25°C. Syringe A contained 0.2 mg/ml phosphorylated SRV and syringe B, 20 mM KSCN.

complex in the consecutive cycle, was ruled out. The possibility remains that  $\text{Ca}^{2+}$ -ATP or  $\text{Ca}^{2+}$ -TNP-ATP complexes have slow "off" rates and that these nucleotides must leave the site before rebinding as  $\text{Mg}^{2+}$ -complexes. Analysis of these "off" rates has not previously been performed and may form the basis of a future study.

### 3.5 EFFECTS OF MODIFICATION OF WATER ACTIVITY ON TNP-ATP FLUORESCENCE

Entrance of water to the catalytic site is essential for hydrolysis of the acyl-phosphate bond. Catalytic sites of enzymes have been shown to contain water in specific arrangements between polar groups that constitute charges essential for ligand binding (Cooke and Kuntz, 1974). Dupont *et al.* (1983) have proposed that the changes in TNP-ATP fluorescence that indicate altered hydrophobicity, monitor water activity in the catalytic site. In the present study, the nature of the interaction was explored by the use of chaotropes that disorder water structure and by deuterium oxide ( $\text{D}_2\text{O}$ ) that substitutes as a more highly ordered form of water.

Phosphoenzyme-induced TNP-ATP fluorescence is sensitive to chaotropic anions. Maximal fluorescence was developed from ATP in the presence of an ATP-regenerating system (Fig. 3.23). Addition of 10 mM KSCN decreased fluorescence to 50% of the initial level after the addition of the same volume of water. ATP restored fluorescence, indicating that the slow decay observed after KSCN addition was a result of ATPase activity and not enzyme inactivation by the chaotrope. Increasing KSCN concentration in the range 0.1 to 20 mM, resulted in decreasing fluorescence to levels approaching that of TNP-ATP bound to the non-phosphorylated enzyme (Fig. 3.24). There was no change in the emission maximum wavelength at 525 nm at decreased fluorescence signals, nor was there any change in the baseline fluorescence spectrum

(data not shown). The KSCN fluorescence quenching effect had an apparent affinity in the millimolar range ( $[SCN^-]_{0.5} = 10$  mM) and was non-cooperative ( $n_H = 1.13$ ). Experiments were also performed in the presence of 10  $\mu$ M TNP-ATP and showed no significant change in  $K_{0.5}$  for  $SCN^-$  (Fig. 3.24).

TNP-ATP fluorescence was found to be sensitive to other known chaotropes. The order of effectiveness was Trichloroacetate =  $SCN^- > I^- > Cl^-$ , with apparent half maximal effects at 13.3, 13.1, 40.3 and 48.4 mM respectively (Table 3.2), that follows the order of effectiveness of the Hofmeister series (Aviram, 1973). A previous study also found this series for the inhibition of ATP binding to the catalytic site (The and Hasselbach, 1975). These authors have proposed that chaotropes exert their effect by preferential binding at hydrophobic clefts that constitute nucleotide binding sites, because chaotrope concentrations are approximately 500-fold lower than those required to disorder water structure.

The kinetics of the quenching of the fluorescence signal were further studied at 5°C. Rapid addition of KSCN to the phosphorylated enzyme decreased fluorescence at an observed rate of 52 sec<sup>-1</sup> (Fig. 3.25). This is equivalent to the rate of quench by millimolar ATP and ADP, and also to the extrapolated "off" rate of TNP-ATP from its binding site on the ATPase (see Fig. 3.10). However, the diffusion rate of added salts is rapid and, assuming a pseudo-first order process, would be expected to exceed the observed rate by many orders of magnitude (Gutfreund, 1972). These results are compatible with chaotrope entry into the TNP-ATP binding site.

The mechanism of non-competitive inhibition seen in figure 3.24, is not immediately evident. Chaotropes are bulky molecules, with low charge densities and have

TABLE 3.2

The apparent chaotrope  $K_{0.5}$  for inhibition of phosphoenzyme-dependent TNP-ATP fluorescence

Conditions were 0.1 mg/ml SRV, 2  $\mu$ M TNP-ATP, 5mM  $MgCl_2$ , 50  $\mu$ M  $CaCl_2$ , 250  $\mu$ M ATP, 20% glycerol, and 20 mM Tris-maleate, pH 8.0, and 25°C. Chaotrope  $K_{0.5}$  values are the mean of 3 titrations and Hill coefficients for chaotrope interaction were  $0.96 \pm 0.20$  for all titrations.

Chaotrope added	$K_{0.5}$ (mM)
Trichloroacetate	$13.25 \pm 0.65$
KSCN	$13.06 \pm 1.67$
KI	$40.26 \pm 0.20$
KCl	$48.40 \pm 0.80$

previously been described to bind to relatively hydrophobic clefts on the enzyme molecule (The' and Hasselbach, 1975). A complete displacement of TNP-ATP has been found, consistent with these findings. Results showing no change in apparent affinity of TNP-ATP, may well be explained by photoselection of the bound TNP-ATP molecules that are not affected by chaotrope entry to that site.

THE EFFECTS OF D<sub>2</sub>O ON TNP-ATP FLUORESCENCE TNP-ATP emission fluorescence peak was blue-shifted 5 nm from 555 nm in H<sub>2</sub>O, to 550 nm in D<sub>2</sub>O (Fig. 3.26), consistent with its viscosity-dependent fluorescence emission, previously observed by Moczldowski and Fortes (1982). D<sub>2</sub>O is a more highly ordered form of water with the same dielectric constant, but a 1.23 higher viscosity.

Total replacement of the water content of SRV by reconstitution with D<sub>2</sub>O resulted in a higher baseline fluorescence of TNP-ATP bound to non-phosphorylated enzyme (Fig. 3.27a), consistent with the higher light scattering of D<sub>2</sub>O observed in Fig. 3.26. Phosphorylation of the enzyme increased the fluorescence signal by the same amount for SRV in D<sub>2</sub>O as in H<sub>2</sub>O. The emission maxima peaked at the same wavelengths (528 nm) (Fig. 3.27b), indicating a similar environment for the bound probe. The enhanced fluorescence of the probe has previously been attributed to movement of water out of the catalytic site (Dupont *et al.*, 1983). Exclusion of H<sub>2</sub>O or D<sub>2</sub>O would therefore result in the same degree of hydrophobicity of the site, and identical emission maxima as confirmed in Fig. 3.27b. The fact that the fluorescence signal deflections are identical implies that the range of polarity change brought about by phosphorylation does not differ for either D<sub>2</sub>O or H<sub>2</sub>O occupation of the site. TNP-ATP fluorescence in the sites on the phosphorylated or non-phosphorylated enzyme would then appear to be independent of the solvent properties of D<sub>2</sub>O and H<sub>2</sub>O that exist in the bulk medium.

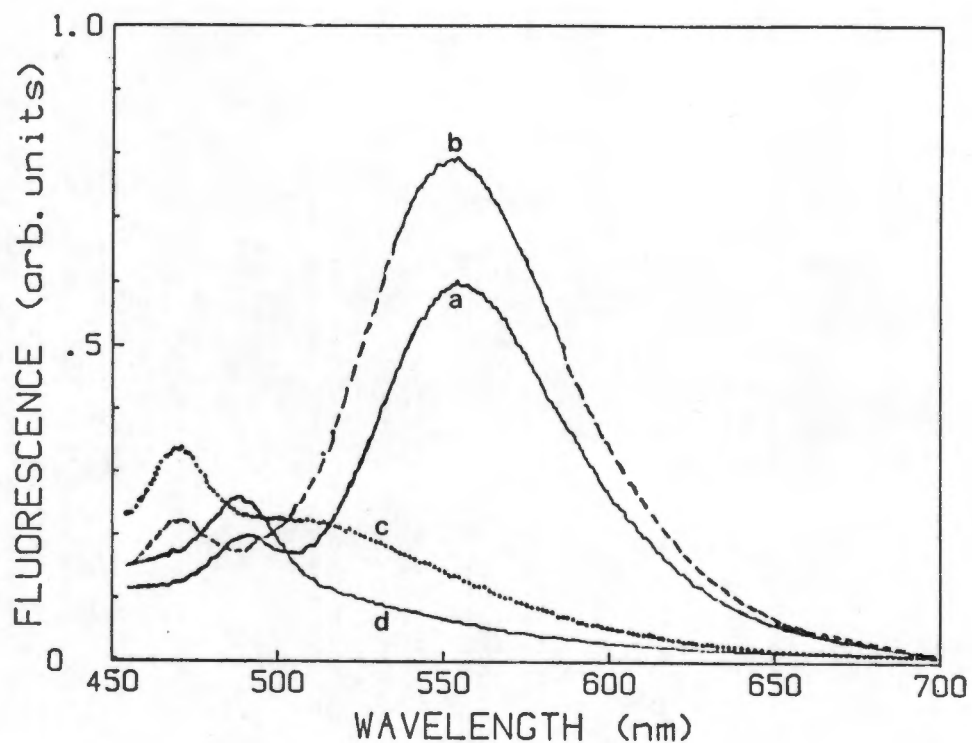


**Figure 3.26** The properties of TNP-ATP fluorescence in  $\text{H}_2\text{O}$  and  $\text{D}_2\text{O}$

TNP-ATP (10  $\mu\text{M}$ ) fluorescence emission was scanned at an excitation wavelength of 418 nm, in 100 mM Mops-Tris pH 7.0 at 25  $^\circ\text{C}$  using  $\text{H}_2\text{O}$  (a) or  $\text{D}_2\text{O}$  (b) as the hydration medium. The scatter spectra of  $\text{D}_2\text{O}$  (c) and  $\text{H}_2\text{O}$  (d) were scanned in the absence of TNP-ATP.

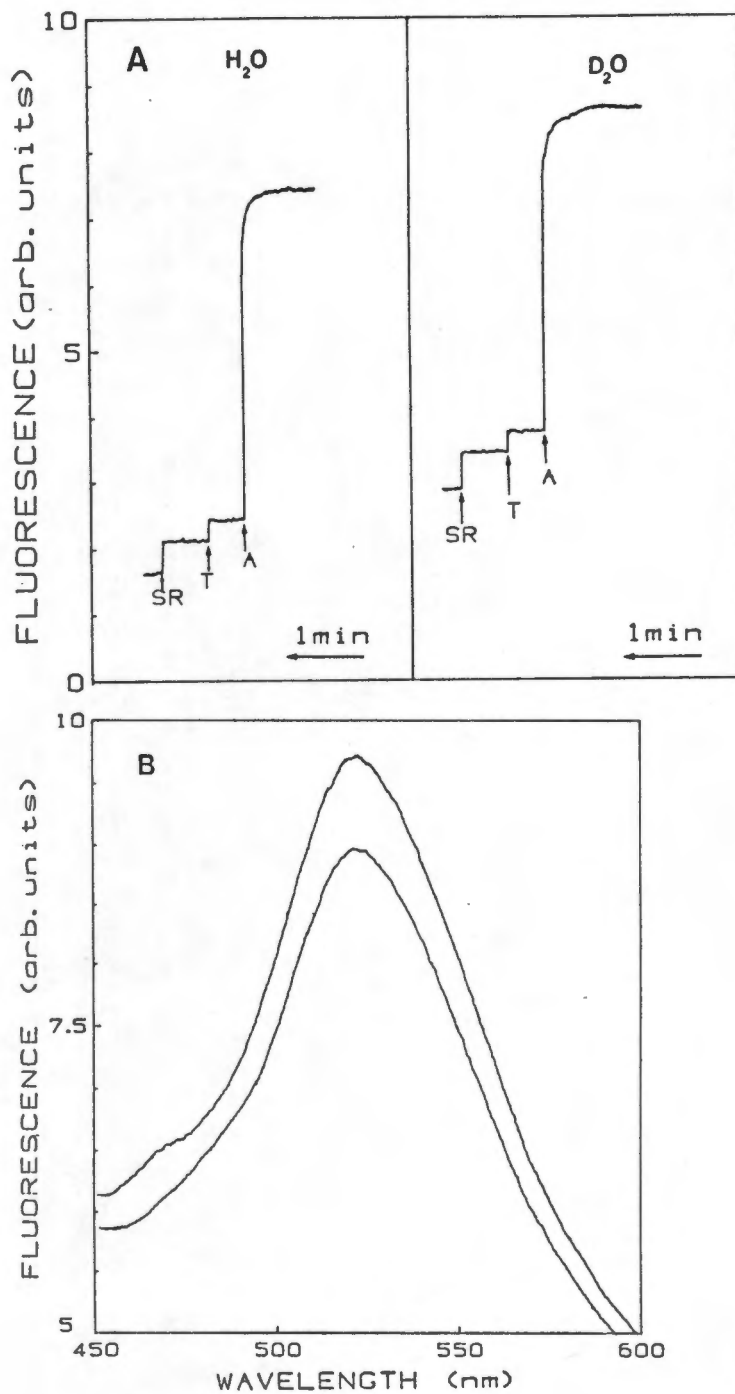


**Figure 3.27** The effects of H<sub>2</sub>O and D<sub>2</sub>O on phosphoenzyme dependent TNP-ATP fluorescence

SRV (0.1 mg/ml) in 20 mM Tris-maleate pH 8.0, 20% glycerol, 5 mM MgCl<sub>2</sub>, 50 μM CaCl<sub>2</sub>, were dehydrated under vacuum at -80°C and reconstituted (SR<sub>2</sub>) in (A) in either H<sub>2</sub>O or D<sub>2</sub>O. Additions were T, 2 μM TNP-ATP, and A, 100 μM ATP. In (B), fluorescence emission was scanned at an excitation wavelength of 418 nm in the same cuvette as in A on the same fluorescence scale.

### 3.6 THE EFFECT OF MONOVALENT CATIONS ON TNP-ATP FLUORESCENCE

Monovalent cations have previously been shown to accelerate ATPase activity and  $\text{Ca}^{2+}$  uptake (Duggan, 1976; Shigekawa and Pearl, 1976; Shigekawa *et al.*, 1978). Rate acceleration by  $\text{K}^+$  is mainly attributed to acceleration of a rate limiting step of phosphoenzyme decomposition (Shigekawa and Pearl, 1976; Guillain *et al.*, 1984). The apparent affinity of the phosphoenzyme for  $\text{K}^+$  is 51 mM for this effect (Shigekawa *et al.*, 1978).

Phosphoenzyme-induced TNP-ATP fluorescence is sensitive to  $\text{K}^+$ . The effects of KCl are shown in Fig. 3.28. Maximal fluorescence developed in the absence of KCl. Increasing KCl concentration in the range 0.2 to 500 mM resulted in decreasing fluorescence to levels approaching that of TNP-ATP bound to the non-phosphorylated enzyme. KCl binding, as monitored by a decrease in TNP-ATP fluorescence, had an apparent affinity in the millimolar range ( $[\text{K}^+]_{0.5} = 48 \text{ mM}$ ) and was non-cooperative ( $n_H = 0.93$ ) (Table 3.4).

TNP-ATP enhanced fluorescence was found to be sensitive to other group IA alkali cations. Fluorescence was decreased by monovalent cations in the series  $\text{K}^+ > \text{Rb}^+ = \text{Cs}^+ > \text{Na}^+ \gg \text{Li}^+$ , with apparent half-maximal effects at 48, 73, 75, 93 and 246 mM, respectively (Table 3.4). These results are consistent with the order of effectiveness for stimulation of E-P hydrolysis, as described by Shigekawa and Dougherty, 1978).

The mechanism of monovalent cation interaction was further explored. Initial studies on the  $\text{Na}^+/\text{K}^+$ -ATPase showed that  $\text{K}^+$  decreased the affinity of the enzyme for TNP-ATP (Moczydlowski and Fortes, 1982). A recent study showed that  $\text{K}^+$  decreased the  $K_d$  of the  $\text{Ca}^{2+}$ -ATPase for TNP-AMP from 0.4 to 3.6  $\mu\text{M}$  (Bishop *et al.*, 1986).

TNP-ATP fluorescent binding assays showed apparent affinities of the ATP-induced phosphoenzyme for TNP-ATP to be 0.61 and 3.10  $\mu\text{M}$ , in the absence and presence of KCl,

respectively (Fig. 3.29). These results are consistent with those of Bishop et al., 1986). Total phosphoenzyme levels remained unaltered (Table 3.4). However the TNP-ATP affinities in the Pi-induced phosphoenzyme (in 10% (v/v) Me<sub>2</sub>SO), were 0.95 and 2.8  $\mu$ M in the absence and presence of KCl, respectively (Fig. 3.29b), while equilibrium E-P levels decreased from 3.05 to 1.9 nmol/mg upon the addition of KCl.

A comparative study of [<sup>14</sup>C]TNP-ATP binding by the filtration method showed TNP-ATP bound to the Pi-induced phosphoenzyme with an apparent affinity of 0.76 and 3.13  $\mu$ M, in the absence and presence of K<sup>+</sup> respectively (Fig. 3.30). While the Pi-induced affinities for TNP-ATP agree with the fluorescent and <sup>14</sup>C- labelled TNP-ATP methods, they are inconsistent with the results of Bishop et al., (1986). Their study expressed apparent affinities as ratios of TNP-ATP bound to total phosphoenzyme, under the assumption that all phosphoenzyme levels produce enhanced TNP-ATP fluorescence.

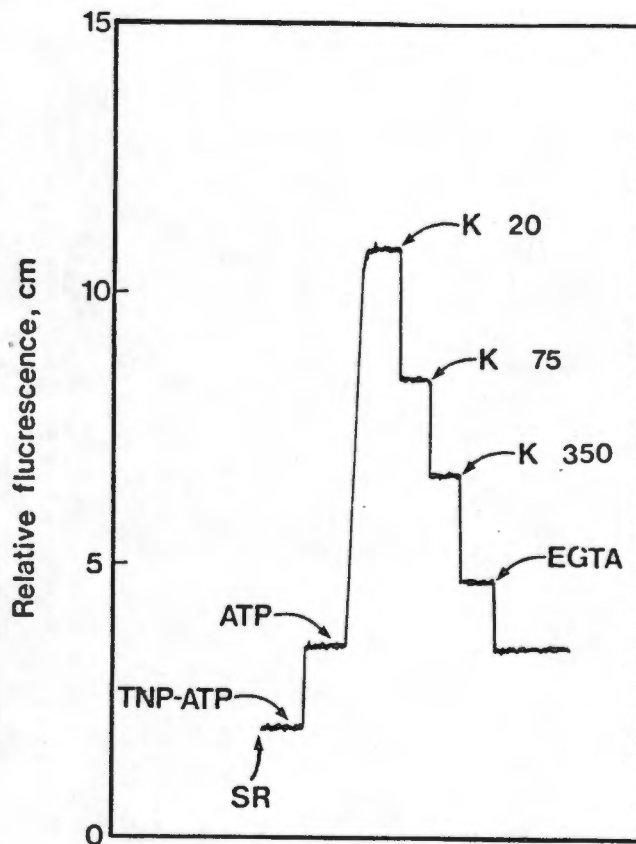
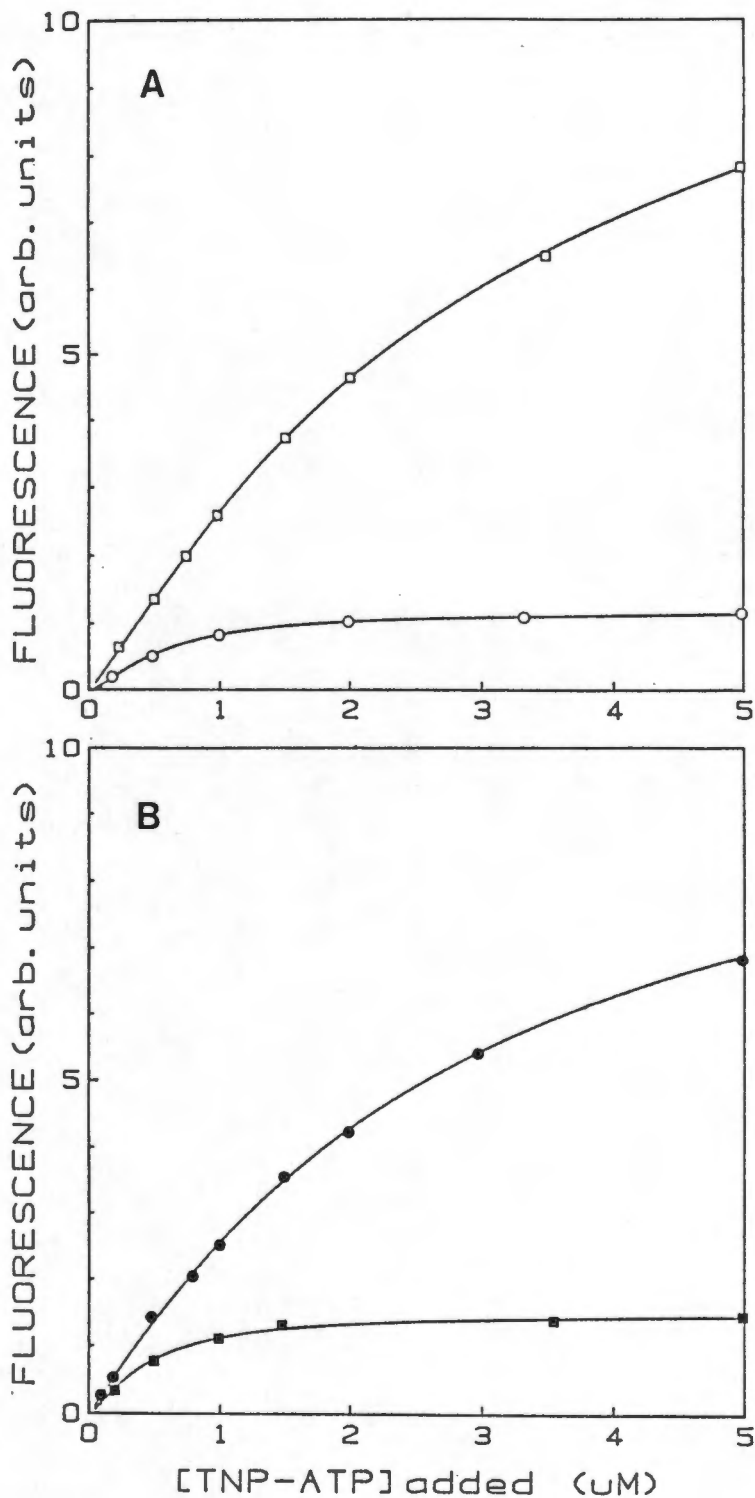


Figure 3.28 The effect of KCl on TNP-ATP fluorescence

Experiments were initiated by addition of 0.1 mg/ml SRV in 3.0 ml of 20 mM Tris-maleate, pH 8.0, 20 % glycerol, 5 mM  $\text{MgCl}_2$ , 50  $\mu\text{M}$   $\text{CaCl}_2$ , at 25 °C. Further additions, indicated by arrows, were 2  $\mu\text{M}$  TNP-ATP, 250  $\mu\text{M}$  ATP. Sequential additions of KCl gave cumulative concentrations as indicated. Finally EGTA, 0.2 mM, was added. Excitation was at 418 nm and emission at 525 nm with 10 nm bandpasses.



**Figure 3.29** TNP-ATP fluorescence binding assays in the presence of KCl

TNP-ATP was titrated into a cuvette containing 0.1 mg/ml SRV, 0.1 M Mops/Tris, pH 7.0, 5 mM  $MgCl_2$ , and 100 mM KCl, with either A, 50 uM  $CaCl_2$  (O), and ATP (□), or in B, 10 % (v/v)  $Me_2SO$ , 0.5 mM EGTA (■) and 5 mM Pi (●). Data have not been corrected for fluorescence of unbound TNP-ATP.

TABLE 3.4

Effects of KCl on phosphoenzyme levels from ATP and Pi

Conditions	E-P (nmol/mg)	E-P + KCl (nmol/mg)
E + ATP	3.35 ± 0.45	3.30 ± 0.50
E + Pi	3.05 ± 0.16	1.90 ± 0.35

Conditions for phosphorylation from ATP and Pi were as described in Fig. 3.30

We have shown earlier that the fluorescence species appears to be dependent on E<sub>2</sub>-P, and that the ADP-insensitive phosphoenzyme represents approximately 30% of total E-P (Fig. 3.16). The effect of KCl was to decrease E<sub>2</sub>-P by 50% with a compensatory increase in E<sub>1</sub>-P. The K<sup>+</sup>-induced decrease in E<sub>2</sub>-P resulted in a 90 % decrease of TNP-ATP fluorescence. The change in fluorescence cannot therefore be entirely attributed to changes in the apparent affinities of the enzyme for TNP-ATP.

A kinetic analysis of the rates of decrease of fluorescence was performed at low temperatures that have previously been found to slow the rate of phosphoenzyme decomposition (deMeis et al., 1980). Addition of K<sup>+</sup> to the enhanced fluorescent state would be expected to decrease fluorescence at the "off" rate of TNP-ATP from its site (see Fig. 3.10), under conditions that decrease the affinity for

TNP-ATP. However,  $K^+$  decreased the fluorescence at a rate approximately 1000-fold slower ( $.027 \text{ sec}^{-1}$ ) (Fig. 3.31) than the "off" rate constant of TNP-ATP ( $30 - 50 \text{ sec}^{-1}$ ). The slow rate is compatible with the rate of E-P decomposition at  $5^\circ\text{C}$  and pH 7.0 (data not shown).

In addition, KCl titrated onto the enzyme had an effect additive to that of TNP-ATP quenching by 10 mM KSCN (data not shown). The  $K_{0.5}$  of KCl (49 mM) was not altered by the presence of the chaotrope. These results indicate two different mechanisms for the action of TNP-ATP fluorescence signal quenching by cations and chaotropic anions. The former appears to accelerate phosphoenzyme decomposition, while the latter occupies the TNP-ATP binding site in a non-competitive manner.

### 3.7 THE INTERACTION OF VALINOMYCIN AS INDICATED BY TNP-ATP FLUORESCENCE.

Valinomycin has previously been shown to inhibit  $\text{Ca}^{2+}$ -dependent ATPase activity in the presence of 100 mM KCl. Inhibition was apparent at both saturating and subsaturating levels of  $\text{Ca}^{2+}$  (Arav et al., 1983). The effects of valinomycin on ATPase activity are shown in Fig. 3.32. Addition of KCl or of NaCl stimulated ATPase activity approximately 2 and 1.6-fold respectively. The presence of 15  $\mu\text{M}$  valinomycin resulted in 30% inhibition of ATPase activity in the absence of added monovalent cations, and diminished the stimulatory effect of high KCl concentrations.

Inhibition of ATPase activity by valinomycin in the absence of added KCl did not appear to be explained by endogenous  $K^+$ , since total  $K^+$  measured by flame photometry was less than 0.5 mM. The possibility that valinomycin might be acting by increasing  $K^+$  conductance across the membrane, and thus charge redistribution, was considered, since  $\text{Ca}^{2+}/K^+$  countertransport has been suggested by Chiu and Haynes (1980).

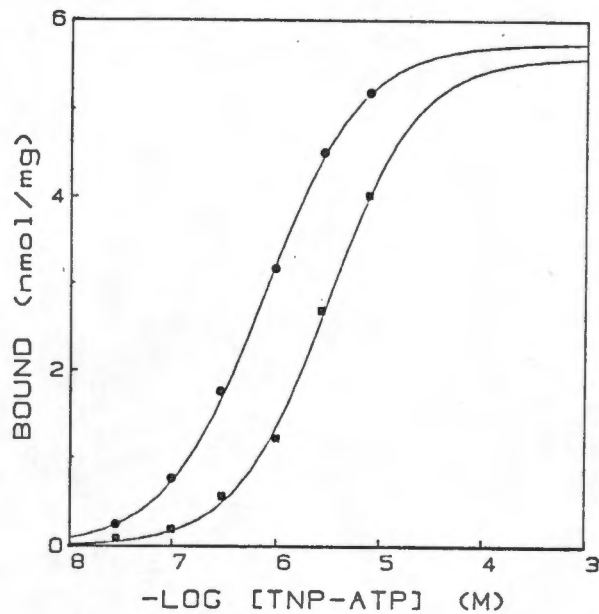


Figure 3.30  $[^{14}\text{C}]\text{TNP-ATP}$  binding in the presence of KCl

Binding assays were performed under identical conditions as in Fig. 3.5 except that the medium contained 10% (v/v)  $\text{Me}_2\text{SO}$  and 5 mM Pi in the absence (●) and presence (■) of 100 mM  $\text{KCl}$ . Binding parameters were  $K_{0.5} = 0.76$  and  $3.13 \mu\text{M}$ ; Maximal binding = 5.4 and 5.3 nmol/mg; and  $n_{\text{H}} = 0.93$  and  $0.91$  in the absence and presence of KCl respectively.

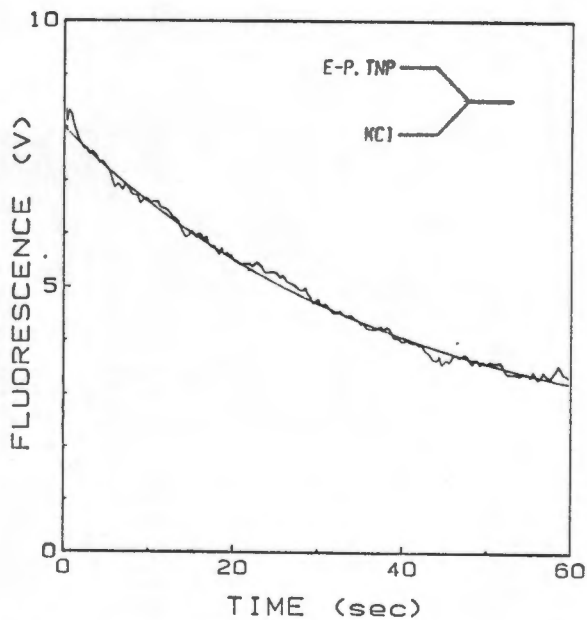
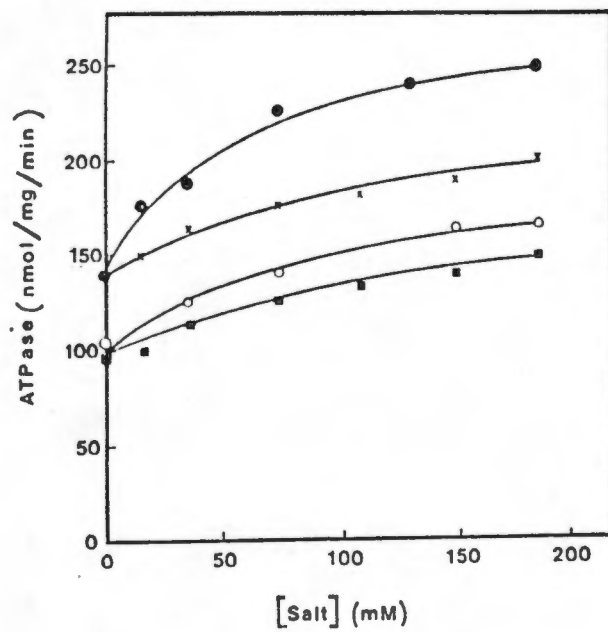


Figure 3.31 Kinetics of the rate of decrease of TNP-ATP fluorescence by KCl

Stopped flow fluorimeter conditions and buffers were as in Fig. 3.30, in the absence of  $\text{Me}_2\text{SO}$ , and identical to the conditions of Fig. 3.25 for  $\text{KSCN}$  fluorescence quenching: syringe A, 0.2 mg/ml SRV,  $2 \mu\text{M}$  TNP-ATP and  $100 \mu\text{M}$  ATP and syringe B, 200 mM KCl at  $5^\circ\text{C}$ . The non-linear least squares fit (solid line) showed an observed rate constant of  $0.027 \text{ sec}^{-1}$



**Fig. 3.32** The effects of KCl, NaCl and valinomycin on ATPase activity.

ATPase activity was determined by the pH stat Method at pH 8.0 and 25 °C, as described under "Methods". Additions were KCl (●), NaCl (x), NaCl + 15 uM valinomycin (○) and KCl + 15 uM valinomycin (■).

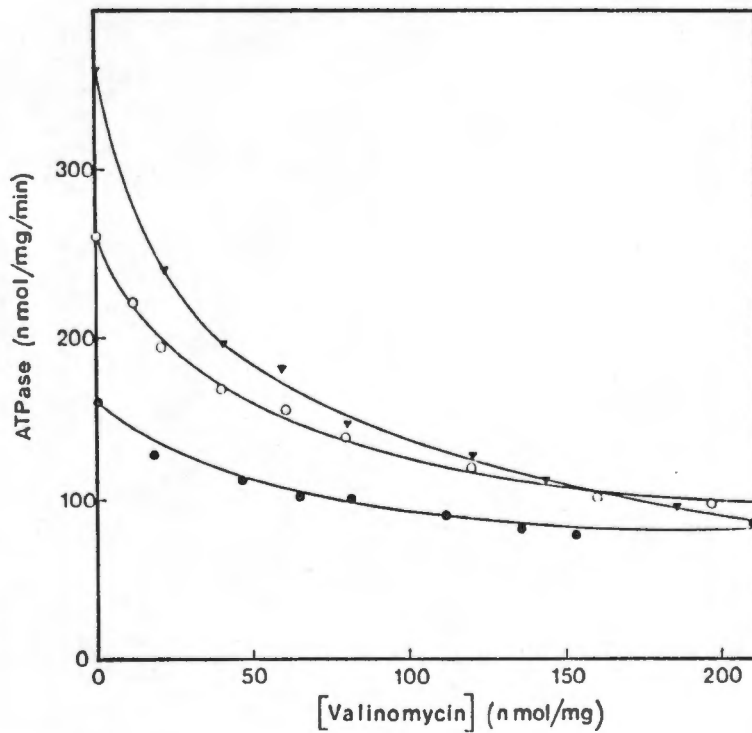


**Figure 3.33** Inhibition of ATPase activity by valinomycin.

Measurements were made as in Fig. 3.32. Additions were, no added KCl (●), 136 mM KCl(▽)and 149 mM NaCl (■).

The experiments shown in Fig. 3.32 were conducted in the presence of the  $\text{Ca}^{2+}$ -specific ionophore, A23187, which excluded the possibility of a transmembrane potential from  $\text{Ca}^{2+}$  gradient formation during enzyme turnover. In addition, the carboxylic ionophores, nigericin (8  $\mu\text{M}$ ), which facilitates  $\text{K}^+$  for  $\text{H}^+$  exchange, and monensin which facilitates  $\text{Na}^+$  for  $\text{K}^+$  exchange, had no effect on ATPase activity, both in the presence and absence of 100 mM KCl or NaCl (results not shown).

The concentration dependence of valinomycin effects are shown in Fig. 3.33. Increasing amounts of valinomycin partially inhibited ATPase activity, in the absence and the presence of KCl (150 mM) and NaCl (150 mM), with half maximal effects at 30-40 nmol/mg SR protein. At high concentrations of valinomycin, the curves converged and the stimulatory effects of the cations were thus abolished.

TNP-ATP enhanced fluorescence reached maximal levels in the absence of added KCl (Fig. 3.34). Addition of valinomycin to the enzyme during the hydrolysis of ATP, in the absence of added KCl, caused a small but significant increase in fluorescence signal (Compare to Fig. 3.28). Subsequent additions of KCl had less inhibitory effects on fluorescence, than in the absence of valinomycin. The apparent  $K_{0.5}$  values for KCl gave values for  $K_{0.5}$  of 48 and 135 mM (Fig. 3.35), in the absence and presence of valinomycin respectively. Valinomycin had no effect on the apparent affinity of the enzyme for TNP-ATP under turnover conditions (Fig. 3.36).

The effects of valinomycin on the apparent affinities of  $\text{Li}^+$ ,  $\text{Na}^+$ ,  $\text{K}^+$ ,  $\text{Rb}^+$ , and  $\text{Cs}^+$  are shown in Table 3.5. The data, in the absence of valinomycin, are consistent with the order of effectiveness for stimulation of E-P hydrolysis, as described by Shigekawa and Dougherty, (1978). The main effect of valinomycin is to increase the  $K_{0.5}$  for the KCl effect, such that the order of effectiveness is altered to

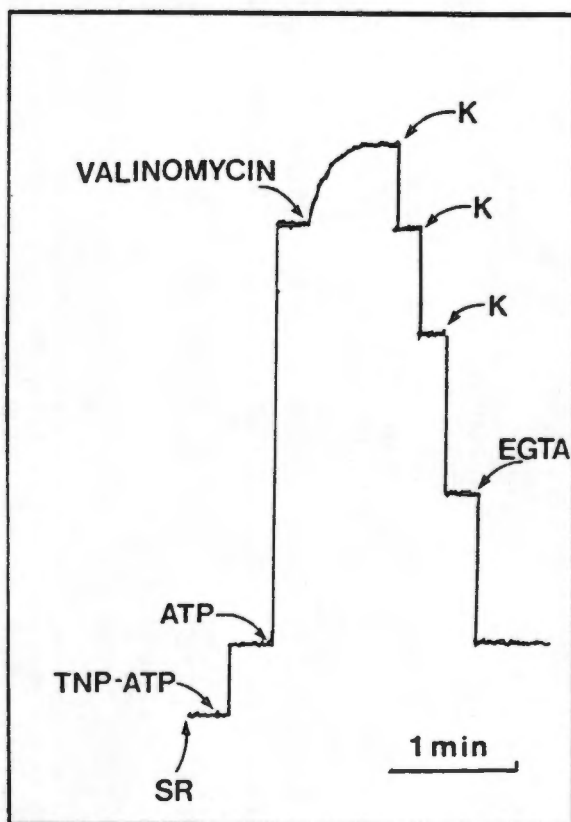


**Figure 3.34** Effects of valinomycin on inhibition of TNP-ATP fluorescence by KCl

Experimental conditions were identical to those of Fig. 3.28. Valinomycin (15  $\mu$ M) in ethanol was added where indicated.

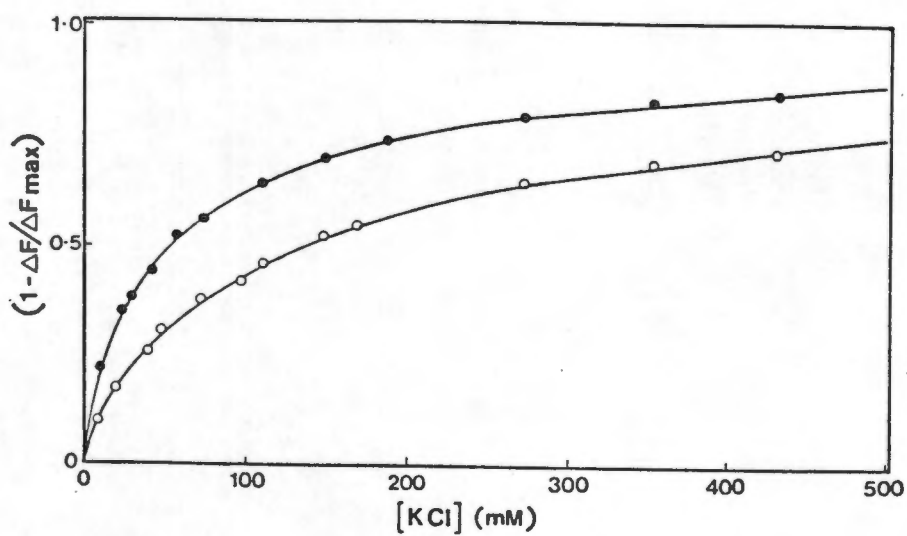


**Figure 3.35** The effects of valinomycin the KCl concentration dependence of inhibition of TNP-ATP fluorescence.

Fluorescence inhibition by KCl in the absence (●) and presence (○) of 15 μM valinomycin under conditions of Fig. 3.28 and 3.34, respectively.

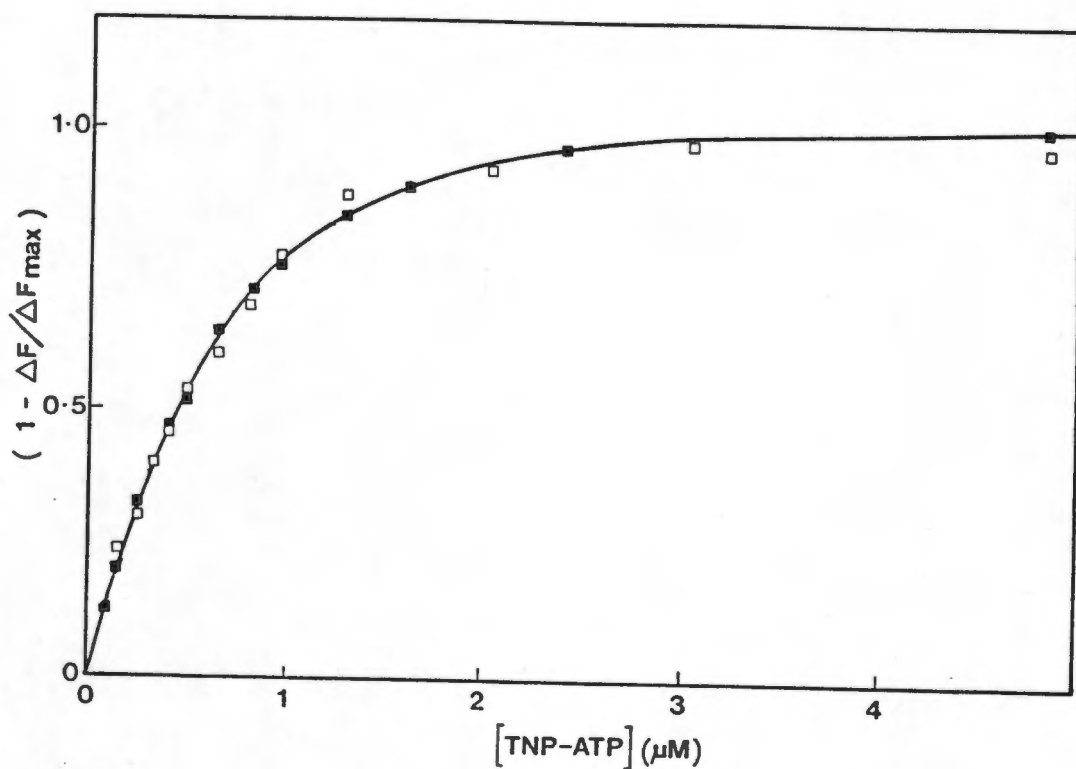


**Figure 3.36** TNP-ATP binding to SRV in the presence of valinomycin.

Binding was measured by fluorescence under steady state turnover conditions identical to those of Fig. 3.28 in the absence of added KCl. TNP-ATP was titrated into the cuvette, in the absence (■) or presence (□) of valinomycin. No correction for inner filter effects was made.

$\text{Cs}^+ > \text{Rb}^+ > \text{K}^+ = \text{Na}^+ > \text{Li}^+$ . The effect of valinomycin, therefore, appears to decrease the affinity and specificity of the site to which  $\text{K}^+$  binds.

The nature of the increase in the fluorescence signal upon addition of valinomycin in the absence of KCl (Fig 3.34) is of interest. It does not appear to be due to non-specific light scattering of valinomycin itself. This conclusion is based on the observations a) that EGTA quenched the total signal following addition of ATP and valinomycin that did not depend on their order of addition and b) that valinomycin added to SR, TNP-ATP and  $\text{Ca}^{2+}$  prior to ATP addition, only produced a slight increase in apparent fluorescence, which was 6 to 10-fold greater when added after ATP, and c) a scan of emission spectra of enhanced TNP-ATP fluorescence, following addition of valinomycin, showed no shift in emission maximum, consistent with the enhanced fluorescence being due to increase in quantum yield of the bound probe.

Valinomycin thus appears to modify the function and characteristics of the  $\text{Ca}^{2+}$ -ATPase in the absence of monovalent cations. The ionophore decreases  $V_{\text{max}}$  of  $\text{Ca}^{2+}$ -dependent ATPase (Fig 3.33) and increases fluorescence emission of TNP-ATP, bound to the enzyme in the steady state (Fig. 3.34).

TABLE 3.5

The effect of valinomycin on the apparent  $K_{0.5}$  for inhibition of TNP-ATP fluorescence induced by enzyme turnover

---

Cation	Control	Plus 15 $\mu$ M valinomycin
(as chloride salt)	$K_{0.5}$	$K_{0.5}$
	(mM)	(mM)
Li <sup>+</sup>	246 $\pm$ 24	270
Na <sup>+</sup>	93 $\pm$ 9	136 $\pm$ 3
K <sup>+</sup>	48 $\pm$ 8	134 $\pm$ 10
Rb <sup>+</sup>	73 $\pm$ 4	111 $\pm$ 3
Cs <sup>+</sup>	75 $\pm$ 7	79

---

Conditions were 0.1 mg/ml SRV, 2  $\mu$ M TNP-ATP, 5 mM MgCl<sub>2</sub>, 50  $\mu$ M CaCl<sub>2</sub>, 333  $\mu$ M ATP, 20 % glycerol and 20 mM Tris-maleate, pH 8.0 and 25 °C.  $K_{0.5}$  values are the mean of 3 or more titrations, where standard deviations are indicated. Hill coefficients for monovalent cation binding were 0.93  $\pm$  0.10 for all titrations.

## 4.0 DISCUSSION

Previous studies on the mechanism of  $\text{Ca}^{2+}$  transport, and its relationship to phosphoenzyme intermediates, have been performed by analysis of enzyme, ligand and product status prior or subsequent to catalysis and vectorial events. TNP-ATP provides a useful probe for direct observation of catalytic events during energy transduction. However, reports on the relationship of TNP-ATP fluorescence changes to phosphoenzyme intermediates, and the nature of the TNP-ATP site, whether catalytic or regulatory, are contradictory. Previous studies have been performed in the presence or absence of  $\text{K}^+$ , which we have shown has a profound effect on TNP-ATP fluorescence levels. In addition, models have been proposed for the interaction of TNP-ATP with the enzyme without accurate measures of binding stoichiometry. In consequence, we have synthesized [ $^{14}\text{C}$ ]TNP-ATP to establish the relationship between bound TNP-ATP and its fluorescence levels. This study is oriented towards the identification of the phosphoenzyme intermediate(s) responsible for enhanced fluorescence, the nature of the site, whether catalytic, regulatory or both, and the relationship of changes in polarity to water activity.

### 4.1 TNP-ATP BINDING STOICHIOMETRY

[ $^{14}\text{C}$ ]TNP-ATP binding studies were performed at equilibrium by filtration. In practice, the number of moles of ligand exposed to the binding sites must exceed the number of moles of sites available. TNP-ATP binding parameters to the non-phosphorylated and phosphorylated enzyme, using large volumes of filtrate at low ligand concentrations, yielded a stoichiometry of 5.2 and 5.6 nmol/mg respectively. Differential absorbance studies yielded values of 5.3 nmol/mg under the same conditions.

These values are closely related to [ $^{14}\text{C}$ ]ATP (6.1 nmol/mg) and  $^{45}\text{Ca}^{2+}$  (11.2 nmol/mg) binding stoichiometries measured by the filtration method. The value of 6 nmol/mg, as representative of a one mol/mol stoichiometry, has previously been reported for ATP (Guillain et al., (1984) and AMP-PCP (Cable et al., 1985) under these conditions.

The range 5 to 6 nmol/mg, obtained in the present study, is in disagreement with values reported for the stoichiometry in a recent study of Dupont et al., (1982b). Their choice of filters gave high non-specific binding. In view of their reported value of 3.2 nmol/mg for ATP binding, (Dupont et al., 1982; 1982b), a stoichiometry of 2 mol/mol sites for [ $\gamma$ - $^{32}\text{P}$ ]TNP-ATP binding was concluded, implying a model in which two discrete families of sites, the catalytic and the regulatory, are simultaneously accessible to nucleotide binding. The alternate model is one in which a single family of sites exist. A recent kinetic study of Bishop et al., (1984), demonstrated that phosphorylation of the enzyme, ( $\text{E}_1\text{TNP}$ ), by ATP occurs at the rate of dissociation of TNP-ATP from the site of low fluorescence. A possible interpretation is that a single site on the non-phosphorylated enzyme is occupied either by TNP-ATP or ATP as shown in Scheme V



#### Scheme V

The present study demonstrates unambiguously a single family of sites for TNP-ATP, and is therefore compatible with the model proposed in Scheme V in which ATP and TNP-ATP compete for the same site on the nonphosphorylated enzyme.

#### 4.2 TNP-ATP BINDING TO THE PHOSPHORYLATED ENZYME

Under equilibrium conditions,  $E_2 + Pi \rightleftharpoons E.Pi \rightleftharpoons E-P$ , where E-P levels were 3 nmol/mg, TNP-ATP bound to the enzyme with a  $K_{0.5}$  of 0.95  $\mu$ M. A previous study by Bishop et al. (1986) derived a  $K_d$  of 3.3  $\mu$ M for TNP-AMP from binding data expressed as ratios of fluorescence signal to  $E_2-P$  levels, under the assumption that  $E_1-P$  also contributes to fluorescence. Fluorescent titrations for TNP-nucleotide binding require corrections for inner filter effects, and for the fractional fluorescence contribution from probe binding to the low fluorescent non-phosphorylated enzyme.

[ $^{14}C$ ]TNP-ATP binding measurements obviate the problem of differences in relative fluorescence of TNP-ATP, bound to either  $E_2$  or  $E_2-P$ . With this protocol, binding was approximately equal to these two species. Since total [ $^{14}C$ ]TNP-ATP bound is not increased upon phosphorylation, the increase in fluorescence is not attributed to increased binding of the probe.

TNP-ATP binding to other protein components was considered. The ratio of 53 kDa glycoprotein is relatively constant in various vesicle fractions at about 3 : 2 (Michalak et al., 1980; Campbell and McLennan, 1981). However, previous rapid kinetic studies have shown a close correlation of E-P formation and enhanced TNP-ATP fluorescence in the millisecond time scale (Bishop et al., 1984; Andersen et al., 1985), inconsistent with relatively slower conformational change expected if events of E-P formation exhibited allosteric linkage to TNP-ATP bound on another protein. Alternatively, the stoichiometric values are too low to represent 2 mol/mol binding sites. The results of this study indicate a one mol/mol stoichiometry for both the phosphorylated and nonphosphorylated enzyme, in contrast to the measurements obtained in separate studies that two nucleotide binding sites exist simultaneously on the

E<sub>2</sub>-P and E<sub>2</sub> conformations respectively (Watanabe and Inesi, 1982; Dupont et al., 1985). It should be noted that in the latter report, apparent high stoichiometry was due to non-specific binding to cellulose Millipore filters. Use of glass-fibre filters corrects this problem.

#### 4.3 COMPETITION OF ATP AND ADP WITH TNP-ATP

Previous studies have shown the existence of regulatory sites that binds ATP, ( $k_d = 1 \text{ mM}$ ), and stimulate catalysis (deMeis and Vianna, 1979). The secondary regulatory effects of ATP have been evidenced by the fact that nonhydrolysable ATP analogues such as AMP-PCP and AMP-CPP are able to activate ATPase activity (Dupont, 1977; Taylor and Hattan, 1979).

Various models have been proposed for the regulatory site location on the enzyme; the enzyme possesses one single site, but a second molecule of ATP is able to bind to the phosphorylated active site with decreased affinity once ADP has been liberated (MacIntosh and Boyer, 1983; Pick and Karlish, 1982); or the enzyme possesses regulatory sites which are discrete from the catalytic site (Dupont, 1977; Verjovski-Almeida and Inesi, 1979). In the present study, binding isotherms indicate that ATP and ADP compete with TNP-ATP for the same site. The apparent  $K_m$  for ATP (1.24 mM), and ADP (0.54 mM), fall within the ranges previously described. ADP binding at high concentrations has previously been used to differentiate the ADP-sensitive from the ADP-insensitive phosphoenzyme. The decrease in E-P levels is bi-exponential and the initial phase is rapid (Pickard and Jencks, 1982). This corresponds to rapid formation of E<sub>1</sub>-P, followed by a slow phase of phosphoenzyme decomposition that liberates Pi, corresponding to the E<sub>2</sub>-P. The mono-exponential decay in fluorescence induced by ADP, implies that TNP-ATP is displaced from its site prior to the

bi-exponential decay of E-P. ATP, at high concentrations, also decreases fluorescence in a mono-exponential pattern, even though this nucleotide does not accelerate the E<sub>1</sub>-P decomposition that is observed with ADP. In addition, the observed rate of fluorescence decay caused by both nucleotides, correlates well with the "off" rate constant of TNP-ATP from the site. The similarity of observed rates of fluorescence signal decay is indicative of a single process; i.e. TNP-ATP displacement, prior to commencement of the activating effects of the nucleotides.

The competitive nature of the nucleotide binding and the monoexponential decay patterns of fluorescence that showed equivalent values to the "off" rate constant for TNP-ATP, are consistent with TNP-ATP binding to the regulatory site. This site is therefore responsible for enhanced fluorescence of the bound probe, and consequently it must differ significantly in its dielectric properties from the site detected on the non-phosphorylated enzyme.

#### 4.4. TNP-ATP FLUORESCENCE AND ENZYME CONFORMATIONAL CHANGE

Several studies have investigated the remarkable increase in TNP-ATP fluorescence that occurs following phosphorylation of the enzyme. The nature of the E-P species involved is of special interest. It appears that fluorescence enhancement is closely related to levels of E-P formed (Nakamoto and Inesi, 1984; Bishop et al., 1984; Bishop et al., 1986). The rate of increase in fluorescence parallels the formation of total E-P at pH 8.0 and 25°C (Bishop et al., 1984). Studies at lower temperatures (2°C) allow greater resolution of phosphorylated intermediates. Andersen et al. (1985) showed that fluorescence enhancement closely follows the formation of E<sub>2</sub>-P. However, in this study, total E-P was not determined.

Dupont and Pougeois (1983) found that X-537A decreases fluorescence by decreasing steady-state levels of  $E_2$ -P. However, the fluorescent nature of this ionophore and the overlap in emission spectra with those of TNP-ATP (Verjovski-Almeida, 1981), precludes an absolute conclusion from this data. Alternatively, Bishop *et al.*, (1986), have concluded that all phosphoenzyme intermediates ( $E_1$ -P and  $E_2$ -P) produce equivalent levels of enhanced TNP-AMP fluorescence. Their conclusion relies on the assumption that the fluorescence of bound TNP-ATP is insensitive to pH, and on expected changes in relative levels of  $E_2$ -P during  $Ca^{2+}$  accumulation. However, Hiratsuka and Uchida (1973), have previously shown a strong pH dependence ( $pK = 5.1$ ), of the spectrophotometric properties of the trinitrophenol moiety of TNP-nucleotides. Nakamoto and Inesi (1984) have shown an inhibitory effect of TNP-AMP on E-P formation from  $P_i$ , with little inhibition by TNP-ATP in the range 1 to 3  $\mu M$ . The use of the former nucleotide analogue for fluorescence to E-P ratio determination in the range of up to 20  $\mu M$  in the study of Bishop *et al.*, (1986), is contentious. In addition, the apparent affinity for TNP-AMP is measured by protocols that rely on an estimate of the amount of low fluorescent conformation, (E), that is subtracted from total fluorescence.

It is apparent, therefore, that strong evidence for a definitive conformational relationship to fluorescence is required. In the present study procedures that redistribute phosphoenzyme intermediates have been employed for identification of a conformational association with enhanced fluorescence. Methods included were Strontium-induced transport that favours increased  $E_2$ -P, and  $Ca^{2+}$ -oxalate precipitation that diminishes steady-state  $E_2$ -P levels. In addition, modification of those thiols responsible for E-P decomposition results in decreased  $E_2$ -P levels.

### REDISTRIBUTION OF E-P INTERMEDIATES BY STRONTIUM IONS

Strontium ions can substitute for  $\text{Ca}^{2+}$  in vectorial transfer by the  $\text{Ca}^{2+}$  pump (Mermier and Hasselbach, 1972).  $\text{Sr}^{2+}$ -induced turnover favours accumulation of relatively higher levels of  $\text{E}_2\text{-P}$  than during  $\text{Ca}^{2+}$  transport (Guimares-motta et al., 1984). The associated TNP-ATP enhanced fluorescence levels were 10% higher than  $\text{Ca}^{2+}$ -induced signals for the same levels of total phosphoenzyme formed. TNP-ATP fluorescence was found to be  $\text{Mg}^{2+}$ -dependent, consistent with previous findings that  $\text{Ca}^{2+}$ -induced phosphoenzyme formation in the absence of  $\text{Mg}^{2+}$  fails to alter probe fluorescence (Dupont et al., 1983; Bishop et al., 1986), even though TNP-ATP binds with high affinity to the enzyme under these conditions (Dupont et al., 1982). Although it has been reported that  $\text{Sr}^{2+}$  competes for  $\text{Mg}^{2+}$  binding sites on the enzyme,  $\text{Sr}^{2+}$  alone does not substitute functionally for  $\text{Mg}^{2+}$  (Guimares-motta et al., 1984), and is unable to increase phosphoenzyme-associated TNP-ATP fluorescence in the absence of  $\text{Mg}^{2+}$ . Since  $\text{Sr}^{2+}$  does not appear to affect binding parameters of TNP-ATP or other ligands, enhanced fluorescence could be a result of altered relative E-P species levels. The increased fluorescence signal during  $\text{Sr}^{2+}$ -induced turnover, is therefore compatible with increased  $\text{E}_2\text{-P}$  levels.

### REDISTRIBUTION OF E-P INTERMEDIATES BY OXALATE

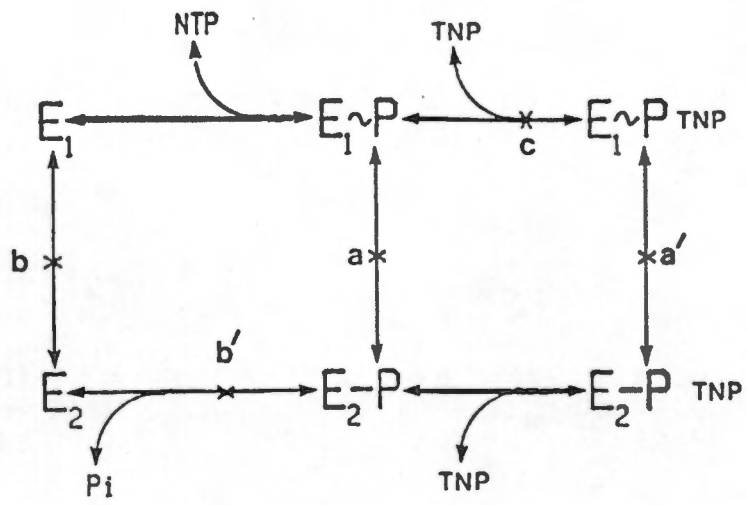
Oxalate accelerates  $\text{Ca}^{2+}$ -uptake by the formation of insoluble  $\text{Ca}^{2+}$ -oxalate precipitates within the vesicle. The  $\text{Ca}^{2+}$  "off" rate is increased from low affinity binding sites oriented towards the vesicle lumen and  $\text{E}_2\text{-P}$  accumulation is maintained at a lower steady-state level than that present during the development of a  $\text{Ca}^{2+}$  gradient (Kometani and Kasai, 1978). Oxalate (5 mM) decreased steady-state TNP-ATP fluorescence to 60%, without decreasing total phosphoenzyme levels. Fluorescent changes were not observed in vesicles rendered

permeable to  $\text{Ca}^{2+}$  by the  $\text{Ca}^{2+}$  ionophore, A23187, supporting the conclusion that oxalate alters  $\text{E}_2\text{-P}$  levels without exerting any direct quenching effects on TNP-ATP fluorescence. This provides further evidence that enhanced TNP-ATP fluorescence is associated with the  $\text{E}_2\text{-P}$  conformation. Depletion of medium  $\text{Ca}^{2+}$  in the presence of oxalate resulted in a sharp decrease in TNP-ATP fluorescence that was restored upon readdition of  $\text{Ca}^{2+}$ . Of practical interest is that the time taken to inhibit TNP-ATP fluorescence is a reflection of the rates of  $\text{Ca}^{2+}$  transport, which were well correlated with  $^{45}\text{Ca}^{2+}$  uptake data. Such an approach might provide a convenient method for studying transport at low medium  $\text{Ca}^{2+}$  levels.

#### REDISTRIBUTION OF E-P INTERMEDIATES BY SULPHYDRYL

MODIFICATION Derivatization of specific thiol groups on the  $\text{Ca}^{2+}$ -ATPase has provided a useful method for the modification of the distribution of phosphorylated intermediates. The decrease of ATPase activity and  $\text{Ca}^{2+}$  uptake under conditions that do not alter total E-P levels, is essentially in agreement with previous studies involving selective SHd modification (Yamada and Ikemoto, 1978; Kawakita *et al.*, 1980; Yasuoka-Yabe and Tonomura, 1982; Yasuoka-Yabe *et al.*, 1983). Previous studies have described the effect of SHd modification as an inhibition of conversion of ADP-sensitive to ADP-insensitive E-P (Nakamura and Tonomura, 1982; Ikemoto, 1982). Nakamura and Tonomura (1982) have cited this as evidence as the basis for their conclusion that  $\text{Ca}^{2+}$  ions are occluded by the  $\text{E}_1\text{-P}$  species.

The finding in the present studies, that the SHd-modified enzyme cannot be phosphorylated in the reverse direction by  $\text{P}_i$ , suggests at least two possibilities. Either the  $\text{E}_2\text{-P}$  conformation cannot be attained from both the forward and reverse phosphorylation processes (steps a and b, b', Scheme VI), or the transition from  $\text{E}_1$  to  $\text{E}_2$ , whether



Scheme VI

phosphorylated or not, is inhibited (steps a and b, Scheme VI). The latter argument raises the possibility that the E<sub>1</sub> conformation can exist in the absence of bound Ca<sup>2+</sup>.

SHd modification has previously been described as Ca<sup>2+</sup> sensitive (Kawakita et al, 1980). The protocol may, in fact, be introducing a complication of uncoupling, brought about by incubation of SRV in low [Ca<sup>2+</sup>] (10<sup>-7</sup> M), as described by McIntosh and Berman (1978). This would also complicate the interpretation of Ca<sup>2+</sup> modulated conformational sensitivity toward SHd modification. Hence the protocol, as described by Kawakita et al. (1980), using high Ca<sup>2+</sup> only, was employed in the present study. Whatever the mechanism involved in the modification of conformational transitions, it appears that the E<sub>2</sub>-P conformation is strongly inhibited in the presence of Ca<sup>2+</sup>.

The aim of the present sulphhydryl investigation was to determine the nature of the phosphorylated species that result in increased hydrophobicity of the non-catalytic binding site on the Ca<sup>2+</sup>-ATPase to which TNP-nucleotides bind and show enhanced fluorescence. Under conditions of NEM modification that did not alter E-P levels during catalysis, TNP-ATP fluorescence was inhibited from both ATP plus Ca<sup>2+</sup> and from Pi in the absence of Ca<sup>2+</sup>. This would indicate that E<sub>1</sub>-P, the predominant species under these conditions, is unaltered by SHd modification. Furthermore, this species cannot be responsible for enhanced fluorescence. Two possible mechanisms were considered. The first is that E<sub>2</sub>-P formation, and its level, determine enhanced TNP-ATP fluorescence. The decreased fluorescence during turnover, of approximately 50 % following SHd modification, correlate well with the decrease in ADP-sensitive E-P from 1.3 to 0.7 nmol/mg; a change of approximately 50 % (Scheme VI, blocked at step a').

A second mechanism that requires consideration is related to the possibility that catalytic and regulatory

nucleotide sites may be non-identical, in which case events at the catalytic site would be transmitted to the non-catalytic site by a conformational transition. Berman and Meltzer (1986) and Berman (1986), have shown dissociation of TNP-ATP enhanced fluorescence from E-P formation under conditions that uncouple transport from catalytic activity and E-P levels, and have proposed that intermediate conformational events of a strictly ordered type couple catalytic intermediates to the transport cycle. SHd modification would then block conformational changes originated at the catalytic site from being transmitted to the regulatory site (step c, Scheme VI), thus preventing enhanced fluorescence of the  $E_1$ -P conformation. In view of the parallel decreases in ADP-sensitive to ADP-insensitive transitions, as well as the block for phosphorylation from Pi in the reverse direction, the latter proposal of  $E_1$ -P dependent enhanced fluorescence appears unlikely. The above discussion, based on  $Sr^{2+}$ , oxalate and NEM-derivitization studies, lead to the conclusion that the  $E_2$ -P species is the most probable intermediate responsible for enhanced TNP-ATP fluorescence.

#### 4.5 THE ROLE OF WATER DURING $Ca^{2+}$ PUMP ACTIVITY

The large increase in fluorescent quantum yield and blue shift in emission maximum of TNP-ATP bound to the phosphorylated enzyme, indicate a major alteration in the dielectric properties of the probe microenvironment. This has previously been equated with exclusion of approximately 18 water molecules from the catalytic site (Dupont and Pougeios, 1983). Dupont (1984), hypothesised that the  $Ca^{2+}$ -ATPase functions as a water pump which essentially removes water from the catalytic site and rehydrates  $Ca^{2+}$  ions at the inward oriented site, increasing their effective diameter and preventing reverse migration to the vesicle exterior (see

Scheme 1.4). The present study further explores interactions of water at the regulatory nucleotide site by the use of chaotropic anions that disorder water structure, and by replacement of H<sub>2</sub>O by the more highly ordered form of water, namely D<sub>2</sub>O.

Chaotropes in general decreased the enhanced TNP-ATP fluorescence in the range 1 to 20 mM, but simultaneously only slightly increased phosphoenzyme levels from 3.2 to 3.6 nmol/mg. The order of effectiveness was trichloroacetate = SCN<sup>-</sup> > I<sup>-</sup> > Cl<sup>-</sup>, with apparent half maximal effects at 13.3, 13.06, 40.3, and 48.4 mM, respectively. Although this follows the order of effectiveness of the Hofmeister series for chaotropic anions, the effective concentration range is too low to significantly alter the structure of bulk water (Hamabata and von Hippel, 1973).

The' and Hasselbach (1975) have previously reported that chaotropes, at concentrations of less than 50 mM, inhibit ATP binding to the catalytic site of the Ca<sup>2+</sup>-ATPase. The order of effectiveness was that expected from the Hofmeister series. These authors proposed that chaotropes, due to their low charge densities, exert their effect by binding to hydrophobic clefts that constitute nucleotide binding sites on the enzyme. KCl has previously been shown to cause an 11-fold increase in the "off" rate of ADP from E<sub>1</sub>-P. The effect was enhanced by the use of KSCN, indicating an anionic rather than cationic-mediated process (Shigekawa and Kanazawa, 1982). In support of their findings, the rate of quench of fluorescence signal by chaotropes  $k_{obs} = 56-60 \text{ sec}^{-1}$  at 5°C (Fig. 3.25), correlates well with the "off" rate of TNP-ATP from its site ( $k_{off} = 40 \text{ sec}^{-1}$ ) (Fig. 3.10).

It is concluded that chaotropes can enter the regulatory site after bound TNP-ATP has departed. The use of chaotropes therefore, is of limited value in determination of the water activity relationship of binding site water and TNP-ATP fluorescence.

TNP-ATP fluorescence, in vesicles under non-turnover conditions, with D<sub>2</sub>O substituting for H<sub>2</sub>O, showed equivalent changes in the range of fluorescent signal magnitude and emission maxima. The extent of change of the phosphoenzyme-induced enhanced fluorescence was identical for vesicles in both media. TNP-ATP fluorescence in these media alone, in the absence of SR vesicles, showed a higher fluorescence quantum yield, and a 5 nm blue shift in emission maximum in D<sub>2</sub>O. This is attributed to the 1.23-fold higher viscosity of D<sub>2</sub>O over H<sub>2</sub>O, since the dielectric constant of the two media are approximately equal. However, these parameters were not reflected by TNP-ATP bound to sites on the non-phosphorylated or phosphorylated enzyme.

It has previously been shown that cosolvents such as Me<sub>2</sub>SO and glycerol, increase the stability of the acyl-phosphate bond (deMeis *et al.*, 1980). Dipolar aprotic solvents such as Me<sub>2</sub>SO, significantly decrease the phosphate solvation energies and therefore favour partitioning of Pi to the active site (deMeis, 1983; 1985). There is little evidence for a direct interaction of cosolvents involving water structure during hydrolysis of the of the acyl-phosphate bond in the active site. NMR studies have shown specific water structures in the active sites of enzymes such as crambin (Teeter, 1984) and rubredoxin (Waughtenpaugh, 1978). Active site water in the Ca<sup>2+</sup>-ATPase may also have a specific arrangement that overrides the functional differences between H<sub>2</sub>O and D<sub>2</sub>O under conditions of enhanced fluorescence. Conformational transitions may exert altered structures on these water molecules. Wiggins (1982) has proposed that the properties of interfacial water is strongly dependent upon the geometrical arrangement of protein surface hydrogen bond donors and acceptors, and that these arrangements can decrease the structural temperature of water from 25 to 5 °C.

An alternative possibility is that TNP-ATP fluorescence

is altered primarily by protein conformational change, not mediated through the associated water environment. Hiratsuka (1975), has proposed that the trinitrophenylated moiety of TNP-ATP folds back to become sandwiched between the base of ATP and a tryptophan residue in the active site of heavy meromyosin, resulting in enhanced fluorescence from pi-electron transfer. Nakamoto and Inesi (1984) have demonstrated energy transfer between a tryptophan residue of the  $\text{Ca}^{2+}$ -ATPase and bound TNP-ATP. It is possible, therefore, that approximation of a hydrophobic residue, such as tryptophan, or a relatively apolar sequence of the ATPase is exposed to the binding site in the  $\text{E}_2$ -P conformation, forming an interface that is conducive to enhanced fluorescent state of the probe.

It is of interest that the proposed step in the catalytic cycle ( $\text{E}_2$ -P) that results in an enhanced fluorescence state of bound TNP-ATP, coincides with a major change in affinity of the binding sites for  $\text{Ca}^{2+}$ , as well as reorientation of sites access to the vesicle lumen (deMeis and Vianna, 1979). Formation of the  $\text{E}_1$ -P conformation is associated with  $\text{Ca}^{2+}$  occlusion from both access points of the  $\text{Ca}^{2+}$  channel (Fassold *et al.*, 1981; Chiesi and Inesi, 1979). A recent study by Petithory and Jencks (1986) shows kinetic evidence for non-random binding of  $\text{Ca}^{2+}$ , followed by ATP, prior to phosphorylation. It is possible that a small conformational change in the vicinity of the active site during phosphorylation of the enzyme occludes  $\text{Ca}^{2+}$  to the exterior. A subsequent step is necessary to reorient the  $\text{Ca}^{2+}$  sites. The energy required for this step is predictably small (Inesi, 1985), whereas the energy changes necessary for the decrease in affinity of the sites for  $\text{Ca}^{2+}$  are large. It is possible, therefore, that enhanced fluorescence of the regulatory nucleotide site probe, TNP-ATP, reflects a minor conformational change of the enzyme during the catalytic cycle that is not essentially linked to the catalytic cycle,

but nevertheless represents a prerequisite for vectorial transfer of  $\text{Ca}^{2+}$  ions.

#### 4.6 INTERACTION OF $\text{K}^+$ AND VALINOMYCIN WITH THE $\text{Ca}^{2+}$ -ATPase

Phosphoenzyme dependent enhanced fluorescence is sensitive to monovalent cations and decreases in a manner compatible with binding of monovalent cations to the monovalent cation site previously characterized and which promotes E-P hydrolysis (Shigekawa and Dougherty, 1978). The specificity of the site for monovalent cations ( $\text{K}^+ > \text{Rb}^+ > \text{Cs}^+ > \text{Na}^+ > \text{Li}^+$ ) is consistent with their effectiveness in promoting E-P hydrolysis. The  $k_{0.5}$  for KCl stimulation of E-P hydrolysis (51 mM) (Shigekawa and Dougherty, 1978) is similar to the  $K_{0.5}$  (48 mM) for inhibition of fluorescence. However, it should be noted that under certain conditions, KCl diminishes TNP-ATP fluorescence without concomitant decrease in steady state E-P levels (Bishop *et al.*, 1984). The possible mechanisms for fluorescence decrease are : a) that KCl accelerates E-P hydrolysis thereby decreasing relative levels of  $\text{E}_2\text{-P}$ , while total E-P levels remain unchanged ; or (b) that KCl decreases the affinity of the nucleotide binding site for TNP-ATP. Bishop *et al.* (1986) have shown, in support of the latter mechanism, that the affinity for TNP-AMP decreases 10-fold upon the addition of KCl, and that the fluorescence lifetimes of the probe remains unchanged. The present study showed similar changes in affinity for [ $^{14}\text{C}$ ]TNP-ATP, ( $K_{0.5} = 0.76$ ) in the absence and ( $K_{0.5} = 3.13 \mu\text{M}$ ) in the presence of 100 mM KCl. However, the fact that fluorescence was decreased by 90% is incompatible with the expected fluorescence changes from the affinity changes of TNP-ATP, even after correction for loss of equilibrium levels of E-P.

It follows that the apparent decrease in affinity of TNP-ATP binding is caused by an increase in the "off" rate

constant of TNP-ATP from the site. We have shown above that ATP, ADP, chaotropes, and values derived from the observed "on" rate, all indicate an "off" rate constant of TNP-ATP in the range of 30 to 60 sec<sup>-1</sup> at 5°C. However, fluorescence decreased at an observed rate constant of 0.027 sec<sup>-1</sup> i.e. 1000-fold slower, which is equivalent to the rate of E-P decomposition at 5°C. It appears that the K<sup>+</sup> effect cannot be attributed to affinity changes of the site for TNP-ATP as postulated in a recent study by Bishop et al., (1986). Although apparent changes were observed under conditions of equilibrium of E and Pi producing 3 nmol/mg E<sub>2</sub>-P, addition of K<sup>+</sup> decreased E<sub>2</sub>-P to new equilibrium levels of 1.9 nmol/mg. Acceleration of the rates of various steps in the phosphorylation/dephosphorylation process by KCl may alter the apparent affinity of the site for TNP-nucleotides. Nevertheless, monovalent cation binding has been demonstrated by a spectrophotometric method that is convenient and relatively simple to perform.

#### 4.7 THE EFFECTS OF VALINOMYCIN ON MONOVALENT CATION BINDING

The interaction of valinomycin with lipid bilayers and naturally occurring biological membranes has been well characterized with respect to its K<sup>+</sup> specific conduction through hydrophobic barriers (Benz et al., 1973; Pressman, 1976). In the present study, the effects of valinomycin on the Ca<sup>2+</sup>-ATPase and on other properties that are directly related to its catalytic function do not appear to be readily explained by its ionophoric effects. However, the possibility that valinomycin effects were mediated by increased cation conductance was considered. McKinley and Meisner have characterized two populations of SR vesicles, which they have termed type I and type II (McKinley and Meisner, 1977). The former are freely permeable to K<sup>+</sup>, while the latter are relatively impermeable. It has been suggested

that this heterogeneity is due to a limited number of  $K^+$ -specific conductance channels, which are distributed among SRV such that type II do not contain  $K^+$  channels. The question of electrogenicity of the  $Ca^{2+}$  pump is unsettled. Zimniak and Racker(1978) have evidence for electrogenic function in reconstituted systems, while Chiu and Haynes (1980) have concluded that development of a transmembrane potential, positive inside, is prevented by either counter transport of  $K^+$  or  $H^+$  or of cotransport of anions, particularly chloride. The enhanced  $Ca^{2+}$  release by valinomycin from SR of frog semitendinosus muscle during tetany is consistent with increased  $K^+$  uptake, resulting in charge neutralization (Kitazawa et al, 1984). However, the valinomycin effects noted in our study were not altered by  $Ca^{2+}$  ionophore, A23187, nor by overnight pre-equilibration of the vesicles in high  $[K^+]$ . Significant effects of valinomycin were also noted in the absence of added  $K^+$  or other monovalent cations. The main support for direct interaction between valinomycin and the  $Ca^{2+}$ -ATPase comes from its specific effects on the monovalent cation binding site. The natural  $K^+$  specificity of the site was abolished by valinomycin and the inhibition of TNP-ATP fluorescence followed a simple lyotropic series for monovalent cations ( $Cs^+ > Rb^+ > K^+ = Na^+ \gg Li^+$  ).

Valinomycin inhibited steady state ATPase activity and  $Ca^{2+}$  transport (Arav et al., 1983), and also enhanced the TNP-ATP fluorescence. These findings are consistent with interaction of valinomycin with a site, whose occupation by the ionophore inhibits E-P hydrolysis and enhances steady state fluorescence of bound TNP-ATP. The type of interaction of valinomycin with the site is uncertain. Although it would appear from the total  $K^+$  content of the final medium that the monovalent cation site is unoccupied in the absence of added salt, it cannot be excluded that a tightly bound  $K^+$  ion does reside at the site, in which case an enzyme- $K^+$ -valinomycin

ternary complex is possible. An alternate explanation is that valinomycin, previously shown to exhibit a variety of conformation transitions compatible with media of varying dielectric constants (see Fig. 1.2 and Ovchinnikov et al., 1974), binds in its unliganded form to the monovalent site, possibly aided by steric matching of amino acid side chains of the enzyme and side chains of the ionophore respectively, and then complexes with the monovalent cation. Of these two mechanisms, it appears that once bound, valinomycin, either specifically prevents access of  $K^+$  ions to the enzyme site, or promotes their off rate constant, resulting in the observed lower affinity for  $K^+$ , but with little effect on the binding of other monovalent cations. It is of interest that valinomycin does not effect the apparent affinity of chaotropic anions as determined from their ability to decrease in TNP-ATP fluorescence. This finding supports the proposal that valinomycin specifically alters monovalent cation interactions with the site through a mechanism of ion chelation. The selectivity patterns among monovalent cations have been formulated in terms of a balance between the attractive energies of ions for negatively charged sites versus their dehydration (Eisenman, 1961). In terms of such a proposal, the altered pattern or "Eisenman sequence", induced by valinomycin, could be due to alteration in either of these parameters (for review, see Eisenman and Horn, 1983).

Vignais et al.(1986) have reported a puzzling effect of valinomycin in rat heart mitochondria. They have shown that the binding capacity of the mitochondria for atractyloside, an inhibitor of ADP/ATP transport, is diminished by valinomycin in the presence of KCl. The effect is only partial and on  $V_{max}$  alone. The inhibitory effect was reversed by the protonophore, nigericin, and by carbonyl cyanide-p-trifluoromethoxyphenyl hydrazine (FCCP). They have suggested that the valinomycin effect may be due to

modification of membrane surface charge, the electrostatic effect of which leads to a change in conformation of the ADP/ATP translocator. However, it is difficult to explain how an all-or-none phenomenon, such as binding capacity of only some of the translocators in the membrane, is modified by surface charge. A direct interaction of valinomycin with the enzyme may be considered.

A previous study in this laboratory described an interaction between the  $\text{Ca}^{2+}$  ionophore, A23187 and tightly bound  $\text{Ca}^{2+}$ , resident on the  $\text{Ca}^{2+}$ -ATPase of SR (Diamond et al., 1980) It was postulated that interaction of the ionophore with a hydrophobic pocket in or on the pump protein, where access to such a hydrophobic site may be either from the medium, or via the lipid bilayer, to an intramembranous protein-lipid contact surface (Berman, 1982). Whatever the molecular explanation for interaction of ionophores with the  $\text{Ca}^{2+}$ -ATPase, it appears that such interaction between ionophores and membrane proteins might be the mechanism for phenomena that cannot readily be explained as a result of their ionophoric properties that redistribute small ions across the lipid bilayers of biological membranes.

## 5.0 CONCLUSION

The fluorescence and high affinity binding properties of the ATP analogue, TNP-ATP have been exploited to study a number of properties and characteristics of the  $\text{Ca}^{2+}$ -ATPase of sarcoplasmic reticulum. TNP-ATP binds with one mol/mol stoichiometry to both the phosphorylated and nonphosphorylated enzyme with high affinity ( $K_{0.5} = 0.2$  to  $0.7 \mu\text{M}$ ). Binding to the non-phosphorylated enzyme appears to occur at the catalytic site. The TNP-ATP binding site that results in enhanced fluorescence has been identified as the regulatory site, on the basis of competition for ATP and ADP binding in the millimolar range.

Various models have been proposed for the spatial location of regulatory sites on the enzyme (Fig 4.1), on the basis of previous evidence that two nucleotide binding sites exist simultaneously (Watanabe and Inesi, 1982; Dupont et al., 1985). A dimeric enzyme may have catalytic and regulatory sites on different polypeptide chains, with allosteric linkage (model 1). The enzyme may possess regulatory sites on the same polypeptide chain, which are discrete from the catalytic site (Model 2). These two models are, however, incompatible with the present findings for only one mol/mol stoichiometry. The enzyme may possess one single site, but a second molecule of ATP is able to bind to the phosphorylated active site with decreased affinity, once ADP has been liberated (model 3). We propose, consequently, that the fluorescence changes of TNP-ATP represent events occurring at the catalytic site during various conformations of the enzyme. It follows that the regulatory site should be a modified conformation of the phosphorylated catalytic site.

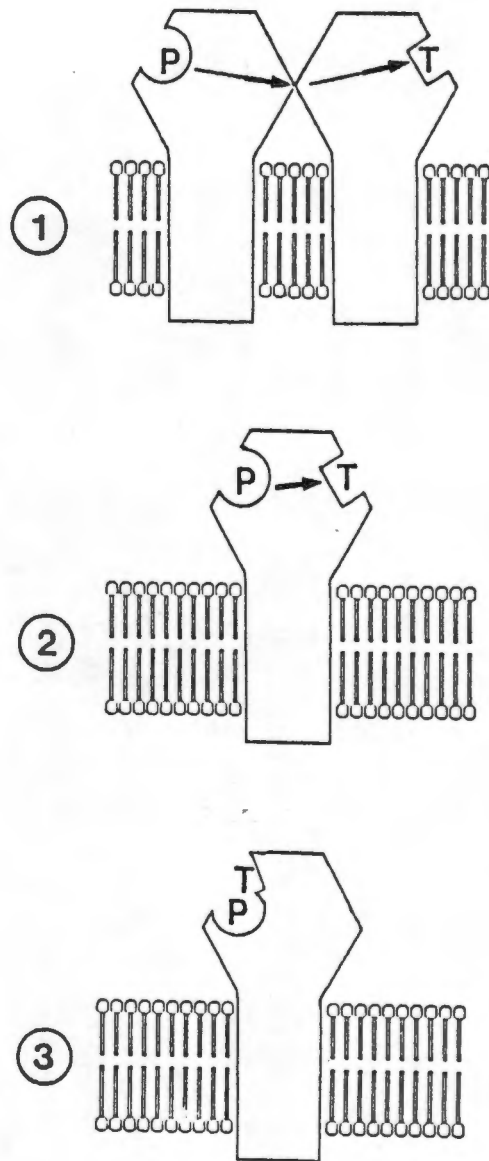


**Figure 4.1** Models of Catalytic-Regulatory Site Interaction: Site-site interaction between phosphorylated and TNP-nucleotide sites.

Model 1: Site-site interaction on dimer with structural symmetry and functional asymmetry.

Model 2: Interaction between two non-identical sites on a monomer.

Model 3: TNP-nucleotide bound at the phosphorylated catalytic site.

The regulatory site, therefore, only exists in the phosphorylated conformations of the enzyme. Following ADP departure from the phosphorylated catalytic site, TNP-ATP can rebind. It is uncertain, however, whether TNP-ATP can bind to the high energy  $E_1$ -P conformation. The present study indicates that enhanced fluorescence of the probe occurs in the  $E_2$ -P conformation, and consequently this binding site must differ significantly in its dielectric properties from the site detected on the non-phosphorylated enzyme.

Chaotropic agents, which have previously been shown to displace ATP molecules from the active site, displace TNP-ATP from the regulatory site.  $K^+$  ions that accelerate phosphoenzyme hydrolysis have no effect on TNP-ATP binding. The partitioning of large molecules of low charge density, such as chaotropic anions, and the exclusion of monovalent cations, may be the result of a specific water-free configuration of the regulatory site. Valinomycin, a  $K^+$ -specific ionophore, accelerates the "off" rate of  $K^+$  from its binding site, but has no effect on chaotropic anions. Anion and cation interactions therefore either operate via different sites, or at different sections of the regulatory site.

Exclusion of water molecules from the regulatory site in the  $E_2$ -P conformation, as previously proposed by Dupont 1983, may not be linked to phosphoenzyme hydrolysis. There are a number of possible interpretations for changes in polarity of the regulatory site. TNP-ATP fluorescence may be a result of approximation of a hydrophobic peptide chain to the trinitrophenyl moiety of the TNP-ATP molecule in the  $E_2$ -P conformation. Alternatively, water activity at the regulatory site may be altered, either by exclusion of water from the site, or by alteration of the water structure, imposed by the architecture of charged groups lining the solvent accessible surface of the site. Movement of relatively hydrophobic residues from the protein interior

into the bulk water medium, or into areas of controlled water activity, may be a transient stage in energy transduction for storage of energy derived from chemical potential energy. Return of the residues to their original "resting" conformation can then be expressed as osmotic potential energy.

It is of interest that the proposed step in the catalytic cycle ( $E_2$ -P) that results in an enhanced fluorescence state of bound TNP-ATP coincides with a major change in affinity of the binding sites for  $Ca^{2+}$ , as well as reorientation of access of these sites to the vesicle lumen (deMeis and Vianna, 1979). Formation of the  $E_1$ -P conformation is associated with  $Ca^{2+}$  occlusion from both access points of the  $Ca^{2+}$  channel (Fassold *et al.*, 1981; Chiesi and Inesi, 1979). A recent study by Petithory and Jencks (1986) shows kinetic evidence for non-random binding of  $Ca^{2+}$ , followed by ATP, prior to phosphorylation. It is possible that a small conformational change in the vicinity of the active site during phosphorylation of the enzyme occludes  $Ca^{2+}$  to the exterior. A subsequent step is necessary to reorient the  $Ca^{2+}$  sites. The energy required for this step is predictably small (Inesi, 1985), whereas the energy changes necessary for the decrease in affinity of the sites for  $Ca^{2+}$  are large. It is possible, therefore, that enhanced fluorescence of the regulatory nucleotide site probe, TNP-ATP, reflects a major conformational change of the enzyme during the catalytic cycle that is essentially linked to the catalytic cycle, and represents a prerequisite for vectorial transfer of  $Ca^{2+}$  ions.

Hydrophobic sites on proteins determine specificity of ligand binding, as well as providing domains, within which phosphorylation and dephosphorylation reactions can occur under conditions that allow energy capture and energy transduction. These reactions are readily studied by monitoring site polarity and site-ligand interactions, and

could possibly lead to further insight and understanding of the mechanisms of biological membrane energetics. The present studies, which were originally aimed at characterization of changes in properties of the active site of the  $\text{Ca}^{2+}$ -ATPase of sarcoplasmic reticulum, may have more general relevance for energy transfer systems in membrane proteins.

## 6.0 BIBLIOGRAPHY

- Amis, E.S. and Hinton, J.F. (1973) Solvent effects on Chemical Phenomena Academic Press N.Y., 46-181.
- Andersen, K. W. and Murphy, A. J. (1983), J. Biol. Chem. 258, 14276-14278.
- Arnett, E. and McKelvey, D. (1966) J. Am. Chem. Soc. 88, 5033-5034
- Andersen, J. P., and Moller, J. V. (1977), Biochem. Biophys. Acta. 485, 188-191.
- Andersen, J. P., Jorgensen, P. L. and Moller, J. V. (1985) P. N. A. S. 85, 4573-4577.
- Arav, R., Aderem, A.A. and Berman, M.C. (1983), J. Biol. Chem 258, 10433-10438.
- Aviram, I. (1973) Eur. J. Biochem 40, 631-636.
- Beil, F.U., von Chak, D. and Hasselbach, W. (1977) Eur. J. Biochem 81 151-164.
- Barlogie, B., Hasselbach, W. and Makinose, M. (1971) FEBS Lett. 12, 267-268.
- Beil, F.U., Von Chak, D., and Hasselbach, W. (1977) EJB 81, 151-164.
- Bennet, J. P., McGill, K. A. and Warren, G. B. (1980) Curr. Top. Membr. Transport 14, 127-164.
- Benz, J., Stark, G., Janko, K. and Lauger, P. (1973) J. Membr. Biol., 14, 329-364.
- Berman, M.C. (1982) Biochem. Biophys. Acta. 694, 95-121.
- Berman, M.C., McIntosh, D.B. and Kench, J.E. (1977) J. Biol. Chem. 252, 994-1001.
- Bernal, J. D. (1964) Proceedings of the Royal Society of London A. 280, 299-322.
- Bergmeyer, H. (1965) Methods of Enzymatic analysis, Academic Press, New York, 573-577.
- Bishop, J. E., Johnson, J. D. and Berman, M. C. (1984) J. Biol. Chem. 259, 15163-15171.

- Bishop, J. E., Nakamoto, R. K. and Inesi, G. (1986)  
 Biochemistry 25, 696-703.
- Birktoft, J.T. Blow, D. (1972) J. Mol. Biol. 68, 187-240.
- Boyer, P. D., Cross, R. L., and Momsen, W. (1973), Proc.  
 Natl. Acad. Sci. 70, 2837-2839.
- Cable M. B. Fehrer, J. J. and Briggs, F. N. (1985)  
 Biochemistry 24, 5612-5619.
- Campbell, K. P. and MacLennan, D.H.(1981), J. Biol. Chem.  
256, 4626-4632.
- Campbell, K. P. and MacLennan, D.H.(1983), J. Biol. Chem.  
258, 1391-1394.
- Carvalho, M.G.S., Souza, D.O. and deMeis, L. (1976) J. Biol.  
 Chem. 251, 3629-3636.
- Caswell, A.H. and Pressman, B.C. (1972) Biochem. Biophys.  
 Res. Comm. 49, 292- 298.
- Chaloub, R.M. and deMeis, L. (1980) J. Biol. Chem. 255, 6168-  
 6172.
- Champeil, P., Gingold, M.P. and Guillain, P. (1983) J. Biol.  
 Chem. 258, 4453-4458.
- Champeil, P., Buschlen-Boucly, S., Bastide, F. and Gary-bobo,  
 C. (1978) J. Biol. Chem. 253, 1179-1186.
- Chiesi, M. and Inesi, G. (1979) J. Biol. Chem. 254, 10370-  
 10375.
- Chiesi, M. and Inesi, G. (1980) Biochemistry 19, 2912-2918.  
 Chiesi, M. and Inesi, G. (1981) Arch. Biochem. Biophys.  
108, 586-592.
- Chiu, V.C.K., and Haynes, D.H., (1980) J. Membr. Biol. 56,  
 203-218.
- Coll, R. J. and Murphy, A. J. (1985) FEBS. Lett. 187, 131-  
 134.
- Connoly, M.L. (1983) Science 221, 709-713.
- Coan, C. R. and Inesi, G. (1977), J. Biol. Chem. 252, 3044-  
 3049.
- Coan, C. R., Verjovski-Almeida, S. and Inesi, G. (1979) J.  
 Biol. Chem. 254, 2968-2974.

- Cooke, R., and Kuntz, I.D. (1974) *Ann. Rev. Biophysics and Bioengineering* 3, 95-127.
- Davidson, G. A. and Berman, M. C. (1985) *J. Biol. Chem.* 260, 7325-7329.
- Deamer, D.W. and Baskin, R. J. (1969) *J. Cell. Biol.* 42, 296-307.
- Degani, C. and Boyer, P.D. (1973) *J. Biol. Chem.* 248, 8222-8226.
- deMeis, L., Behrens, M.I. and Petretski, J.H. (1985) *Biochemistry* 24, 7783-7789.
- deMeis, L. and deMello, M.C.F. (1973) *J. Biol. Chem.* 248 3691-3701.
- deMeis, L., Martins, O.B. and Alves, E.L. (1980) *Biochemistry* 19, 4252- 4261.
- deMeis, L. and Masuda M. (1974) *Biochemistry* 13, 2057-2062.
- deMeis, L. and Tume, R. (1977) *Biochemistry* 16, 4455-4463.
- deMeis, L. and Vianna, A.L. (1979) *Annu. Rev. Biochem.* 48, 275-292.
- deSouza, D. and deMeis, L. (1976) *J. Biol. Chem.* 251, 6355-6359.
- Diamond, E.M., Norton, K.B., McIntosh, D.B. and Berman, M.C. (1980) *J. Biol. Chem.* 255, 11351-11356.
- Dijkstra, B.W., Hol, W.G.S. and Drenth, J. (1981) *J. Mol. Biol.* 147, 97- 123.
- Drost-Hansen, W. (1973) *Ann. NY Acad. Sci.* 204, 100-113.
- Duggan, P.F. (1977) *J. Biol. Chem.* 252, 1620-1627.
- Dupont, Y. (1976) *Biochem. Biophys. Res. Comm.* 71, 544-550.
- Dupont, Y. (1977) *Eur. J. Biochem.* 72, 185-190.
- Dupont, Y. (1978) *Biochem. Biophys. Res. Comm.* 82, 893-900.
- Dupont, Y. (1980) *Eur. J. Biochem.* 109, 231-238.
- Dupont, Y. (1983) *FEBS Lett.* 161, 14-20
- Dupont, Y. (1982) *Biochem. Biophys. Acta.* 688, 75-87.
- Dupont, Y. Bennet, N. and Lacapere, J.J. (1982) *Ann. NY Acad. Sci.* 402, 569-572.

- Dupont, Y., Chapron, Y. and Pougeois, R. (1982b) *Biochem. Biophys. Res. Comm.* 106, 1272-1279.
- Dupont, Y., Harrison, S. C. and Hasselbach W. (1973) *Nature* 244, 555- 558.
- Dupont, Y. and Pougeois, R. (1983) *FEBS Lett.* 156, 93-98.
- Dupont, Y. and Leigh, J.B. (1978) *Nature* 273, 396-398.
- Dupont, Y. and LeMaire, M. (1980) *FEBS Lett.* 115, 247-252.
- Dutton, A. Reis, E. D. and Singer, S. J. (1976) *Proc. Natl. Acad. Sci.* 73, 1532-1536.
- Ebashi, S. (1960) *J. Biochem. (Tokyo)* 48, 150-115.
- Ebashi, S. and Lipmann, F. (1962) *J. Cell Biol.* 14, 389-400.
- Ebashi, S., Otsuka, M. and Endo, M. (1962) *Excerpta Med. Int. Congr. Ser.* 48, 899-905.
- Eisenman, G. (1961) In: *Symposium on Membrane Transport and Metabolism.* A. Kleinzeller and A. Kotyk eds. 163-179  
Academic Press. NY.
- Eisenman, G., and Horn, R. (1983) *J. Membr. Biol.* 76, 197-225.
- Eletr, S., and Inesi, G. (1972) *Biochem. Biophys. Acta.* 282, 174-179.
- Fassold, E., von Chak, D. and Hasselbach, W. (1981) *Eur. J. Biochem.* 113, 611-616.
- Felber, S.M., and Brand, M.D. (1982) *FEBS Lett.* 150, 122-124.
- Fernandez-Belda, F., Kurzmack, M. and Inesi, G. (1984) *J. Biol. Chem.* 259 9687-9698.
- Fleicher, S., Wang C. T., Saito, A., Pilarska, M. and McIntyre, J. O. (1979) Flux across Biomembranes Y. Mukohata and L. Packer eds. Academic Press N.Y., 193-205.
- Frank, H.S. (1958) *Proceedings of the Royal Society of London A.* 247, 481-492.
- Frank, H.S. and Wen, Y. (1957) *Discussions Faraday Soc.* 57 133.
- Froehlich, J.P. and Heller, P.F. (1985) *Biochemistry* 24, 126-136.

- Froehlich, J.P. and Taylor, E.W. (1975) J. Biol. Chem. 250, 2013-2021.
- Froehlich, J.P. and Taylor, E.W. (1976) J. Biol. Chem. 251, 2307-2315.
- Garrahan, P.J., Rega, A.F. and Alonso, G.L. (1976) Biochem. Biophys. Acta. 448, 121-132.
- George, P., Witonsky, R.J., Trachtman, M., Wu, C., Dowart, W. Richman, L., Richman, W., Shurayh, F. and Lentz, B. (1970) Biochem. Biophys. Acta. 223, 1-15.
- Glynn, I. M. and Chappel, J. B. (1964) Biochem. J. 90, 147-149.
- Glynn, I. M. and Karlsh, D. (1975) Annu. Rev. Physiol. 37, 13-56.
- Grubmeyer, C. and Penefsky, H. S. (1981) J. Biol. Chem 256, 3718-3727.
- Guillain, F. Champeil, P. an Boyer, P. D. (1984) Biochemistry 23, 4754- 4761.
- Guillain, F., Champeil, P., Lacapere, J.J. and Gingold, M. (1981) J.Biol Chem. 256, 6140-6147.
- Guillain, F., Gingold, M.P. Buschen, S. and Champeil, P. (1980) J. Biol. Chem. 255, 2072-2076. 0
- Guillain, F., Champeil, P., Lacapere, J. J. and Gingold, M. C. (1981) J. Biol. Chem. 256, 6140-6147.
- Guillain, F., Gingold, M. P. and Champeil, P. (1982) J. Biol. Chem. 257, 7366-7371.
- Guimares-Motta, M. Sande-Lemos, M.P. and deMeis, L. (1984) J. Biol. Chem. 8699-8705.
- Gutfreund, H. (1972) Enzymes: Physical Principles, Wiley-Interscience, London.
- Hamabata, A. and von Hippel, P.H. (1973) Biochemistry 12, 1264-1271.
- Hasselbach, W. (1978) Biochem. Biophys. Acta. 515, 23-53.
- Hasselbach, W. and Makinose, M. (1961) Biochem Z. 333, 518-528.

- Hasselbach, W. and Makinose, M. (1963) *Biochem Z.* 339, 94-111.
- Hatefi, Y. and Hansten, Y.G. (1974) *Methods Enzymol.* 31, 770-790.
- Haynes, D.M., Kenyon, G.L. and Kollman, P.A. (1978) *J. Am. Chem. Soc.* 100, 4331-4340.
- Haynes, D.H. and Simkowitz, P. (1977) *J. Mol. Biol.* 33, 63-108.
- Haynes, D. H., Weins, T. and Pressman, B.C. (1974) *J. Mol. Biol.* 18, 23.
- Hill, T., and Morales, M. F. (1951) *J. Am. Chem. Soc.* 73, 1656-1660.
- Hiratsuka, T. (1975) *J. Biochem. (Tokyo)* 78, 1135-1147.
- Hiratsuka, T. (1982) *Biochem. Biophys. Acta.* 719, 509-517.
- Hiratsuka T. and Uchida K. (1973) *Biochem. Biophys. Acta.* 330, 635-647.
- Henke, J. A. M. (1970) *J. Chem. Physiol.* 56, 521-541.
- Herbette, L., Marquardt, J., Scarpa, A. and Blaisie, J. K. (1977) *Biophys. J.* 20, 245-272.
- Hobbs, A. N., Wayne-Albers, R., Froehlich, J. P. and Heller, P.F. (1985) *J. Biol. Chem.* 260, 2035-2037.
- Horgan, D. J., Tume, R. K. and Newbold, R. P. (1972) *Analytical Biochemistry* 48, 147-152.
- Huxley, H. E. (1964) *Nature* 202, 1067-1071.
- Ikemoto, N. J. (1975) *J. Biol. Chem.* 250, 7219-7224.
- Ikemoto, N. J. (1976) *J. Biol. Chem.* 251, 7275-7277.
- Ikemoto, N. J. (1982) *Annu. Rev. Physiol.* 44, 297-317.
- Inesi, G. (1971) *Science* 171, 901-903.
- Inesi, G. (1985) *Annu. Rev. Physiol.* 47, 573-601.
- Inesi, G., Maring, E., Murphy A. J., and McFarland, B. H. (1970) *Arch Biochem. Biophys.* 138, 285-294.
- Inesi, G., Kursmack, M., Coan, C., Lewis, D. E. (1980) *J. Biol. Chem.* 255, 3025-3031.
- Inesi, G., Watanabe, T., Coan, C. and Murphy, A. (1982) *Ann. N.Y. Acad. Sci.* 402, 515-534.

- Jencks, W. P. (1980) *Adv. Enzymol.* 51, 75-106.
- Jencks, W. P. (1983) *Curr. Top. Membr. Transp.* 19, 1-19.
- Kanazawa, T. and Boyer, P. D. (1973) *J. Biol. Chem.* 248, 3163-3172.
- Kanazawa, T., Yamada, S. Yamamoto, T. and Tonomura, Y. (1971) *J. Biochem. (Tokyo)* 20, 95-123.
- Kauzmann, W. (1959) *Adv. Protein Chem.* 14, 1-63.
- Kawakita, M., Yasuoka, K., Kaziro, Y. (1980) *J. Biochem. (Tokyo)* 87, 609-617.
- Kitazawa, T., Somlyo, A. V. and Somlyo, A. V. (1984) *J. Physiol. (Lond)* 350, 253-268.
- Klemens, M. R., Andersen, J. P. and Grisham, C. M. (1986) *J. Biol. Chem.* 261, 1495-1498.
- Klip, A., Reithmeier, R. A. F., and MacLennan, D. H. (1980) *J. Biol. Chem.* 255, 6526-6568.
- Klotz, I. M. (1959) *Science* 128, 815-822.
- Klotz, I. M. (1962) *Horizons in Biochemistry*, Kasha M. & Pullman, B. Eds. Academic Press N. Y.
- Knowles, A. F. (1980) *Ann. Rev. Biochem.* 49, 877-919.
- Knowles, A. F. and Racker, E. (1975a) *J. Biol. Chem.* 250, 1949-1951.
- Knowles, A. F. and Racker, E. (1975b) *J. Biol. Chem.* 250, 3538-3544.
- Koenig, S. H., and Schillinger, W. E. (1969) *J. Biol. Chem.* 244, 3283-3289.
- Kometani, and Kasai, M. (1978) *J. Mol. Biol.* 41, 295-308.
- Kurzmack, M., Verjovski-Almeida, S. and Inesi, G. (1977) *Biochem. Biophys. Res. Comm.* 78, 772-776.
- Lacapere, J.J., Gingold, M. P., Champeil, P. and Guillain, F. (1981) *J. Biol. Chem.* 256, 2302-2306.
- Laemmli, U. (1970) *Nature (Lond.)* 227, 680-685.
- Lakowicz, J. R. (1983) Principles of Fluorescence Spectroscopy, Plenum Press, N. Y.

- Laggner, P., Suko, J., Punzengruber, C. and Prager, R. (1981) *Z. Naturforsch., B.: Anorg. Chem, Org. Chem.* 36b, 1136-1143.
- Laemmli, U. K. (1970) *Nature* 227, 680-687.
- Lee, C. Y., McCammon, J. A., Rossky, P. J. (1984) *J. Chem. Phys.* 80, 4448-4455.
- Lee, B., and Richards, F. M. (1971) *J. Mol. Biol.* 55, 379-384.
- Loomis, C. R., Martin, D. W., McCaslin, D. R. and Tanford, C. (1982) *Biochemistry* 21, 151-156.
- Louis, C. F., Nash-Adler, P. Fudyma, G., Shigekawa, M. and Katz, A. M. (1980) *Biochem. Biophys. Acta.* 599, 610-622.
- Low, P.S., and Somero, G. N. (1975) *Proc. Natl. Acad. Sci.* 72, 3014-3309.
- MacLennan, D. H. (1970) *J. Biol. Chem.* 254, 4508-4518.
- MacLennan, D. H., Brandt, C. J., Korczak, B. and Green, N. M. (1985) *Nature* 316, 696-700.
- Makinose, M. (1971) *FEBS. Lett.* 12, 269-270.
- Makinose, M. (1973) *FEBS Lett.* 37, 140-143.
- Makinose, M. and Hasselbach, W. (1965) *Biochem. Z.* 343, 360-382.
- Makinose, M. and Hasselbach, W. (1971) *FEBS Lett.* 12, 271.
- Makinose, M and Boll, W. (1979) in Cation fluxes Across Biomembranes Mukohata y., and Packer L. eds., 89-100, Academic Press, N.Y.
- Makinose, M. and The, R. (1965) *Biochem. Z.* 343, 383-393.
- Martin, D. W. and Tanford, C. (1981) *Biochemistry* 20, 4597-4602.
- Martonosi, A. and Feretos, R. (1964), *J. Biol. Chem.* 239, 648-658.
- Martonosi, A. (1969) *J. Biol. Chem.* 244, 613-620.
- Martonosi, A. and Fortier, F. (1974) *Biochem. Biophys. Res. Comm.* 60, 382-389.
- Masuda, H. and deMeis, I. (1973) *Biochemistry* 12, 4581-4585.

- McIntosh, D.B., and Boyer, P.D. (1983) *Biochemistry* 22, 2867-2875.
- McKinley, D. and Meissner, G. (1977) *FEBS Lett.* 82, 47-50.
- McMurray, W. and Beggs, M. (1959) *Arch. Biochem. Biophys.* 84, 546.
- Meltzer, S. and Berman, M. C. (1985) *J. Biol. Chem.* 259, 4244-4253.
- Mermier, P. and Hasselbach, W. (1976) *Eur. J. Biochem.* 69, 79-86.
- Michalak, M. Campbell, K. P. and MacLennan, D. M. (1980) *J. Biol. Chem.* 255, 1317-1326.
- Mitchinson, C., Wilderspin, A. F. Trumanian, B. J. and Green. N. M. (1982) *FEBS Lett.* 146, 87-92.
- Moczdowski, E. G. and Fortes, P. A. (1981) *J. Biol. Chem.* 256, 2346-2356.
- Moller, J. V., Andersen, J. P. and LeMaire, M. (1982) *Molecular and Cellular Biochemistry* 42, 83-107.
- Moller J. V., Lind, K. E., and Andersen, J. P. (1980) *J. Biol. Chem.* 255, 1912-1920.
- Moore, C. and Pressman, B. C. (1964) *Biochem. Biophys. Res. Comm.* 15, 562.
- Murphy, A. J. (1976) *Biochemistry* 15, 4492-4494.
- Nagasaki, K. and Kasai, M. (1980) *J. Biochem. (Tokyo)* 87, 709-716.
- Nakamura, Y., and Tonomura, Y. (1982) *J. Biochem. (Tokyo)* 91, 449-461.
- Nakamoto, R. K. and Inesi, G. (1984) *J. Biol. Chem.* 259, 2961-2970.
- Napolitano, C. A., Cooke, P. Segalman, K. and Herbette, L. (1983) *Biophys. J.* 42, 119-125.
- Negendank, W. and Schaller, C. (1982) *Biochem. Biophys. Acta.* 688, 316-322.
- Nemethy, G. and Sheraga, H. A. (1962) *J. of Chemical Physics.* 36, 3382-3417.

- Newbold, R. P., and Tume, R. K. (1979) *J. Mol. Biol.* 48, 205-213.
- Norten, A. H. and Levy, H. A. (1969) *J. Phys. Chem.* 73, 26-33.
- Nowak, T. (1976) *J. Biol. Chem.* 251, 73-78.
- Oosta, G. M., Mathewson, N. S. and Catravas, G. N. (1978) *Anal. Biochem.* 89, 31-34.
- Ovchinnikov, Y. U. A., Ivanov, V. T. and Shkrob, A. M. (1974) Membrane Active Complexes *Biochem. Biophys. Acta. Library* vol. 12 Elsevier N.Y.
- Painter, G. R. and Pressman, B. C. (1982) *Topics in Current Chemistry* 101, 83-110.
- Panet, R., Pick, U. and Selinger, Z. (1971) *J. Biol. Chem.* 246, 7349-7356.
- Pang, D. and Briggs F. (1977) *J. Biol. Chem.* 252, 3262-3266.
- Peachey, L. D. (1965) *J. Cell. Biol.* 25, 209-231.
- Penefsky, H. S. (1985) *J. Biol. Chem.* 260, 13735-13741.
- Phipps, D. A. (1976) Metals and Metabolism, Oxford Press.
- Pick, U. (1981) *Eur. J. Biochem.* 121, 187-195.
- Pick, U. and Karlsh, S. J. D. (1982) *J. Biol. Chem.* 257, 6120-6126.
- Pick, U. and Racker, E. (1979) *Biochemistry* 18, 108-113.
- Pickart, C. M. and Jencks, W. P. (1982) *J. Biol. Chem.* 257, 5319-5322.
- Pickart, C. M. and Jencks, W. P. (1984) *J. Biol. Chem.* 259, 1629-1643.
- Pierce, D. H. and Scarpa, A., Topp, M. R. and Blaise, J. K. (1983) *Biochemistry* 22, 5254-261.
- Pfieffer, D. R., Reed, P. W. and Lardy, H. A. (1974) *Biochemistry* 19, 4007.
- Porter, J. (1961) *Biophys. Biochem. Cytol. Suppl.* 10, 219-226.
- Pressman, B. C. (1967) *Proc. Natl. Acad. Sci.* 58, 1949-1951.
- Pressman, B. C. (1976) *Am. Rev. Biochem.* 45, 501-530.
- Pucell, A. and Martonosi, A. (1971) *J. Biol. Chem.* 249, 3389-3397.

- Punzenbruber, C., Prager, R., Kolossa, N., Winkler, K. and Suko, J. (1978) *Eur. J. Biochem.* 92, 349-359.
- Raskin, A.A., Iofin, M. and Honig, B. (1986) *Biochemistry*, 25, 3619-3625.
- Saito, K., Imamura, Y. and Kawakita, M. (1984) *J. Biochem. (Tokyo)* 95, 1297-1304.
- Scarpa, A., Beldassere, J. and Inesi, G. (1972) *Gen. Physiol.* 60, 35- 739.
- Scatchard, G. (1949) *Chem. Rev.* 44, 7.
- Schwartzbach, G. (1957) *Complexometric Titration* (translated by Inving, H. M.) Methuen, London.
- Scofano, H., Vierya, A. and deMeis, L. (1979) *J. Biol. Chem.* 254, 10227-10231.
- Scott, H. L. (1984) *Chem Phys. Lett.* 109, 507-573.
- Shamoo, A. E., Ryan, T. E. Stewart, P. S. and MacLennan, D. H. (1976) *J. Biol. Chem.* 251, 4147-4154.
- Shigekawa, M. and Akowitz, A.A. (1979) *J. Biol. Chem.* 254, 4726-4730.
- Shigekawa, M. and Dougherty, J. P. (1977) *Biochem. Biophys. Res. Comm.*, 76, 784-789.
- Shigekawa, M. and Dougherty, J. P. (1978) *J. Biol. Chem.*, 253, 1451-1464.
- Shigekawa, M., Dougherty, J. P. and Katz, A. M. (1978) *J. Biol. Chem.* 253, 1442-1450.
- Shigekawa, M. and Kanazawa, T. (1982) *J. Biol. Chem.* 257, 7657-7665.
- Shigekawa, M. and Pearl, L. J. (1976) *J. Biol. Chem.* 251, 6947-6952.
- Shigekawa, M., Wakabayashi, S., and Nakamura, H. (1984) *J. Biol. Chem.* 259, 8698-8707.
- Somlyo, A. V., Schuman, H., Somlyo, A. P. (1977) *J. Cell. Biol.* 74, 828-857.
- Sumida, M. and Tonomura, Y. (1974) *J. Biochem. (Tokyo)* 75, 283-297.

- Sumida, M. and Sasaki, S. (1975) *J. Biochem. (Tokyo)* 75, 283-297.
- Sumida, M., Wang, T., Mandel, F., Froelich, J. P. and Schwartz, A. (1978) *J. Biol. Chem.* 253, 8772-8777.
- Tada, M., Yamada, T. and Tonomura, Y. (1978) *Physiol. Rev.* 58, 1-79.
- Takakuwa, Y. and Kanazawa, T. (1981) *J. Biol. Chem.* 256, 2691-2695.
- Takakuwa, Y. and Kanazawa, T. (1982) *J. Biol. Chem.* 257, 426-431.
- Takisawa, H. and Makinose, M (1981) *Nature* 290, 271-273.
- Takisawa, H. and Makinose, M (1983) *J. Biol. Chem.* 258, 2986-2992.
- Tan, K. H. and Lovrien, R. (1972) *J. Biol. Chem.* 247, 3278-3285.
- Tanford, C. (1980) The Hydrophobic Effect Wiley-Interscience, N. Y.
- Tanford, C. (1983) *Ann. Rev. Biochem.* 52, 379-409.
- Taylor, J. S. (1981) *J. Biol. Chem.* 256, 9793-9795.
- Taylor, J. S. and Hattan, D. (1979) *J. Biol. Chem.* 254, 4402-4407.
- Teeter, M. M. (1984) *Proc. Natl. Acad. Sci.* 81, 6014-6018.
- The, R. and Hasselbach, W. (1975) *Eur. J. Biochem* 53, 105-113.
- Thorley-Lawson, D.A. and Green, N. B. (1973) *Eur. J. Biochem.* 40, 403-413.
- Thorley-Lawson, D. A. and Green, N. B. (1977) *Biochem J.* 167, 739-748.
- Verjovski-Almeida, S. (1981) *J. Biol. Chem.*, 256, 2662-2668.
- Verjovski-Almeida, S. and Inesi, G. (1979) *J. Biol. Chem.* 254, 18-21.
- Verjovski-Almeida, S., Kurzmack, M. and Inesi, G. (1978) *Biochemistry* 17, 5006-5013.
- Vignais, P. V., Michejda, J. W. and Doussiere, J. (1983) *J. Bioenerg. and Biomem.* 15, 243-256.

27 APR 1987

- Vishwanath, C. K. and Easwaran, K. R. K. (1982) *Biochem.* 21, 2612-2621.
- Watanabe, T., and Inesi, G. (1982) *J. Biol. Chem.* 257, 11510-11516.
- Wautenpaugh, K. D., Margulis, T. N., Sieker, L. C., and Jensen, L. H. (1978), *J. Mol. Biol.*, 122, 175-190.
- Weber, A., Herz, R. and Reiss, I. (1966) *Biochem. Z.* 345, 329-369.
- Welch, G. R., Somogyi, B. and Damjanovich, S. (1982) *Progr. Biophys. Mol. Biol.* 39, 109-146.
- Wiggins, P. M. (1982) *J. Theor. Biol.* 99, 645-664.
- Wilkinson, G. N. (1961) *Biochem J.* 80, 324-332.
- Wolfenden, G (1983) *Science*, 1087-1093.
- Yamada, S. and Ikemoto, N. (1972) *J. Biochem.* 71, 1101-1104.
- Yamada, S., and Ikemoto, N. (1978) *J. Biol. Chem.* 253, 6801-6807.
- Yamada, S. and Ikemoto, N. (1980) *J. Biol. Chem.* 255, 3108-3119.
- Yamamoto, F., Takisawa, H. and Tonomura, Y. (1979) *Curr. Top. Bioenerg.* 9, 179-236.
- Yamamoto, T. and Tonomura, Y. (1967) *J. Biochem. (Tokyo)* 62, 558-575.
- Yamaguchi, M. and Kanazawa, T. (1984) *J. Biol. Chem.* 259, 9526-9531.
- Yasuoka-Yabe, K., Kawakita, M. and Kaziro, Y. (1982) *J. Biochem. (Tokyo)* 91, 1629-1637.
- Yasuoka-Yabe, K., Tsuji, A. and Kawakita, M. (1983) *J. Biochem. (Tokyo)* 94, 677-688.
- Zimniak, P. and Racker, E. (1978) *J. Biol. Chem.* 253, 4631-4637.